

Aus dem Institut für Immunologie und Serologie
der Medizinischen Fakultät Mannheim
(Direktor: Prof. Dr. med. Stefan Meuer)

The influence of fibronectin modulation on tumor growth

Inauguraldissertation
zur Erlangung des Doctor scientiarum humanarum (Dr. sc. hum.)
der
Medizinischen Fakultät Mannheim
der Ruprecht-Karls-Universität
zu
Heidelberg

vorgelegt von
Hiba Ghura

aus
Latakia (Syrien)
2019

Dekan: Prof. Dr. med. Sergij Goerd
Referentin: Prof. Dr. med. Inaam Nakchbandi

TABLE OF CONTENT

	Page
LIST OF ABBREVIATIONS.....	1
1 INTRODUCTION.....	4
1.1 Cancer.....	4
1.1.1 Exogenous factors that promote cancer.....	4
1.1.2 The genes involved in cancer development.....	5
1.1.3 The hallmarks of cancer.....	5
1.1.4 Tumor microenvironment.....	6
1.1.4.1 Immune cells.....	6
1.1.4.2 Cancer-associated fibroblasts.....	9
1.1.4.3 Pericytes.....	9
1.1.4.4 Extracellular matrix (ECM).....	10
1.1.5 The metastasis.....	10
1.1.5.1 The epithelial-to-mesenchymal transition (EMT).....	11
1.1.5.2 Invasion.....	11
1.1.5.3 Intravasation.....	11
1.1.5.4 Survival of metastatic cells in the circulation.....	11
1.1.5.5 Extravasation.....	12
1.1.5.6 Micrometastasis formation (premetastatic niche).....	12
1.1.5.7 Metastatic colonization.....	12
1.2 Fibronectin.....	13
1.2.1 Fibronectin isoforms.....	14
1.2.1.1 EDA fibronectin.....	14
1.2.1.2 EDB fibronectin.....	14
1.2.1.3 The variable region.....	15
1.2.2 Fibronectin interactions and physiological functions.....	15
1.2.3 Role of fibronectin in cancer.....	16
1.2.4 Fibronectin as a therapeutic target in cancer.....	17
1.3 The goal of the work.....	18

2 MATERIAL AND METHODS	19
2.1 Materials.....	19
2.1.1 Instruments.....	19
2.1.2 Companies	20
2.1.3 Chemicals and reagents	22
2.1.4 Media, buffers and solutions.....	24
2.1.5 Used materials.....	26
2.2 Animal experimentation methods	28
2.2.1 Animals.....	28
2.2.2 Anesthesia of laboratory animals.....	28
2.2.3 Intratibial injection of human breast cancer cells	29
2.2.4 Bioluminescence imaging.....	29
2.2.5 Radiography of bone lesions	30
2.2.6 B16 - Melanoma - animal experiment model	30
2.2.7 Therapeutic treatment with peptides.....	30
2.2.8 Killing of the experimental mice	31
2.3 Cell biology methods	31
2.3.1 Murine melanoma cell line B16-F10	31
2.3.2 Human breast cancer cell line MDA-MB-231B/luc ⁺	31
2.3.3 Isolation of immune cells from tumors	32
2.3.4 Depletion of immune cells from tumors.....	32
2.3.5 Determination of cell number	32
2.3.6 Passaging and preparation of tumor cells for <i>in vivo</i> injections	32
2.4 Protein biochemical methods	33
2.4.1 Production of matrix lysates.....	33
2.4.2 Production of protein lysates for analysis of western blot or ELISA... 33	
2.4.3 Protein concentration by Bradford-assay.....	33
2.4.4 ELISA (Enzyme linked immunosorbent assay).....	34
2.4.5 Human and murine plasma fibronectin ELISA	34
2.4.6 SDS gel electrophoresis	34
2.4.7 Western blot	35
2.4.8 Purification of peptides using a nickel-NTA column.....	36
2.5 Molecular biology methods.....	37
2.5.1 Detection of mycoplasma by PCR	37
2.5.2 RNA isolation and the reverse transcription of RNA	37

2.5.3	Flow cytometry analysis.....	37
2.6	Histological methods	38
2.6.1	Preparation of tumor sections.....	38
2.6.2	Immunohistochemical staining of frozen sections.....	38
2.7	Statistical evaluations	39
3	RESULTS.....	40
3.1	Confirming of the role of fibronectin of cancer cells in tumor growth	40
3.1.1	Knocking down of fibronectin in MDA cells	40
3.1.2	Induction of local bone metastasis.....	41
3.1.3	Analysis of tumor growth	41
3.1.4	Radiographic analysis of osteolytic lesions.....	41
3.1.5	Investigation of immune cells in MDA tumors	42
3.2	Investigation of the effect of fibronectin accumulation inhibitor peptides in MDA human breast cancer model	43
3.2.1	Investigation of the effect of recombinant pUR4 and its Scrambled peptide on fibronectin of MDA cells <i>in vitro</i>	43
3.2.2	Investigation of the effect of recombinant pUR4 on MDA tumor growth <i>in vivo</i>	44
3.2.3	Investigation of pUR4 entry into MDA tumors.....	45
3.2.4	pUR4 decreases fibronectin content of MDA tumors.....	46
3.2.5	Radiographic analysis of MDA tumors before and after of recombinant peptides injection.....	46
3.2.6	Investigation of immune cells in MDA tumors treated with recombinant peptides.....	48
3.2.7	Investigation of cancer and stromal cells in MDA tumors treated with recombinant peptides	49
3.3	Evaluation of the effect of synthetic peptides in MDA tumors	50
3.3.1	Investigation of the effect of synthetic pUR4 and its scramble on fibronectin of MDA cells <i>in vitro</i>	50
3.3.2	Investigation of the effect of synthetic pUR4 and its scramble peptide in MDA cells <i>in vivo</i>	50
3.3.3	Evaluation of fibronectin content of MDA tumors treated with synthetic peptides.....	51
3.3.4	Radiographic analysis of MDA tumors treated with synthetic peptides	52
3.3.5	Evaluation of immune cells of MDA tumors treated with synthetic peptides.....	53

3.3.6	Evaluation of cancer and stromal cells of MDA tumors treated with synthetic peptides.....	54
3.4	Effect of pUR4 in immunocompetent mice	54
3.4.1	Investigation of the effect of recombinant pUR4 and its scramble peptide on fibronectin of B16 melanoma cells <i>in vitro</i>	54
3.4.2	Investigation of the effect of synthetic pUR4 and its scramble peptide on fibronectin of B16 melanoma cells <i>in vitro</i>	55
3.4.3	Investigation of the effect of synthetic peptides on B16 tumors growth <i>in vivo</i>	56
3.4.4	Effect of the synthetic pUR4 on the immune cells of B16 tumors	57
3.4.5	Effect of the synthetic pUR4 on cancer and stromal cells of B16 tumors	59
3.5	Evaluation of modified pUR4 effect on MDA cells	59
3.5.1	Evaluation of modified synthetic peptides <i>in vivo</i>	60
3.5.2	Evaluation of fibronectin content in MDA tumors treated with synthetic modified peptide	61
3.5.3	Radiographic analysis of MDA tumors treated with the synthetic modified peptide	61
3.5.4	Characterization of immune cells in MDA tumors treated with the synthetic modified peptide	62
3.5.5	Characterization of cancer and stromal cells in MDA tumors treated with the modified synthetic peptides	64
3.6	Investigation of the effect of modified peptide in B16 melanoma cells.....	64
3.6.1	Investigation of the effect of synthetic modified peptide on fibronectin of B16 melanoma cells <i>in vivo</i>	64
3.6.2	Effect of the synthetic modified peptide on the immune cells of B16 tumors in immune competent mice.....	65
3.6.3	Effect of the synthetic modified peptide on B16 melanoma cells and stromal cells of B16 tumors in immune competent mice.....	66
3.7	Investigation of the fractions of the modified synthetic peptide <i>in vitro</i>	67
3.8	Cytokines expression of MDA tumors.....	69
3.9	Immunohistochemical staining of MDA tumors.....	70
4	DISCUSSION	73
4.1	Effect of tumor-cell-fibronectin on tumor growth	73
4.1.1	Knock down of fibronectin in MDA-MB-231 cells	73
4.1.1.1	Effect on the growth of MDA-MB-231B / luc + - breast cancer cells	73
4.2	Modulation of fibronectin of cancer cells using a bacterial peptide	74

4.2.1	pUR4 inhibits fibronectin accumulation of human breast cancer cells <i>in vitro</i> and reduces cancer growth <i>in vivo</i>	74
4.2.2	pUR4 diminishes tumor growth of murine B16 melanomas	75
4.2.3	The effect of the modification of pUR4 <i>in vivo</i> and <i>in vitro</i>	76
4.3	Changes in the expression of cytokines profile of tumors.....	77
5	SUMMARY	79
6	REFERENCES	80
7	CURRICULUM VITAE	94
8	ACKNOWLEDGEMENT	96

LIST OF ABBREVIATIONS

Alb	Albumin
Ang-1	Angiopoietin-1
bp	Base pairs
BSA	Bovine serum albumin
CAFs	Cancer associated fibroblasts
CD	Cluster of differentiation
CD1	Caesarean derived 1
cFN	Cellular fibronectin
COX	Cyclooxygenase enzyme
cpp	Cell penetrating peptides
CT	Control
CTLs	Cytotoxic T lymphocytes cells
DAPI	4,6-diamidino-2-phenylindole
DMEM	Dulbecco's modified eagle medium
DMSO	Dimethyl sulfoxide
DNA	Deoxyribonucleic acid
dNTP	Deoxyribonucleotide triphosphate
D-PBS	Dulbecco's PBS
ECM	Extracellular matrix
EDA	Extra domain A
EDB	Extra domain B
EGF	Epidermal growth factor
ELISA	Enzyme linked immunosorbent assay
EMMPRIN	Extracellular matrix metalloprotease inducer
FCS	Fetal calf serum
FGFs	Fibroblasts growth factors
Fig.	Figure
FN	Fibronectin
Foxn1	Forkhead box N1
FUD	Functional upstream domain
G418	Geneticin
H ₂ O _d	Distilled water
H ₂ O _{dd}	Double distilled water
HBEGF	Heparin-binding EGF-like growth factor
HBV	Hepatitis B virus
HPV	Human papilloma viruses
HRP	Horseradish peroxidase
i.p.	Intraperitoneal
IGF-1	Insulin-like growth factor 1
IgG	Immunoglobulin G
IgM	Immunoglobulin M
IL	Interleukin
iNOS	Induced nitrogen synthetase
JNK	Jun N-Terminal Kinase
Kd	Knockdown
kDa	Kilo Dalton

LIST OF ABBREVIATIONS

LDV	(Leu-Asp-Val)
LOX	Lysyl oxidase
MSCs	Mesenchymal stem cells
Maspin	Mammary serine protease inhibitor
MCP-1	Monocytes chemotactic protein-1
M-CSF	Macrophages colony stimulating factor
MDSC	Myeloid-derived suppressor cells
MFI	Mean fluorescence intensity
MIF	Migration inhibitory factor
min	Minute
mM	Millimoles
MMP	Matrix metalloprotease
MPI	Max Planck Institute
mRNA	Messenger RNA
MSC	Mesenchymal stem cell
NF- κ B	Nuclear factor 'kappa-light-chain-enhancer' of activated B-cells
NK	Natural Killer
ns	Not significant
oFN	Oncofetal fibronectin
OPN	Osteopontin
P53	Tumor protein
PBS	Phosphate buffered saline
PBS-T	Phosphate buffered saline-Tween
PCR	Polymerase chain reaction
PDGF	Platelet derived growth factor
PD-L1	Programmed-death-ligand
Pen / Strep	Penicillin/Streptomycin
pFN	Plasma fibronectin
qPCR	Quantitative real time PCR
RANKL	Receptor activator of NF- κ B ligand
RB1	Retinoblastoma
REDV	(Arg-Glu-Asp-Val)
RGD	Arginine-glycine-aspartic acid
RLU	Relative luminescence unit
RNA	Ribonucleic acid
RNAi	RNA interference
RT	Room temperature
s	Second
SDF-1	Stromal cell-derived factor 1
shRNA	Short hairpin RNA
siRNA	Small interfering RNA
TAMs	Tumor associated macrophages
Taq	Thermus aquaticus polymerase
TBE	Tris-boric acid EDTA
TBS	Tris buffered saline
TBS-T	Tris buffered saline-Tween
TGF	Transforming growth factor
Th	T helper cells
TNF	Tumor necrosis factor

LIST OF ABBREVIATIONS

TNF- α	Tumor necrosis factor- α
UV	Ultraviolet
VCAM-1	Vascular cell adhesion molecule 1
VEGF	Vascular endothelial growth factor
VEGFR1+	Vascular endothelial growth factor receptor 1 positive
vs.	Versus
α MEM	Advanced minimum essential medium
α -SMA	α -smooth muscle actin

1 INTRODUCTION

1.1 Cancer

Cancer is a life-threatening disease with uncontrolled growth of cells that have a potential to spread in the body. 9.6 million deaths from cancer worldwide were recorded in 2018 and more than four in ten of all cancer deaths was caused by lung, liver and gastrointestinal cancer. Moreover, 17 million new cases of cancer were reported in 2018. Therefore, developing curable therapeutics approaches is important [1].

1.1.1 Exogenous factors that promote cancer

Many exogenous factors that could be involved in cancer promotion were recognized. These factors are chronic inflammation, tobacco smoke, alcohol, radiation, stress and diet [2]. Chronic inflammation due to viral infection is responsible for 15% of cancer cases worldwide. For example, human papillomaviruses (HPVs) and hepatitis B virus (HBV) are leading contributors to the development of cervical cancer and liver cancer, respectively [3, 4]. Furthermore, tobacco is a major risk factor for cancers of the respiratory system, bladder, kidney and stomach. Its carcinogenic effect arises from its ability to enhance chronic inflammation. It acts as a tumor stimulus by inhibiting apoptosis and promoting angiogenesis. On the other hand, it leads to mutations in critical genes and disables their functionality such as *TP53* and *KARS* genes by specific chemicals such as aromatic amines, aldehydes, tobacco-specific nitrosamines and polycyclic aromatic hydrocarbons. Epidemiological data also suggest that alcohol consumption is carcinogenic. Many findings correlated the immune inhibition effects of alcohol with tumor development and metastasis [5, 6]. However, its mechanism needs to be further clarified [7]. Mutations in DNA which lead to cancer could also be caused by radiation especially ionizing radiation and ultraviolet (UV) radiation. Ionizing radiation is another cause of lung cancer and most of its sources come from the radioactive elements in nature [8]. UV radiation which comes from the sunlight is recognized as a risk factor for melanoma and other skin cancers [9]. There is also an epidemiological link between obesity and cancer incidence and the mechanism of that arises from the hormonal imbalance which affects normal metabolic pathways and especially the estrogen hormone which is known to promote cell proliferation [10]. Stress could also affect the secretion of the steroid hormone cortisol and that may contribute to the development of some forms of cancers [11]. It was reported that stress response can affect cancer progression by different mechanisms. Chronic stress results in enhancing VEGF production and increasing burden of ovarian tumors [12]. Furthermore, catecholamines production which is enhanced by stress response was implicated in an induction of *IL-6* gene transcription which displays a crucial angiogenic effect in tumor progression [12]. Clinical studies also showed that ovarian cancer patients with low social interactions exhibit higher levels of IL-6 in plasma [13]. It was also shown that stress hormones support tumor migration and invasion by enhancing the ovarian tumor cells to produce matrix metalloproteinase and this process was confirmed in several other tumors including colon cancers and head and neck cancers [14-16]

1.1.2 The genes involved in cancer development

The transformation of cancer cells from normal to malignant ones is mediated by genes which normally regulate cell growth and differentiation. That includes two main categories, the oncogenes and the tumor suppressor genes [17]

Genes that are involved in coordinating of proliferation and apoptosis are characterized as proto-oncogenes that can transform into oncogenes as a result of mutations. These include point mutations, deletions, insertions, chromosomal rearrangement leading to replication of entire chromosomes and chromosome translocation or to gene amplification. These changes result in modifications either in the amount or in the location of genes. The classical model is due to the development of an oncogene, which is a mutation of one copy of a gene leading to tumor development [18]. Another model is due to inactivation of tumor suppressor genes that normally control cell cycle progression and restrain cell growth. These genes are normally recessive, requiring mutated maternal as well as paternal copies of these tumor suppressor genes for the tumor to develop. Nevertheless, the presence of only one mutated copy increases the risk of cancer development. *P53* and *RB1*, two retinoblastoma genes are the most frequent genes inactivated in human cancers. Cancers, however, can have both, activation of oncogenes and inactivation of tumor suppressor genes together [19]

1.1.3 The hallmarks of cancer

Cancer cells can be distinguished from normal ones by several characteristics. Cell division of normal cells is tightly controlled whereas this control is lost in cancer cells. In addition, cancer cells are able to enhance their own growth. They can evade apoptosis [20], and become immortal in contrast to normal cells [21]. Angiogenesis, invasion and metastatic potential are the other properties of cancer cells that support cancer development [22].

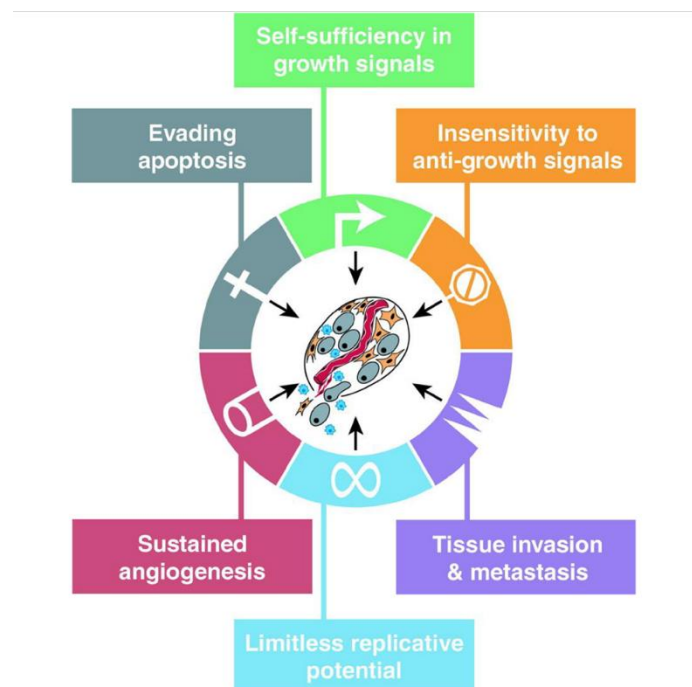


Figure 1.1.3 The hallmarks of cancer

INTRODUCTION

Special functional characteristics are required for the malignant transformation. Reproduced unmodified from [23].

1.1.4 Tumor microenvironment

The tumor microenvironment is complex. Many cell types are recruited and extracellular matrix is produced. The cells consist of immune cells, fibroblasts, and vascular cells, some of which produce the matrix. These cells as well as matrix play a critical role in tumor growth and metastasis [22].

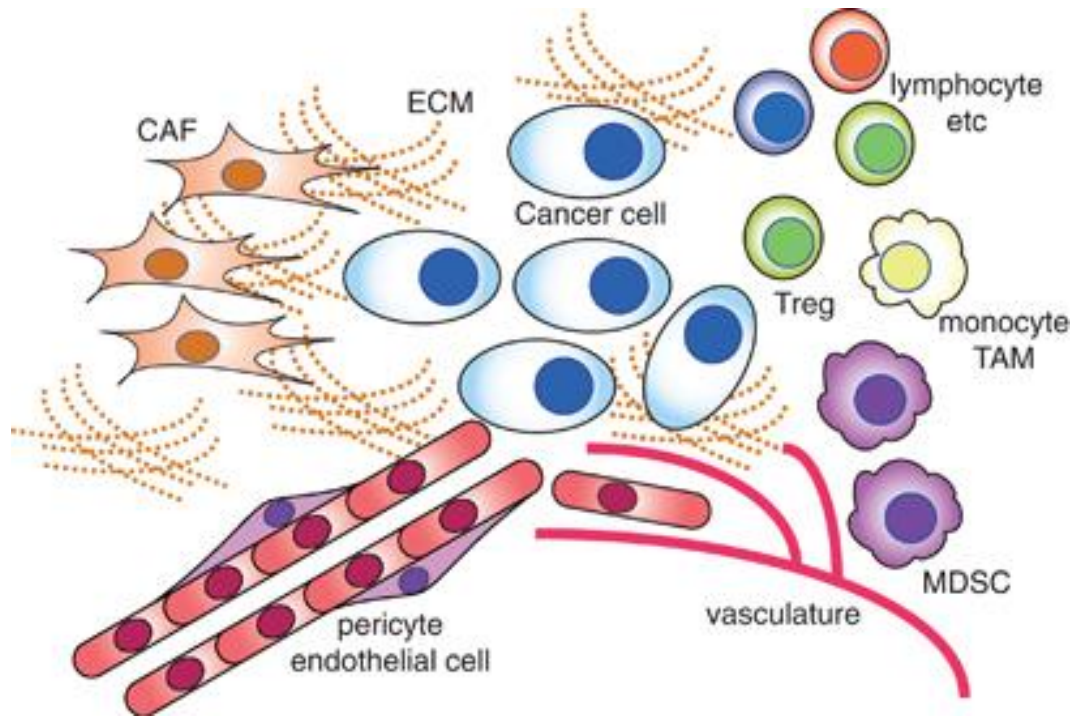


Figure 1.1.4 Tumor microenvironment.

The tumor microenvironment is a heterogeneous and complex mixture of cellular components from mesenchymal origin like cancer associated fibroblasts (CAFs) and endothelial cells. CAFs are a prominent population and can support tumor progression by different mechanisms. The tumor also includes cells from hematopoietic origin (lymphoid and myeloid cells). Tumor associated macrophages (TAMs) are an abundant cell population in tumor tissue. They can be reprogrammed according to the tumor microenvironment, therefore their role in tumor progression is tumor type-dependent and needs to be further characterized. The noncellular component is the extracellular matrix (ECM). Reproduced unmodified from [24].

1.1.4.1 Immune cells

In tissue injury, inflammatory cells are recruited to the site of injury and then leave after having fulfilled their function. This is in contrast to conditions of chronic inflammation as is the case in cancer where immune cell function is mediated and controlled by various players in the tumor environment [25].

The leukocytes including the myeloid and lymphoid cells can be detected in all solid tumors [26, 27]. The role of these cells in tumor progression depends on the tumor type and location [28]. These infiltrating immune cells supply mutagenic signals that directly enhance the proliferation of cancer cells or indirectly through interactions with other cells [29]. The main mutagenic soluble mediators produced by infiltrating immune cells

INTRODUCTION

include epidermal growth factor (EGF), tumor necrosis factor- α (TNF- α), transforming growth factor- β (TGF- β), fibroblasts growth factors (FGFs) and various interleukins and chemokines [29].

Immune cells are also involved in sustaining proliferation signals and activation of invasion and metastasis by modulating the structure and function of extracellular matrix. They achieve that by expressing various types of proteolytic enzymes like serine proteases, metalloproteases and cysteine proteases [30, 31]. These enzymes can induce angiogenic responses. They may also selectively cleave ECM molecules and adhesion molecules in order to avoid inhibitory growth signals [32, 33]. Furthermore, the immune cells as a part of stroma components play a crucial role in tumor migration and metastasis by their ability to produce matrix-metalloproteases (MMPs). For example, MMP-2 which is produced by macrophages and mast cells could activate TGF- β which in turn plays a key role in promoting the endothelial mesenchymal transition process (EMT) [34, 35]. On the other hand, it has been reported that this MMP-2 induces cleavage and alteration of specific ECM components such as laminin-5, especially the subunit Laminin-5- γ 2, the cleavage of which leads to enhancing of breast epithelial cells migration [36]. Macrophages also produce MMP-7 [35] which also in turn facilitates the invasion and metastasis by its ability to cleave macromolecules of ECM such as E-cadherin domain [37].

Hypoxia which is the prominent factor in angiogenesis increases recruitment of immune cells. These cells produce various mediators that regulate angiogenesis such as VEGF, TNF- α , TGF- β , platelet derived growth factor (PDGF), chemokines, matrix proteases enzymes and nitric oxide. These mediators then cooperate in order to induce angiogenesis [23, 38].

Macrophages in tumors are referred to as tumor associated macrophages (TAMs). In certain cancer types they represent the major component of the immune cells in the tumor microenvironment. In breast cancer for example they encompass 80% of the immune cell population [39]. The source of these cells is either the monocytes in the circulation which are recruited into tumors by chemotactic cytokines produced by tumors like monocytes chemotactic protein-1 (MCP-1), macrophages colony stimulating factor (M-CSF) and vascular endothelial growth factor (VEGF), or the macrophages can also proliferate locally in the tumor itself [40].

Macrophages have a pleiotropic role in tumor progression. They can exhibit pro- and anti-inflammatory functions depending on the signals that they get [41]. Thus, there are two types: M1 and M2 macrophages. M1 macrophages produce pro-inflammatory cytokines like TNF- α , IL1 and IL6, while M2 macrophages secrete mainly anti-inflammatory cytokines like IL10 and TGF- β that support tissue remodeling and angiogenesis. This anti-inflammatory M2 phenotype seems to be the dominant one in tumors [40, 42]. These M2 cells produce VEGF-A which is the main factor for promoting of angiogenesis by their capacity to produce MMP-9 that in turn increases the bioavailability of VEGF-A in the tumor environment [43].

The immune cells also provide the tumor environment with pro-invasive factors such as extracellular matrix metalloprotease inducer (CD147) and migration inhibitory factor (MIF). These factors are produced in response to TNF- α and activation of JNK signalling. The presence of these factors in tumor microenvironment results in secretion of MMP-2 and MMP-9 [44]. Immune cells of the macrophage type are

implicated in evading the immune-mediated destruction of cancer cells by their involvement in the blocking of cytotoxic T lymphocyte (CTL) activity in the tumor by different mechanisms [45]. It has been reported that this suppression is partially mediated by inducible nitric oxide synthase (iNOS) or arginase I which metabolizes L-arginin and leads to the production of reactive oxygen species (ROS) which themselves have an immune suppressive behavior during tumor progression [45, 46]. Furthermore, TAMs provide the tumor microenvironment with a variety of chemotactic factors which also lead to the suppression of T cells and all T-regulatory (*Treg*) cell factors [45]. Another mechanism by which TAMs are implicated in suppression of CTLs is by upregulation of the checkpoint inhibitor called programmed cell death protein 1 ligand (PDL-1) through IL10 production [45, 47].

Previous findings illustrated the role of the TNF- α related cytokine called receptor activator of NF- κ B ligand (RANKL) that is produced by T cells and macrophages infiltrating prostate cancer. RANKL inhibits the expression of *maspin* gene which is a tumor suppressor gene that affects the expression of integrin adhesion molecules diminishing cell motility and invasion [48]. It has been reported that maspin could alter the integrin expression profile of invasive human breast cancer cells and inhibit their invasive capabilities. *Maspin* can induce an upregulation of α 5 and α 3 integrins and as a result increasing the ability of human breast cancer cells to be more adherent and less invasive [49]. This mechanism highlights the paracrine support of the tumor microenvironment in metastasis progression [50].

Myeloid-derived suppressor cells (MDSCs) are defined as immature myeloid cells not detected in healthy conditions. They are associated with chronic inflammation and play a role in tumor progression and drug resistance mainly due to their capacity to suppress T cells. Two main phenotypes of MDSCs were described in tumor-bearing mice. These are the monocytic MDSCs (M-MDSCs) and the granulocytic MDSCs (G-MDSCs). M-MDSCs are characterized by CD11b⁺ LY6G⁻ and LY6C^{high} expression and experimental findings confirm their ability to differentiate into macrophages and dendritic cells [51, 52]. Their immune-suppressive activity is mediated by production of immune-suppressive cytokines and up-regulation of arginase-1 and inducible nitric oxide synthase (iNOS) [53]. G-MDSCs are defined by CD11b⁺ LY6G^{high} and LY6C⁻ expression. The immune-suppressive mechanism of G-MDSCs is different from M-MDSCs and needs contact with T cells for a prolonged period of time [54]. G-MDSCs were described to have immunosuppressive characteristics on CD8⁺ T cells by different mechanisms. Some studies had already shown that the immunosuppressive function is mediated by ROS-dependent mechanism although they expressed high levels of arginase-1 [55]. On the other hand, it has been reported that their inhibitory functions do not need the presentation of MHC-class I molecules [56]. Finally, Interferon- γ (IFN- γ) was also described to be implicated in the suppression of these cells [56]. Whereas M-MDSCs were reported to induce CD8⁺ Tcell suppression by a nitric-oxide- (NO)-mediated mechanism and partially by IFN- γ /STAT1 dependent mechanism [57]. Other T cells play a crucial regulating role in tumor microenvironment too. The presence of CD4⁺ T helper and CD8⁺ cytotoxic lymphocytes (CTLs) predicts a better prognosis [58]. Th1 cells, which are characterized by having anti-tumor effect by producing IFN- γ , TNF- α and IL2. IFN- γ enhances the expression of PD-L1 [59] which in turn inhibits the immune system. IL17 produced by Th17 cells also supports the activity of IFN- γ produced by Th1 in inducing secretion of CXCL9 and CXCL10, two T cell chemoattractants [60]. Furthermore, long-term contact of T cells in tumor microenvironment with tumor cells leads to the development of exhausted T cells with limited anti-tumor effect [61]. T-regulatory cells (*Tregs*) are a subset of CD4⁺ T cells

that inhibit cytotoxic anti-tumor effects of cytotoxic T cells (CTLs) and natural killer (NK) cells, thus exerting immune-suppressive activity [62, 63], either directly or by secreting cytokines such as IL10 and TGF- β [64, 65]. Another subset of T cells are the Th2 cells that produce cytokines like IL4, IL5 and IL13 and inhibit T cells that mediate cytotoxicity of tumor cells [66-68].

B cells can also affect tumor by regulating blood coagulation and enhancing complement activation [69, 70]. They may exert an anti-tumor effect by presenting tumor antigens to CTLs. but can also exert a pro-tumor effect by producing cytokines such as IL10, activation of Treg cells and suppressing Th1 cells [71, 72]

1.1.4.2 Cancer-associated fibroblasts

Cancer-associated fibroblasts (CAFs) are part of tumor stroma. They include at least two main sub-populations: fibroblasts that provide structural support of tissues and myofibroblasts. Myofibroblasts are found in chronic inflammation and also express α -smooth muscle actin (α -SMA) [73]. They are heterogeneous since they may originate from various precursors such as fibroblasts, endothelial cells, epithelial cells and mesenchymal stem cells [74, 75]. CAFs are an important contributor to tumor proliferation, invasion and metastasis [76].

Because of the heterogeneous origin of CAFs they may support cancer cells to evade growth suppressors [38]. They produce proteases which in turn damage tissue structure that normally suppresses growth. They produce survival factors such as insulin-like growth factor 1 (IGF-1) and insulin-like growth factor 2 (IGF-2) [77, 78]. Moreover, they are implicated in ECM formation and secretion of remodeling enzymes like MMPs, which in turn facilitate metastasis [31]. For example, CAFs, in response to TNF- α and TGF- β in tumor, secrete MMP-9 that degrades the main constituents of basement membrane which are type IV collagen and laminin [79, 80].

CAFs play an important role in angiogenesis by producing VEGF, FGFs, and PDGF and storing them in the matrix [81]. By releasing ECM-degrading enzymes they enrich the tumor environment with these factors [77, 82]. CAFs also secrete CXCL12 that recruits endothelial precursors [74]. In addition, they contribute to recruitment of proangiogenic immune cells [83, 84]. TGF- β produced by CAFs inhibits cytotoxic T cells (CTLs) and NKT cells further enhancing tumor growth [85, 86].

Lastly, CAFs reprogram cell metabolism by producing metabolites such as lactate and pyruvate via anaerobic glycolytic pathway. Thus, they work as an energy supplier for cancer cells [87-90].

1.1.4.3 Pericytes

Pericytes are the perivascular fibroblastic-like cells. They are involved in various steps of cancer development [91]. By secreting a variety of growth factors, pericytes can stimulate the proliferation of endothelial cells and thus enhance angiogenesis. On the other hand, they induce endothelial cells migration and extracellular matrix modulation by proteases secretion [92-94]. Several studies have shown the ability of pericytes to differentiate into different cell types such as adipocytes, chondrocytes, smooth muscle cells and fibroblasts [95]. Pericytes have also properties that they share with mesenchymal stem cells (MSCs) including partial similarity in surface markers and the ability to migrate in response to chemotaxis [96].

1.1.4.4 Extracellular matrix (ECM)

The non-cellular component of tumor microenvironment is the extracellular matrix composed of macromolecules including proteins such as fibronectin and collagen, glycoproteins and polysaccharides that form a three-dimensional network of a high degree of complexity [97]. The main functions of the ECM are in allowing cell adhesion, promoting differentiation and mediating cell-cell communications [98]. In cancer microenvironment, ECM architecture is deregulated and these changes lead to alteration in its biological and physical characteristics and functions [99]

1.1.5 The metastasis

Cancer mortality is related to metastasis in 90% of the cases [100]. It is a complex process involving several steps and includes invasion, intravasation, migration, extravasation, and proliferation of cancer cells in the secondary site of the cancer growth called metastatic site [101]. It needs a coordinated cross-talk among these various steps to avoid cancer cell loss at any of the steps [102]

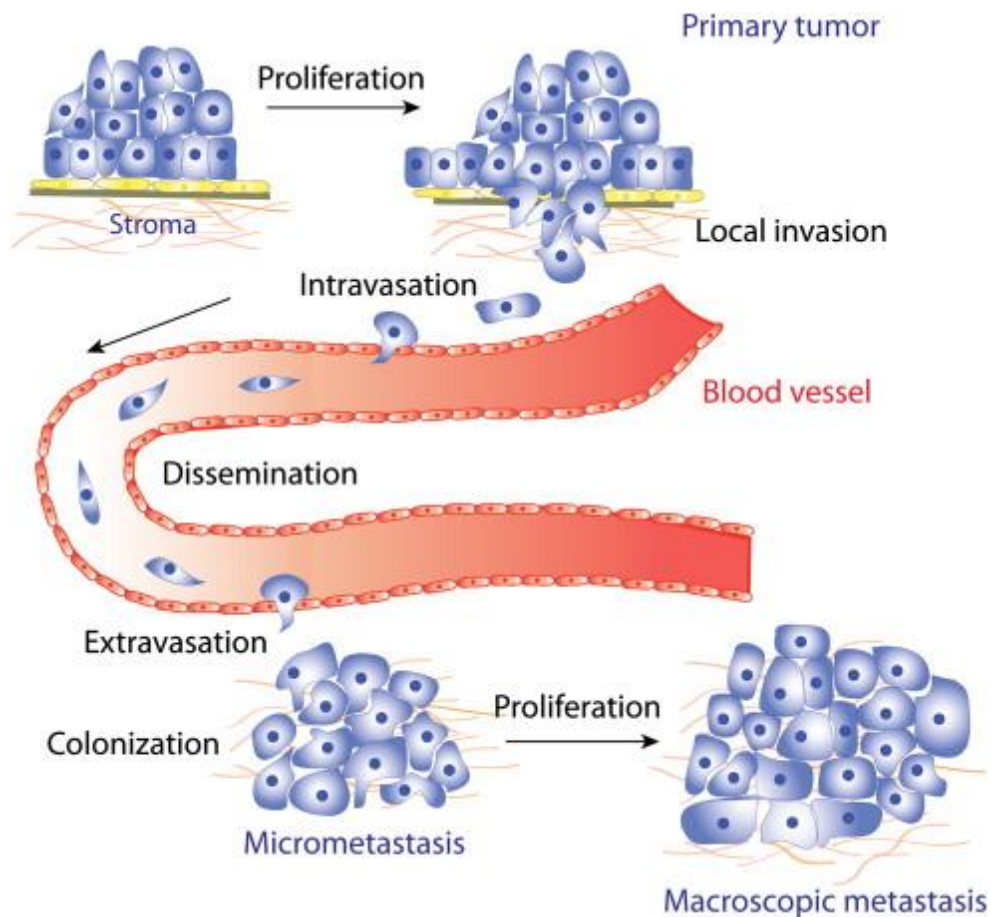


Figure 1.1.5. Schematic presentation of metastatic cascade.

The complex metastasis process starts with dissemination of cancer cells from the primary sites (local invasion and intravasation), transmission and survival in the circulation followed by arrest at the secondary site (extravasation). After adapting to the new environment (micrometastasis formation), tumor cells start proliferation. Reproduced unmodified from [103].

1.1.5.1 The epithelial-to-mesenchymal transition (EMT)

EMT is a program that takes place during embryonic development and in pathological conditions such as wound healing, tissue regeneration, fibrosis and cancer [104]. In tumors, EMT can be induced by hypoxia, TGF- β , FGF and EGF. This leads to loss of markers of epithelial cells (E-cadherin and cytokeratin-18) and expression of mesenchymal markers (α -SMA and vimentin). The process may be incompletely leading only to cells with different expression level of E-cadherin [105].

EMT is characterized by expression of transcription factors like Twist and Snail. Twist and Snail as transcription factors act as molecular switching keys of the EMT program. Their upregulation is required in metastatic carcinomas [106, 107]. It leads to downregulation of E-cadherin and upregulation of N-cadherin. This results in changes in cell-cell adhesion, cell-matrix adhesion and the cytoskeleton [108, 109]. It was also shown that Snail-induced EMT can facilitate tumor metastasis by inducing immune suppression [110].

1.1.5.2 Invasion

Invasion and migration are fundamental to metastasis formation. Cancer cells may locally invade either as a coherent multicellular unit via a process named collective invasion or as individual tumor cells [111]. The movement of individual cancer cells through the ECM can proceed through mesenchymal or amoeboid cell migration [112]. The mesenchymal mechanism is used by normal cells like smooth muscle cells, endothelial cells and fibroblasts and it is protease-dependent [113]. These proteases such as MMPs degrade ECM allowing the cells to induce a breach in the basement membrane that organizes epithelial cells. The matrix provides signals through integrin-mediated cell-matrix adhesions, and upregulation of MMP production is needed for invasion [114]. Cancer cells produce directly MMPs or stimulate the stromal cells to produce them [115]. The amoeboid cell migration is a protease-independent mechanism requiring mechanical forces and is faster than mesenchymal migration [112, 116]. It leads to loss of ECM attachment and cell polarity [101, 117]. Tumor cells reorganize their cytoskeleton by changing cell-cell and cell-matrix adhesion which increases their ability to migrate. For example, modulation of collagen crosslinking through changing of integrin signalling leads to alteration of ECM rigidity and breast cancer progression [118].

1.1.5.3 Intravasation

Intravasation refers to the entry of cancer cells into the lumen of lymphatic and blood vessels [119]. TGF β supports both the invasion generally and penetration of blood vessels walls by mammary cancer cells [120]. Tumor associated microvasculature has weak interactions between the adjacent endothelial cells and often lacks pericyte coverage leading to an unstable structure and facilitating intravasation [121]. Cyclooxygenase-2 (COX-2), MMP-1 and MMP-2 were reported to stimulate neoangiogenesis and hence support the intravasation of breast cancer cells [122]

1.1.5.4 Survival of metastatic cells in the circulation

In the circulation cancer cells represent “metastatic intermediates” [123]. Once in the circulation cancer cells and platelets form micro-aggregates [102]. These allow the cancer cells to overcome the stress of loss of matrix attachment mediated by integrin

which is normally necessary for survival. It also protects them from immune cell action and the mechanical shear stress of blood flow. This process is mediated by fibronectin in the circulation as well as expression of L and P-selectins by cancer cells [124-127]

1.1.5.5 Extravasation

Extravasation requires adhesion and trans-endothelial migration. The paracellular migration is the dominant mechanism of extravasation. This requires disruption of endothelial cell junctions. Tumor cells can enhance this process by secretion of specific factors or expression of particular receptors. For example, it has been reported that the extravasation of breast cancer cells was initiated by the expression of the EGF-receptor ligands such as heparin-binding EGF-like growth factor (HBEGF), the enzyme COX2, which mediates prostaglandin synthesis and the metalloproteinase MMP1 and MMP2 that induce the matrix remodeling. Extravasation of melanoma is augmented by osteonectin secretion and remodeling of endothelial junctions via binding to vascular cell adhesion molecule 1 (VCAM-1). The induction of programmed necrosis in endothelial cells is another mechanism used by tumor. The recruitment of the myeloid cells and platelets to the surrounding of tumor cells after their arrest to the vascular bed not only supports their survival in the circulation but also can promote the extravasation [128].

1.1.5.6 Micrometastasis formation (premetastatic niche)

Forming a micrometastasis requires the survival of the tumor in a distant tissue. The new microenvironment is different from the primary tumor site. The premetastatic niche model was suggested to clarify how cancer adapt to the new site. Data suggest that the primary tumor by releasing systemic signals can change the composition of this niche. Lysyl oxidase (LOX) from the primary tumor leads to fibronectin production in the future niche. The receptor $\alpha 4\beta 1$ on the hematopoietic progenitor cells can mediate their localization to the hematopoietic niche. This integrin can also bind to the vascular cell adhesion molecule-1 (VCAM-1 or CD106) which is expressed on stromal and endothelial cells. Various cells are implicated in releasing a various of chemoattractant factors from the ECM like stromal cell-derived factor 1 (SDF-1) + by their ability to secrete MMP9 [129]. These activities lead to the homing of the cancer cells to the future metastatic site.

1.1.5.7 Metastatic colonization

The cancer cells that reaches the secondary site depends on the stromal components of the new environment [102]. The concept of the “seed-and-soil” observed by Stephen Paget suggests that certain cancer cells prefer metastatic sites that are more suitable for their survival and proliferation [130]. Melanoma cells failed to metastasize to subcutaneous grafts of renal tissues, whereas they metastasize successfully to the subcutaneous grafts of lung tissues [131]. Specific genes facilitate metastasis of breast cancer to either liver [132], lung [133], bone [134] or brain [124]. Various osteolytic cytokines, such as TGF- β modify the crosstalk between osteoclasts and osteoblasts and enhances bone metastasis [134]. Since bone marrow-derived cells recruitment to the metastatic site is required for metastasis, systemic molecules released from cancer such as osteopontin (OPN) and SDF-1 are also important [135, 136]. Angiogenesis is also needed [137, 138], and is stimulated by lack of oxygen (hypoxia) and VEGF production [139].

1.2 Fibronectin

Fibronectin (FN) is a dimer of 500 kDa glycoprotein that is found in the ECM and in various body fluids. FN is either found *in vivo* in its soluble form (produced by hepatocytes) or in an insoluble form (cellular), that is incorporated in the matrix around or on the cells such as fibroblasts, epithelial cells, endothelial cells, and osteoblasts [140, 141].

Its two monomer chains are linked to each other at their C-terminal by disulfide bridges. It consists of three types of modules: type I, II, and III, which are included in each monomer and are responsible for the functional properties of fibronectin. Type I and type II modules contain disulfide bonds whereas type III modules do not [142, 143]. The 12 type I modules at the N (amino) and C (carboxyl) terminal can be involved in the binding of fibrin and collagen. Type II modules are also involved in the binding of collagen. Type III modules include RGD sequence that is composed of 3 amino acids (arginine, glycine and aspartic acid) and is involved in binding to cell surface receptors in addition to other binding sites for integrins and heparin [144].

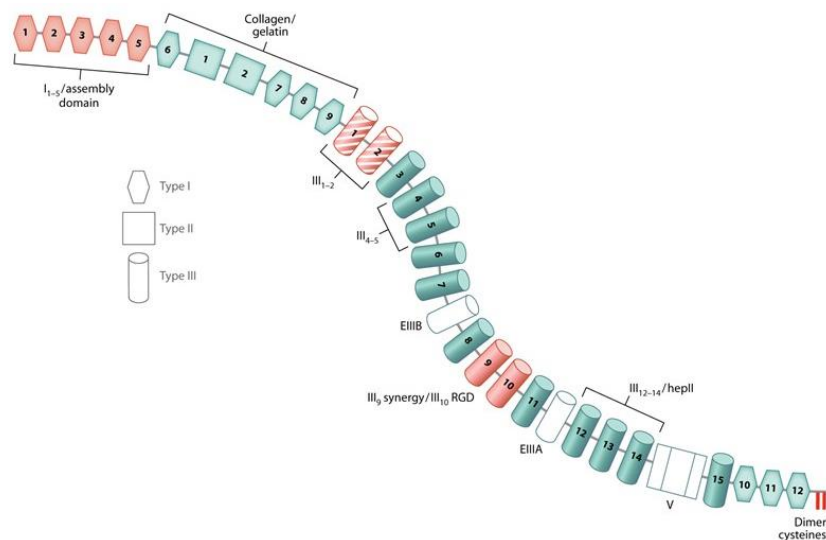


Figure 1.2. Schematic representation of plasma fibronectin structure [145]

The two monomers of fibronectin are linked to each other at the C-terminal by disulfide bridges. Each monomer is composed of repeating units of three different modules (type I (hexagons), type II (quadrants) and type III (cylinders)). The functional domains of fibronectin are characterized by the corresponding binding patterns. Reproduced unmodified from [145].

Assembly of fibronectin means that the protein gets extended and that happens when it binds to the receptors on the cell surface. Two main methods were characterized for initiation of assembly. The first one requires the interaction of cell surface integrins with the integrin-binding motif in ¹⁰FNIII (RGD) [146]. Another mechanism proposed the interaction between the N-terminal 70-kDa domain of fibronectin including N-⁹FNI with the cell surface [147, 148]. It has been reported that the kinetics of binding of N-⁹FNI to the cell surface is similar to that of fibronectin [149]. Therefore, N-⁹FNI has been described as a negative inhibitor of fibronectin assembly [150]. The bacterial peptide pUR4 that binds to a 70-kDa domain of fibronectin which comprises the N-⁹FNI can inhibit FN assembly [151]. However, the N-⁵FNI is also important for assembly and the deletion of one FNI module in the N-⁵FNI abolishes the binding of N-⁹FNI to the cell

surface [152], therefore it seems that FN binds to collagen through several FNI modules. However, the binding sites in N-⁹FNI including NGF and IGD motifs [153, 154] are not necessary for its binding to the region of assembly on the cell surface [155].

1.2.1 Fibronectin isoforms

Fibronectin is encoded by a single gene and produced by several mammalian cell types, however it exists in several isoforms due to the alternative splicing patterns in the IIIICS region, the presence or absence of the extra-domains A (EDA) or B (EDB) of the single fibronectin primary transcript as well as post translational modifications [156]. The IIIICS region, which is modified by alternative splicing, is in a non-homologous segment and is referred to as a variable region or IIIICS (type-III connecting segment). This domain is structurally complex and is composed of 5 sequences of amino acids. Within the main area of type III repeats, exclusion or inclusion of the fibronectin type III EDA and EDB domains [157-159] lead to the formation of several isoforms [160, 161]. This alternative splicing of the fibronectin pre-mRNA is developmentally regulated and is also dependent on the cell type [162, 163]. Therefore, these isoforms differ in solubility, cell adhesion, and binding properties [164, 165]. Taking into account the variants that result from posttranscriptional modifications of the EDA and EDB modules, 20 different fibronectin monomers can be generated in humans [144].

1.2.1.1 EDA fibronectin

EDA isoform is the result of alternative splicing of precursor mRNA at the region between ¹¹FNIII and ¹²FNIII which represents the complete 90 amino acid domain EDA or EIIIA domain [144, 166]. The EDA domain is >90% similar in mouse and human [167]. It is involved in critical functions including cell adhesion [168], mitogenesis and cell cycle progression [169], wound healing [170] and differentiation of myofibroblasts [171]. EDA is highly expressed during embryonic development but its presence in normal tissues in adulthood is restricted. However, it is produced during wound healing, atherosclerosis [172], pulmonary and liver fibrosis [173, 174] and in stroma of various cancer types [175]. EDA fibronectin is detected in normal vasculature [176, 177]. In line with the requirement for fibronectin for angiogenesis and angiogenesis for tumor growth [178], EDA fibronectin was expressed in 50% of invasive ductal breast cancer in humans [179]. Moreover, fibronectin EDA was shown to mediate epithelial-mesenchymal transition in lung and colorectal carcinomas [180, 181]. EDA fibronectin was also highly expressed in primary and metastatic melanoma lesion sections [182]. All of these functions induced by EDA FN might be caused by increasing its binding affinity to the integrin $\alpha 5\beta 1$ [183], or due to its ability to bind to $\alpha 4\beta 1$, $\alpha 4\beta 7$, or $\alpha 9\beta 1$ integrin [184].

1.2.1.2 EDB fibronectin

The EDB isoform is the result of an alternative splicing of precursor mRNA at the region between ⁷FNIII and ⁸FNIII which represents the complete 91 amino acid domain EDB or EIIIB domain [144, 166]. EDB domain is almost analogous in humans and mouse [165, 185, 186]. However, EDA and EDB isoforms show low similarity within species (28% in humans) suggesting that they have distinct functions [166]. The presence of the EDB domain induces activation of vascular endothelial growth factor expression and endothelial proliferation [187]. It is sometimes named oncofetal variant due to its high expression during development leading to some confusion with the isoform

containing O-glycosylations [188, 189]. However, many studies demonstrated that the EDB exon is more excluded in adults than the EDA exon [190, 191]. Its absence from the mature blood vessels but presence in newly formed blood vessels led to its use as a marker for angiogenesis [192].

Deletion of the exons coding EDA and EDB in mice resulted in cardiovascular defects because of the importance of EDA and EDB variants in stabilization of blood vessels and in angiogenesis [193]. EDB was found in the vessels of breast carcinoma [179] and stroma of human colorectal cancers [194]. Furthermore, high expression in the blood vessels in Hodgkin and non-Hodgkin lymphoma was associated with more malignant forms [195]. In melanoma metastatic lesions, EDB was also highly expressed especially in comparison to the primary malignant melanoma [182].

1.2.1.3 The variable region

It is formed by a total of 120 amino acids and located between ¹⁴FNIII and ¹⁵FNIII [174]. Depending on alternative slicing, it can consist of a variety of chains including up to five sequences. Its presence is needed for its secretion, except in chondrocytes. The plasma fibronectin includes at least one variable region and it was reported that synthesized fibronectin lacking the variable region degraded, whereas it is often found in both chains of cellular fibronectin. Therefore, it might be required for the formation and stability of dimer fibronectin [196, 197].

1.2.2 Fibronectin interactions and physiological functions

FN mediates various vital processes including cell differentiation, proliferation, adhesion and migration. FN and other components of extracellular matrix are crucial factors for embryogenesis [198]. It has been shown that FN is required for blood vessel formation, and in its absence leads to failure of vascular angiogenesis in mice and to early embryonic lethality [199]. It exerts its functions through binding to members of integrin receptors family [200].

Numerous integrin recognition sequences have already been characterized and 11 integrin pairs are able to bind to fibronectin [144, 201]. Integrins are cell surface proteins consisting of heterodimers of an α and a β subunit. They mediate cell-cell and cell-matrix interactions [201]. The main sequence that mediates the cell adhesion functions of fibronectin is RGD sequence that is located in ¹⁰FNIII domain and composed of three amino acids (Arg-Gly-Asp). It is also found in other cell adhesion proteins such as vitronectin and laminin [202, 203]. This motif binds to integrin $\alpha 5\beta 1$ and $\alpha v\beta 3$ as well as others such as $\alpha v\beta 1$, $\alpha 8\beta 1$ and $\alpha 9\beta 1$ [184]. The presence of the synergy sequence (PHSRN sequence) that is located in the ⁹FNIII repeats and composed of five amino acids (Pro-His-Ser-Arg-Asp) is required for the binding of RGD to $\alpha 5\beta 1$ [204]. The LDV sequence (Leu-Asp-Val) and REDV (Arg-Glu-Asp-Val) which are found in the variable region of fibronectin are other cell recognition sequences that interact with $\alpha 4\beta 1$ and $\alpha 4\beta 7$ [144, 205]. The EDA domain also includes binding sites for $\alpha 4\beta 1$, $\alpha 4\beta 7$ and $\alpha 9\beta 1$ integrins [206]. Fibronectin can also interact with heparan sulfate proteoglycans located on syndecans by its two main heparin binding domains. The stronger one is located at the C terminus and another one in the N terminus of fibronectin. Syndecans modify the cell response to fibronectin [207]. It has been shown that the connection between $\alpha 5\beta 1$ integrin and syndecan-4 is required for the focal adhesion which occurs during the cell adhesion on fibronectin. Furthermore, integrin-

syndecan interactions might be involved in cell adhesion to both laminin and vitronectin [208].

Two major fibrin-binding sites (Fibrin I and Fibrin II) were also detected in fibronectin and the most important one is found at the N terminus and is formed of ⁴FNI and ⁵FNI. Fibronectin interactions with fibrins affect cell adhesion and migration [209]. Collagen binding sites are found in the FNI and FNII repeats of fibronectin. Collagen is an important component of ECM. Collagen fibers mediate various physiological functions during embryonic development and modify cellular differentiation. It has been reported that the deposition of fibronectin into the matrix is required for the formation of a collagen matrix [209, 210]. The collagen binding site in fibronectin includes four FNI and two FNII modules which are (⁶FNI, ¹⁻²FNII and ⁷⁻⁹FNI) and it is called gelatin-binding domain (GBD). Using antibodies targeting this region leads to an inhibition of collagen deposition in fibroblasts *in vitro* [211]. Binding studies showed that ⁸⁻⁹FNI fragments bind preferably to collagen but the role of other regions in the gelatin-binding domain GBD is not clear. Furthermore, it was reported that collagen chains are also implicated in this interaction through specific binding repeats which have high affinity to ⁷⁻⁹FNI [212]. The mechanism of this interaction requires a sequence containing GESGE which is found in pUR4. This motif can bind with high affinity to ⁷⁻⁹FNI fragment of fibronectin suggesting that this repeat mimics collagen binding sites that were found in other bacterial matrix peptides [213]. Fibronectin is involved in many physiological activities such as wound healing. In healthy organisms, the inactive form of integrin on the hematopoietic cells in the circulation prevents fibril formation. However, when vascular injury develops, the platelets in the bloodstream aggregate and α IIb β 3 integrin is activated, and fibronectin fibrils are formed. Fibronectin in the clot acts as chemoattractant for many cells that are also required for wound healing such as leukocytes, fibroblasts, and endothelial cells [214, 215]. Furthermore, fibronectin plays a critical role in stabilization of clot by its covalent binding with fibrin that is mediated by the blood coagulation factor XIIIa and also by its cross-linking with collagen fibers which support platelets aggregation. It was also reported that fibronectin acts as an opsonin for phagocytosis to allow the removal of the debris and dead cells during tissue injury [214].

1.2.3 Role of fibronectin in cancer

The participation of fibronectin in different stages of tumorigenesis by different mechanisms has already been confirmed in numerous studies. The high expression of total fibronectin and the extra domain (EDA) were associated with the upregulation of α 5 β 1 integrin in malignant breast cancer lines [216]. Furthermore, the interaction between fibronectin and α 5 β 1 integrin mediates downstream signaling of PI3-K/Akt which in turn down-regulates the tumor suppressor gene *p53* and as a consequence enables the cancer cells to evade apoptosis which is one of defining feature of cancer [217]. Upregulated EDA in colorectal tumors and its interaction with its receptor α 9 β 1, which in turn was highly expressed in CD133⁺CD44⁺ cells that are believed to initiate colon cancer, was required for tumor proliferation [218]. An immunosuppressive role of fibronectin has also been observed, since silencing of fibronectin by siRNA resulted in slowing of glioma growth in mice and that was in part explained by reduction of T-regulatory cells (*Tregs*) which inhibit T helper cell action against cancer [219]. Importantly, EDA fibronectin activates the myeloid derived suppressor cells population that weaken the immune response against cancer confirming its pro-tumor effect [220]. The fibronectin isoforms EDA and EDB are also regulators of tumor growth by upregulating the pro-angiogenic VEGF [177, 187, 221]. Fibronectin also facilitates the

invasion of cancer cells by changing ECM stability [109] and by inducing the expression and secretion of certain matrix metalloproteases that dissolve the matrix surrounding the tumor cells and enable their entry into the vascular system [115, 222]. As cancer cell survival during circulation is also crucial for development of metastases, it has also been demonstrated that the fibronectin helps the tumor cells to bind to platelets protecting them from the immune system [223, 224].

1.2.4 Fibronectin as a therapeutic target in cancer

Based on the crucial role of fibronectin in all stages of tumor progression, many potential fibronectin-dependent therapeutic approaches can be envisioned to treat cancer.

Fibronectin can be targeted directly by inhibition of its production and that could be curable. Alternatively, one could try to prevent its accumulation such as by using pUR4. pUR4 is a bacterial peptide derived from F1 adhesion molecule of *streptococcus pyrogens* that inhibits FN polymerization by binding with high affinity to the N-terminal 70-kDa part of FN. Its mechanism as a FN polymerization inhibitor *in vitro* was confirmed [151]. Furthermore, its administration in mice in which a partial ligation of the external and internal carotid arteries was performed diminished fibronectin and collagen accumulation and thus reduced the narrowing of the vessels [225]. The involvement of this peptide in the inhibition of other matrix proteins accumulation such as collagen I and tenascin-C was also elucidated in co-culture of breast cancer cells and fibroblasts *in vitro* [226]. The importance of FN in angiogenesis was shown in an *in vivo* model of breast and prostate cancer, where fibronectin was deleted in the circulation [127, 226].

Targeting of fibronectin expression in the tumor could be another strategy for cancer therapy and that was investigated by RNA interference which led to silencing of fibronectin gene expression [219, 227]. Cell penetrating peptides (cpp) are peptides derived from viral proteins with some modifications consist of (10-30) amino acids and were used to deliver fibronectin siRNA *in vitro* [228]. Because of its ability to penetrate tumor cell membrane, they were used as a delivery vector for fibronectin siRNA to the tumor [229] and also for trans-vascular delivery of siRNA. Using these approaches, they were shown to be an optimistic, non-invasive and safe therapeutic molecules that can pass across the blood brain barrier [230].

Vaccinia viruses were also reported as a strategy for fibronectin targeting in malignant ovarian cancer and fibronectin of fibroblast in the tumor stroma [231] depending on an engineered established form that has an oncolytic effect. They were used for targeting fibroblasts in ovarian tumor stroma and they were able to infect them [232].

Based on the presented evidence, targeting of FN synthesis or accumulation might offer a good alternative to chemotherapy and inhibit angiogenesis and cancer growth. Once a good possibility has been established, one challenge is the delivery system which should specifically deliver the agent to the tumor site [233].

1.3 The goal of the work

Fibronectin is an extracellular matrix protein that is expressed in almost all types of cancers and plays a crucial role in tumor growth promotion, survival and resistance to therapy. We have shown that deleting fibronectin genetically in mice leads to smaller bone metastasis. Furthermore, higher fibronectin expression in breast and prostate cancer lesions shortens survival in affected patients. Under special circumstances fibronectin suppresses the ability of myeloid cells to fight cancer *in vivo* in mice. In a model of liver fibrosis, we had successfully used a peptide that prevents fibronectin fibril formation and hence matrix accumulation. We hypothesized that pharmacologically decreasing fibronectin accumulation in cancer will not only slow down cancer progression by suppressing angiogenesis but may additionally diminish cancer size by stimulating the immune response. Therefore, the main goal of my work is an investigation of fibronectin matrix manipulation as a therapeutic approach in cancer.

2 MATERIAL AND METHODS

2.1 Materials

2.1.1 Instruments

Instrument	Producer
Autoclave	System GmbH, Wettenberg, GE
Camera EOS 350 Digital	Canon Inc., Tokyo, Japan
CASY cell counter	Roche, Mannheim, GE
Centrifuge	Type 1-14, Sigma Labor centrifuge, Biofuge 15, Heraeus Multifuge 1 S-R, Thermo Fisher Scientific Light Cycler 2.0 sample carousel (20µl), Roche SORVALL® RC-5B PLUS Superspeed Centrifuge, Thermo Fisher Scientific Cryostat CM 3050, Leica
Cryomikrotom	Type CP1000, Agfa
Developing instrument	Lab instruments Deutschland GmbH, Crailsheim, GE
ELISA Reader	LSRII, BD Bioscience
Flow cytometry	Privileg, Stuttgart, GE
Freezer -20°C	New Brunswick Scientific, Edison NJ, USA
Freezer -80°C	#3043317, Nunc, Thermo Fisher Scientific
Freezing box	Peqlab Biotechnologie GmbH, Erlangen, DE
Gel system	Bio-Rad Laboratories GmbH, Düsseldorf, GE
Gel documentation	Eppendorf, Hamburg
Heating block	Eppendorf, Hamburg, GE
Thermomixer compact	New Brunswick Scientific, Edison NJ, USA
Incubator	Thermo Fisher Scientific Inc, Waltham MA, USA
Laminar flow cabinet	Light cyclor 2.0 instrument, Roche
Light cyclor	Messer Group GmbH, Sulzbach, GE
Liquid nitrogen tank	Yellow line MSH basic, Carl Roth
Magnet	ASYS Hitech GmbH, Eugendorf, Austria
Micro-plate washer	Leica Microsystems, Wetzlar, GE
Microscope	Microscope DM IL, inverse routine microscope, Leica Vanox-S, Olympus, with sony camera (CCD) Biozero (BZ-8100), Keyence ECLIPSE Ti-E, Nikon
Microscope	LG Electronics, Seoul, Korea
Microwaves	Knick GmbH + Co. KG, Balingen, DE
pH meter	IBS Integra Biosciences, Fernwald GE
Pipet comfort classic	Anthos fluidoType 24200, ASYS
Plate washer	Pharmacia LKB Pump P1, GE Healthcare Econo, Bio-Rad
Pump	CanoScanLiDE 60, Canon
Scanner	New Brunswick Scientific, Edison NJ, USA
Shaking incubator	Biometra, Göttingen, GE
Thermo cyclor	

MATERIAL AND METHODS

UV spectrophotometer	Eppendorf, Hamburg, GE
Vortex	Bender and Hobein AG, Zürich, Switzerland
Scale	Kern and Sohn, Balingen, GE

2.1.2 Companies

Company	Place
Abbott GmbH & Co.	KG Wiesbaden
Abcam plc	Cambridge, UK
Acris Antibodies GmbH	Hiddenhausen
Adipogen AG	Liestal, Schweiz
Agfa Healthcare GmbH	Köln
A.Hatenstein GmbH	Würzburg
Alcan Packaging Neenah	Wiscosin
Amersham	Freiburg
Applichem GmbH	Darmstadt
ASYS Hitech GmbH	Eugendorf, Austria
Axxora Deutschland GmbH	Lörrach
Bachem AG	Budendorf, Switzerland
Bayer AG	Leverkusen
BD Biosciences	Heidelberg
Biocat	Heidelberg
Bender &Hobein AG	Zurich, Switzerland
Biologend Europe BV	Uithoorn, Nederland
Biomers	Ulm
Bio-Rad Laboratories GmbH	München
Biotechne (R&D, Tocris)	Wiesbaden-Nordenstadt
Biozym Scientific GmbH	Oldendorf
Braun	Tuttlingen
Cliper Life Sciences	Rüsselsheim
Carl Roth GmbH & Co.KG	Karlsruhe
Charles River Laboratories	Sulzfeld
Dako Deutschland GmbH	Hamburg
Dianova GmbH	Hamburg
Eppendorf AG	Hamburg
Fermentas GmbH	St. Leon-Rot
GE Healthcare Europe GmbH	Freiburg
Greiner Bio-One GmbH	Frickenhausen
Invitrogen GmbH	Karlsruhe
Kinesis GmbH	Langenfeld
Knick GmbH & Co.KG	Berlin
Lab instruments Deutschland GmbH	Crailsheim

MATERIAL AND METHODS

Lab & Vet Service GmbH	Vienna, Austria
Leica Microsystems	Wetzlar
LG Electronics	Seoul, Korea
Marienfeld GmbH & Co. KG	Lauda-Königshofen
Merck KGaA	Darmstadt
Messer Group GmbH	Sulzbach
Miltenyi Biotec GmbH	BergischGladbach
Minerva Biolabs	Berlin
MorphoSysAbD GmbH	Düsseldorf
New England BioLabs GmbH, (Cell Signalling)	Frankfurt am Main
Nikon GmbH	Düsseldorf
Olympus America Inc.	Center Valley PA, USA
Pall Life Sciences	Dreieich
Pan Biotech GmbH	Aidenbach
PE Applied Biosystems	Waltham MA, USA
PeproTech Germany	Hamburg
Peqlab Biotechnologie GmbH	Erlangen
Perbio Science	Bonn
Polysciences Europe GmbH	Eppelheim
Progen Biotechnik	Heidelberg
Promega GmbH	Mannheim
Qiagen GmbH	Hilden
Restek GmbH	Bad Homburg
Roche Diagnostics	Mannheim
Sanofi-Aventis Deutschland GmbH	Frankfurt
Santa Cruz Biotechnology, Inc.	Heidelberg
Sarstedt	Nürnberg
Serva	Heidelberg
Semperit AG	Vienna, Austria
Sigma-Aldrich Chemie GmbH	Taufkirchen
Sigma Laborcentrifugen GmbH	Osterode am Harz
Sony Corporation	Tokyo, Japan
SsniffSpezialdiäten GmbH	Soest
Stratec Biomedical AG	Birkenfeld
Synchem OHG	Felsberg/Altenburg
Systec GmbH	Wettenberg
Tecan Deutschland GmbH	Crailsheim
Thermo Fisher Scientific Inc.	Waltham MA, USA
Trevigen Inc.	Gaithersburg, USA
Vitaris AG	Baar
VWR International GmbH	Darmstadt

Whatman International Ltd.
Zentrallager Theoretikum

Maldstone, UK
Heidelberg

2.1.3 Chemicals and reagents

Product	Product number, company
Aceton	#40143 Zentrallager Theoretikum
Agarose	#15510-027, Invitrogen
Aluminium sulfate	#192430050, Acros Organics
Albumin Fraction V (BSA)	#8076.2, Carl Roth
Ammonium chloride	#32205, Riedel-de Häen, Zentrallager Theoretikum (Heidelberg university)
Aluminium sulfate	#192430050, Acros Organics
Aqua injection water	#23114.01, Braun
Boric acid	#A3581,1000, Applichem
Cell disassociation buffer	#12151-014, GIBCO, Invitrogen
CFSE	#422701, Biolegend
Chloramine-T-hydrate	#857319-100G, Sigma-Aldrich
Chlorpromazine	#C8138, Sigma-Aldrich
Coomassie brilliant blue R-250 dye	#20278, Thermo Fisher Scientific
DAPI	#6335.1, Carl Roth
Dithiothreitol (DTT)	#D9779, Sigma-Aldrich
Detection reagent ECL	#32106, ECL western-blotting substrate pierce, Thermo Fisher Scientific
4-Dimethylaminobenzaldehyd	#39070, Fluka, Sigma-Aldrich
Dimethyl sulfoxide	#D2650, Sigma-Aldrich
Di-sodium hydrogen Phosphate Dihydrate	#A3567, 0500, Applichem
DMEM	#41966052, Gibco, Invitrogen
DNA Exitus Plus	#A7089, Applichem
DNA marker 100 bp	#T835, Carl Roth
dNTP Mix	#BIO-39044, Bioline
DPBS	#14190, Gibco, Invitrogen
Dynabeads® sheep anti-rat IgG	#110.35, Invitrogen
EDTA	#E5134, Sigma-Aldrich
Enhancer	#01-1030, Peqlab
Eosin G	#7089.1, Carl Roth
Acetic acid	#10296, Grüssing
Ethanol	#32205, Riedel-de Haen, Zentrallager
Fast blue RR salt	#F0500, Sigma-Aldrich
FCS (Fetal Calf Serum)	#P30-3302, Pan Biotech
Formaldehyde	#31245, Riedel-de Haen, Zentrallager
G418 – Disulfate – solution, steril	#A6798,0050, Applichem
Gelatine 2 %	#G1393, Sigma-Aldrich
Gelatin sepharose	#17-0956-01, Amersham, GE Healthcare
Geneticin	#30432, Sigma-Aldrich
Urea	#U5128, Sigma-Aldrich
HBSS 10x	#14185-045, GIBCO, Invitrogen
Imidazole	#104716, Merck
Iodoacetic acid	#35603, Thermo Fisher Scientific

MATERIAL AND METHODS

Potassium chloride	#A3582, 1000, Applichem
Potassium hydrogen carbonate	#P748, Carl Roth
Potassium dihydrogen phosphate	#1.04873.1000, Merck
Potassium hydroxide	#Z12038, Zentrallager Theoretikum
Ketanest®	Pfizer, pharmacy of hospital, Heidelberg university
Sodium chloride 0.9 %	#190/12606084, B.Braun
Collagenase	#17454, Seva
β-Mercaptoethanol	#444203-250 ml, Merck
Methanol	#32213-2.5L, Sigma-Aldrich
2-Methylbutan	#A1263, 1000, Applichem
MgCl ₂ (PCR)	#01-1030, Peqlab
Micro BCA™ protein assay	#23235, Thermo Fisher Scientific
Milk pulver	#T145.1, Carl Roth
MES	#M5287, Sigma-Aldrich
Mowiol 4-88 reagent	#475904, Calbiochem, Merck
Sodium carbonate	#A4332.1000, Applichem
Sodium chloride	#64026, Riedel-de Haen, Zentrallager
Sodium citrate	#S4641, Sigma-Aldrich
Sodium deoxycholate	#3484.1, Carl Roth
Sodium fluoride	#201154-5G-D, Sigma Aldrich
Sodium dihydrate phosphate	#106346, Merck
Sodium dihydrate carbonate	#106323, Merck
Sodium hydroxide	#30620, Sigma Aldrich
Sodium nitrate	#237213, Sigma Aldrich
Sodium orthovanadate	#S6508-50G, Sigma-Aldrich
Sodium thiosulfate	#S7026, Sigma-Aldrich
N-ethylmaleimide	#2251,0005, AppliChem
Ni-NTA Agarose	#R901-01, Thermo Fisher Scientific
NP40	#ab142227, Abcam
Opti-MEM	#31985-062, Gibco, Invitrogen
Penicillin/streptomycin	#15140-122, Gibco, Invitrogen
peqGOLD Trifast	#30-2010, peqlab VWR
Phenolphthalein	#34607, Sigma-Aldrich
Phenylmethylsulfonylfluoride (PMSF)	#A0999,0005, AppliChem
Pierce™ NeutrAvidin™ Agarose	#29200, Thermo Fisher Scientific
Polyinosinic-polycytidylic acid (plpC)	#IAX-200-021-3005, Adipogen
2-propanol	#69595, Riedel-de Häen, Zentrallager
Proteinase k	#3115852001, Roche
Propidium iodide	#421301, Biolegend
Puromycin	#540411, Merck
Redsafe	#21141, Hiss Diagnostics
Revertaid reverse transcriptase together with 5x reaction buffer	#EP0442, Fermentas
Ribolock RNase inhibitor	#EO0381, Fermentas
RNAzol RT	#R5433, Sigma
HCl	#Z-23-88, ZentrallagerTheoretikum
SensiMix™ capillary kit	#QT405-01, Bioline
Taq DNA-polymerase	#01-1030, Peqlab
Taq DNA-polymerase	MPI for Biochemistry Martinsried
Terminale deoxyribonucleotidyl transferase	#16314015, Thermo Fisher Scientific
Tissue-Tek	#4583, O.C.T compound, Sakura, VWR

MATERIAL AND METHODS

Tris	#4855.2, Roth
Tris-HCl	#9090.3, Roth
Triton X-100	#108603, Merck
Tween 20	#9127.1, Roth
TMB	#613544, Merck
Trypan blue 0.4 %	#1525-061, Gibco, Invitrogen
Trypsin-EDTA	#25300, Gibco, Invitrogen
Xylazine	Hospital pharmacy, Heidelberg University

2.1.4 Media, buffers and solutions

Name	Components
ACK-lyse buffer	4.15 g ammonium chloride / 0.5 g potassium-hydrogen carbonate / 100 µl 0.5 M EDTA (pH=7.5) in 500 ml H ₂ O _d , steril filtration 0.22 µm, kept at 4°C until use
Agar	#15510-027, Invitrogen
Agar gel	1.5 % - 2 % Agar in 1xTBE-buffer, heated in microwave, 2 µl Red Safe added and mixed well. Solution was poured carefully and used fresh
Albumin fraktion V (BSA)	#8076.2, Roth
αMEM	#22561, Gibco, Invitrogen
Blocking buffer (ELISA)	3 % BSA in PBS-T
Micro BCA™ protein assay	#23235, Thermo Fisher Scientific
Blocking buffer (ELISA)	3 % BSA in PBS-T
cDNA Synthese kit	iScript select, #170-8896, BioRad
Cell dissociation buffer	#12151-014, GIBCO, Invitrogen
CFSE, for cell staining	Biolegend, dilution 1:10000 / 1x 10 ⁷ cells
Coomassie-staining solution	Imperial protein stain (#24615, Pierce, Thermo Fisher Scientific), protein-gels were stained for 1h, destained with H ₂ O _d for >1h
DAPI	#6335.1, Roth
Detection reagent	#32106, ECL western blotting substrate, Pierce
DMEM	#41966052, Gibco, Invitrogen
DMSO	#D2650, Sigma-Aldrich
DNA Exitus Plus	#A7089, Applichem
DNA-lyse buffer	100 mM tris (pH 8.5) / 200 mM NaCl / 5 mM EDTA (pH 8), 0.2 % SDS, in 10 ml autoclaved H ₂ O _{dd}
DNA-Marker	100 bp-DNA-ladder extended, #T835.1, Roth
dNTPs	#20-3012, Peqlab
D-PBS	#14190, Gibco, Invitrogen

MATERIAL AND METHODS

Dynabeads®	goat anti-rat IgG, #110.35, Invitrogen, Protein G-beads #100.04D, Invitrogen
Enhancer (PCR)	#01-1030, Peqlab
Ethidiumbromid	10 mg/ml, #2218.1, Roth
FACS-buffer	2.5% FCS in D-PBS
FCS	#P30-3302, Pan Biotech
Gelatine Sepharose 4B	#17-0956-01, GE Healthcare
Geneticin	#10131027, Gibco, Invitrogen
Heparin	#H3149-25KU, Sigma Aldrich
HEPES	#15630-056, Gibco, Invitrogen
Carbonate-buffer (ELISA)	0.78 g Na ₂ CO ₃ / 1.5 g NaHCO ₃ in 500 ml H ₂ O _{dd} , pH 9.6, stored at 4°C (used for maximally 2 months)
Ketanest®	Hospital pharmacy, Heidelberg university, Pfizer
Luciferin	#bc219, Synchem
MgCl ₂ (PCR)	#01-1030, Peqlab
Mowiol (Elvanol)	5 g Mowiol 4-88 Reagent, 20 ml PBS (pH 8), overnight rotation at RT. Addition of 10 ml Glycerin followed by incubation for 30 min at 50°C in water. Centrifugation for 30 min / 5000 xg. Solution stored at -20°C
Paraformaldehyd-solution 4 %	22.5 ml H ₂ O _{dd} was mixed with 5 µl 10 M NaOH at 60°C. 1 g Para-formaldehyde and 2.5 ml 10x PBS were added. Solution was allowed to cool down, pH adjusted at 7.4, and stored in aliquots at -20°C
PBS (1x)	100 ml PBS (10x), in 1 L H ₂ O _d , stored at RT
PBS (10x)	400 g NaCl, 58g Na ₂ HPO ₄ / 10 g KH ₂ PO ₄ / 10 g KCl in 5 L H ₂ O _d , pH 7.0, stored at RT
Penicillin / Streptomycin	#15140-122, Gibco, Invitrogen
Sample buffer (DNA, 4x)	50 % glycerine in 4x TBE, with addition of bromphenol blue
Propidium iodide	#421301, Biolegend
Proteinase-K-solution	20 mg/ml proteinase-K in H ₂ O _d
Stopping solution (ELISA)	0.5 M sulphonic acid (H ₂ SO ₄)
TaqMan® master kit	#04735536001, Roche
Taq-reaction buffer	#01-1030, Peqlab
TBE (1x)	100 ml TBE (10x), in 1 L H ₂ O _d , stored at RT

MATERIAL AND METHODS

TBE (10x)	108 g tris / 55.6 g boric acid / 4.65 g EDTA in 1 L H ₂ O _d , stored at RT
TMB	#613544, Merck
Trifast™	peqGOLD, PeqLab
Trypsin-EDTA	#25300, Gibco, Invitrogen
Digestion solution (tumor)	0.025 g collagenase NB4 / 0.05 % DNase I
Dilution buffer (ELISA)	1.5 % BSA in PBS-T
Coating buffer (ELISA)	14.71 mM sodium carbonate 35.71 mM sodium hydrogen carbonate Add up 500 ml millipore H ₂ O _{dd}
DOC lysis buffer	2 % sodium deoxycholate 20 mM tris-HCl, pH 8.8 Proteinase inhibitor 1:100 2 mM EDTA / 2 mM iodoacetic acid 2 mM N-ethylmaleimide
Wash buffer (ELISA)	100 ml PBS (x10), 0.5 ml Tween 20, 900 ml H ₂ O _d
10X transfer buffer	29.2 g glycine, 58 g tris 37.6 ml 10 % SDS solution in 1 L H ₂ O _{dd}
Wash buffer Ni-NTA	3.45 g NaH ₂ PO ₄ , 29.22 g NaCl, 0.68 g imidazole PH 7.4 – 7.8
Elution buffer gelatine sepharose	4 M urea, 0.05 M tris in PBS (240 g urea, 6 g tris in 100 ml PBS, PH at 7.5, add H ₂ O _{dd} up 1 L) stored at RT
Elution buffer Ni-NTA	50 mM NaH ₂ PO ₄ , 1M NaCl, 250 mM imidazole (for 50 ml aqua braun water add 0.345 g NaH ₂ PO ₄ +2.922 g NaCl+0.851 g imidazole, adjust PH to 7.4 – 7.8)
Equilibration buffer for Gelatine Sepharose	0.01 M sodium citrate and 0.005 M EDTA in PBS (for 100 ml 10x solution add 2.94 g sodium citrate and 1.86 g EDTA, PH 7.2). Solution stored at RT
Running buffer 10x (SDS-PAGE)	30.25 g tris, 144 g glycine and 10 g SDS in 1 L H ₂ O _{dd}

2.1.5 Used materials

Alcohol swab	#G602, Servopax
Aluminium foil	#2596.1, Carl Roth

MATERIAL AND METHODS

Cell culture bottles	#169900 25 cm ² , #156800 75 cm ² , #159926 175 cm ² , Nunc
Cell culture plates	#150239 6-well-plate, #144530 24-well-plate
Cells filter	#352360 100 µm cell strainer, BD Biosciences
Centrifuge tubes	#188271 15 ml, #227261 50 ml, Greiner Bio-One
Chamber slides	#177445, Nunc
Cover foil	#300001358, Tecan
Cover-glass	#6101242, Marienfeld
Cryo tubes	#123263, Greiner Bio-One
Dialysis tube	#44145, Servapor, Serva
Embedding molds	#64708955, Heraeus Kulzer GmbH
Frisch foil	#59206, Zentrallager Theoretikum (University of Heidelberg)
Glass capillaries qPCR	#04929292001, Roche
Gloves	#3780872, Sempercare, Semperit AG
Hamilton-pipette	#75 RN, 31/2“3/S, Hamilton
Injection cannula	#304000, Microlance, 30G, BD Biosciences #302200 Microlance, 27G, BD Biosciences
Macrosep	#OD100C36, Pall
Microtiter plates	#439454 Maxi Sorp, Nunc
Microvette	#20.1288, 200 K3E (Blood plasma), Sarstedt
Object-holder	#4951PLUS, Thermo Fisher Scientific
Ointment for eyes and nose	#2182442, Bepanthen, Bayer
Parafilm	#P-996, Alcan Packaging
Pasteur pipettes	#197734230, Neo Lab
PCR-reaction tubes	#711080, Biozym
Petri dishes	#633171, Greiner Bio-One
Pipette tips	#739296, 740290, Greiner Bio-One
PVDF-membrane	#RPN303F, Amersham Hybond-P, GE Healthcare
Radiography films	#10595000 Structurix D4 DW, AGFA
Reaction tubes	#72.706 1.5 ml
Sephadex-columns	#28-9180-07 PD MiniTRAP™ G-25, GE Healthcare

MATERIAL AND METHODS

Serologic pipettes	(2, 5, 10 & 25 ml), Greiner Bio-One
Steril filter	#SLGV033RS Millex GV 0.22 μm , PVDF-membran, millipore
Tubes	#55.1578, Polypropylene 12/75 mm, Sarstedt
Whatman papers	#3030917 3MM CHR, Whatman International Ltd.

2.2 Animal experimentation methods

2.2.1 Animals

In this work, only animals of the genus *mus musculus* (house mouse) were used. These were bred and kept in a pathogen-free facility (IBF-Heidelberg) during the whole period of the experiments. They were kept in a cage of polycarbonate with a size of 360 cm in which up to 3 animals were placed using dust-free softwood granules (#LTE E-001, Lab & Vet service GmbH). The animals were fed exclusively with a pelleted sole diet (# V1166-341, sniff Spezialitäten GmbH), and kept in a temperature of (20-24) $^{\circ}\text{C}$ and a relative humidity of (55-60)%. The animal were exposed to a diurnal cycle lasting 12 hours with lights on from (0700-1900) mid-european time (MEZ). The drinking water of the mice consisted of tap water. Thus, it could be ensured that the experiments always took place under standard conditions. All animal experiments were approved by the Animal Protection Commission of the regional council Karlsruhe and the application numbers are:

- G-13/17 (the effect of matrix on tumor growth of human breast cancer)
- G-34/19 (the effect of matrix on tumor growth of B16 melanoma)
- G-127/15 (the role of EDA and EDB fibronectin in tumor metastasis)

The immune deficient mouse strain used in these experiments was obtained from Charles Rivers. It is based on the CD1 strain (Caesarean Derived 1). These mice carry a mutation in the *FOXP1* gene. Homozygous mice lack the thymus, which means that T lymphocytes cannot mature and thus they are immunodeficient. These immunodeficient mice are among the best characterized laboratory animals that offer the opportunity to study the behavior of human tumors in an experimental setting. B16 melanoma was injected in immune competent mice that have C57BL/6 in their background. Therefore, the melanoma mouse line B16, which was obtained from a C57BL/6 mouse can be used.

2.2.2 Anesthesia of laboratory animals

Mice receiving intratibial injection were anesthetized by subcutaneous injection of 0.5 $\mu\text{g/g}$ medetomidine, 5 $\mu\text{g/g}$ midazolam and 0.05 $\mu\text{g/g}$ fentanyl. The surgical tolerance in this type of anesthesia lasts about 3 hours. Here too the cornea of the eye was protected from dehydration through use of the eye ointment. After surgery, anesthesia was reversed by administering a mixture of antagonists and pain control. This mixture consisted of 2 $\mu\text{g/g}$ atipamezole, 0.412 $\mu\text{g/g}$ flumazenil and 0.06 $\mu\text{g/g}$ buprenorphine, and was injected subcutaneously.

A mixture of ketamine (120 mg/kg body weight) and xylazine (16 mg/kg body weight) was injected into the mice intraperitoneally before radiography of the skeleton.

Anesthesia is adequate after 3-5 minutes, so that high quality X-ray images of the skeleton can be obtained. An eye ointment was applied (Bepanthen, Bayer, # 2182442) to prevent drying of the eye cornea during anesthesia and subsequent loss of vision. The surgical tolerance can be tested by a lack of toe reflex and lasts up to 20 minutes.

2.2.3 Intratibial injection of human breast cancer cells

The intratibial injection of human breast cancer cells is a xenograft model to transfer of human breast cancer cells into immune deficient mice. In this model, the mouse is firstly anesthetized and fixed under a binocular. Under deep anesthesia, a 1 cm long cut through the skin along the tibia is performed with a scalpel. The existing muscle layers are removed away to expose the tibia clearly. Then with the help of a thin dental drill, two small holes are performed at a distance (4-5) mm and a diameter of approximately 0.2 mm through the bone cortex of the proximal tibia. Subsequently, the bone marrow is rinsed by a syringe filled with 1 ml DPBS and a 30 G cannula and the blood that is coming out from the holes is removed using a sterile cotton swap. Then, the cancer cells (1×10^5 cells/5 μ l DPBS) are injected using Hamilton pipette and the holes are closed immediately with surgical bone wax. After removing the rest of the wax and cleaning of the wound, the muscle and skin layer are sutured with an insoluble Supramid thread (Supramid, USP 5/0) with 2-3 stitches. The final closing of the wound was done using a spray plaster and the mouse is awakened by application of the subcutaneous antagonist injection.

Following the intratibial injections, and after administering the antidote mixture that contains buprenorphine against pain, the mice received further injection of buprenorphine (temgesic, 0.05-0.1 mg/kg) every 4-6 hours for 3 days. Instead of continuing injections at night, buprenorphine was added to drinking water for pain therapy 0.3 mg/ml (2.5 ml/80 ml drinking water) at night for the next two nights after surgery. The last injection took place in the evening before changing the water to the mixture buprenorphine/water and was resumed the next morning when changing of the mixture buprenorphine/water to drinking water. This provided an adequate pain control.

2.2.4 Bioluminescence imaging

Since the human breast cancer cells have a luciferase construct, the tumor cells can be visualized in the organism by administration of luciferin which is the substrate of the luciferase that can convert the enzyme into light. This light emits in a range of (500-700) nm with a maximum emission at 612 nm at 37°C and is able to penetrate the biological tissues. The measurement was carried out by (IVIS-100, xenogeny) in the clinical-experimental area of IBF (IBF, Maushotel, Im Neuenheimer Feld, building 347, 69120 Heidelberg). To achieve that, the mice are anesthetized in an inhalation chamber which is connected to the imaging device and is supplied with the anesthetic gas isoflurane. A solution containing luciferin (150 mg/kg body weight) was administrated intraperitoneally. After five minutes of an intraperitoneal injection of luciferin, the mouse is placed under an isoflurane inhalation mask in a dark chamber on a table heated to 37°C. Since this device is provided with a sensitive camera which is located in the light chamber, the position, the number of tumor cells and the size of the tumor can be detected by performing ventral and dorsal measurement for each mouse. The mouse must be aligned so that the entire body is visible (objective distance

10 cm, camera position “field of view C”). The normal recording time is 1 minute with a medium capacity, however that is dependent on the size of the tumor. Therefore, the measurement was done for 1 minute and 2 minutes for each mouse. The system also takes additionally a photographic image of the mouse in order to localize the bioluminescence signal in the mouse. The software “live imaging” (version 2.5, xenogen) was used for quantification. It calculates the relative light unit (RLU) from the emitted light of region of interest (ROI).

2.2.5 Radiography of bone lesions

The osteolytic lesions which are caused by the tumor cells could be characterized by radiography. This was done by an X-ray machine at the immunology and serology institute of Heidelberg university (type 70025320, BIO-RAD). First, the mice were anesthetized with a mixture of ketamine and xylazine and then placed on the X-ray film so that the edges and the whole body of the mouse could be distinguished. The used voltage was 30 kV for 3 minutes. After measurement, the X-ray films were developed and scanned for the evaluation. The area, length and width of the osteolytic lesions were determined using the computer program “ImageJ”.

2.2.6 B16 - Melanoma - animal experiment model

In this model, mice were first anesthetized with Isoflurane and then 10^6 B16 melanoma cells in 100 μ l PBS were injected subcutaneously into the left flank of the mouse. The same anesthesia was applied for tumor size measurement before start of treatment.

2.2.7 Therapeutic treatment with peptides

The peptides were provided by the biochemical core facility of Max Planck institute for Biochemistry in Martinsried. These peptides were isolated from the biomass or from synthetic raw mass using Nickel-columns that bind the preceding 6-HIS-tag (MKHHHHHH-) as described in 2.4.8. After confirmation of identity and concentration, the concentration was adjusted to 5 mg/ml using NaCl 0.9 % and following steril filtration aliquots were frozen at 80°C until use. In the breast cancer model peptide injections started at day 29 until day 39, with killing at day 40. In the melanoma model peptide injections started at day 7 until day 13, with killing on day 14. The injections were administered at a dose of 0.5 mg (100 μ l of a solution of 5 mg/ml) intraperitoneally daily at the same time of the day. In addition to the group receiving scrambled peptide a group only received 100 μ l NaCl 0.9 % administered daily intraperitoneally.

pUR4 peptide which represents the functional upstream domain (FUD) of F1 adhesion molecule of *Streptococcus Pyogenes* and has the following sequence:

KDQSPLAGESGETEYITEVYGNQQNPVIDDKLPNETGFSGNMVETEDT

The peptide consists of 49 amino acids and has a molecular weight of 5376.71 g/mol and an extinction coefficient of 0.54.

The Scrambled peptide was as follows:

EKGYSKPPVGNEGGDQVDEYDTMSQTKLEDEGNTLISPITFENATEQVN

pUR4 was further modified based on the literature [148, 151, 234] and the new modified peptide has the following sequence:
GGKNTPLPSVYDIMTTVSGFEKEIDEEDQTGLQVGKTSNGAEETDPKANQNEY

This new modified peptide includes two main motifs which mimics the ones in pUR4 and can interact with ³FNI and ²FNI modules of fibronectin with high affinity. It consists of 53 amino acids and has a molecular weight of 5734 g/mol and an extinction coefficient of 0.52.

The obtained data indicated that the modified peptide acts as a fibronectin polymerization inhibitor. Therefore, it was interesting to find out which part of this peptide is responsible for that effect. To achieve that, the modified peptide was divided into 3 individual peptides (A, B and C) which have the following sequences:

A: GGKNTPLPSVYDIMTTV (17 amino acids)

B: SGFEKEIDEEDQTGLQV (17 amino acids)

C: GKTSNGAEETDPKANQNEY (19 amino acids)

The next step was to further fractionate and modify the most efficient sequence and 3 new peptides were further designed which have the following sequences:

1: SGFEKEIDE

2: EDTQTGLQV

3: KEIDEEDQT

All of the peptides were injected intraperitoneally at a dose of 0.5 mg in 100 μ l 0.9 % NaCl daily.

2.2.8 Killing of the experimental mice

The euthanasia of the experimental mice was carried out by cervical dislocation. After killing, the mouse was fixed and the tumors were isolated. A piece of tumor was cryopreserved on a Whatman paper and shortly sunken in isopentane, which was previously cooled in liquid nitrogen. Then the tumor was also kept shortly in liquid nitrogen in order to ensure the rapid freezing of the tumor. Finally, the tumors were frozen at -80°C.

2.3 Cell biology methods

2.3.1 Murine melanoma cell line B16-F10

The murine B16-F10 melanoma cell line has been isolated from the skin of C57BL/6 (H-2b) mice and is a highly invasive skin cancer cell line that leads to rapid tumor growth after its subcutaneous application in mice. This cell line is particularly suitable for using in anti-tumor therapeutic trials because of its easy administration, easy monitoring and its rapid growth. The tumor growth of this cell line is controlled by a variety of immune receptors and it has been reported that it is mainly associated with T cell-dependent growth [235].

2.3.2 Human breast cancer cell line MDA-MB-231B/luc⁺

The human breast cancer cell line MDA-MB-231B/luc⁺ was previously isolated in 1973 from a pleural effusion (fluid accumulation in the pleural cavity) of 51 years old caucasian woman at the M.D. Anderson Cancer Center in Houston, USA. They are adenocarcinoma cells originating from the mammary gland tissue. They are frequently used as a cancer research model because they tolerate culture conditions and adhere

well *in-vitro*. In these cells, the letters luc⁺ were added because a reporter gene for luciferase enzyme was transfected using a CMV promoter-controlled expression vector [236]. Since the vector contained a resistance gene against geneticin, following transfection cells are maintained in media containing this antibiotic. The letter B was added because they were developed to seek bone tissue for metastasis formation. To achieve this, cells were selected after four injection cycles in mice after each one, cells tumor cells were only isolated from bone metastases. The clone that is called “bone-seeking clone” that grows exclusively in the bone was generated and by using it, it was possible to investigate bone lesion formation by breast cancer cells.

2.3.3 Isolation of immune cells from tumors

In order to characterize the immune cells of the tumors, each tumor was isolated and put in 1 ml digestion medium (DMEM + 1 mg/ml collagenase A + 0.05 % DNase). After shaking in a thermostatic shaker for 45 minutes at 37°C, digested tumors were resuspended and passed through a 100 µm cell strainer.

2.3.4 Depletion of immune cells from tumors

Filtered cells (see 2.3.3) were resuspended in 1 ml DPBS. Magnetic protein G beads (Dynabeads, Invitrogen) were used. These beads bind all antibodies by their heavy chains. Beads were first washed with DPBS and then held on magnet (MACS®) in order to remove the liquid. This was followed by incubation with 5 µg antibody in 200 µl DPBS for 30 minutes at room temperature (RT) in an electric shaker (30 µl of beads were used for about 1×10^7 cells). Beads were washed again with DPBS and the cells (1×10^7 cells in 1 ml DPBS) were added and incubated with the beads for 30 minutes at room temperature. Then, the beads with the cells were washed with DPBS 3 times. To obtain mRNA from the isolated cells, beads were exposed to 300 µl RNazol with short vortexing.

2.3.5 Determination of cell number

For this purpose, a Casy-TT® cell counter was used. It is also used to characterize the size distribution, cells aggregation and the viability of the cells. A specific program could be created for each cell type. By using Casy®-Blue solution, the dead cells and debris could be distinguished from the healthy cells because they have a different flow behavior through the device and a different size.

The measurements are carried out by pulling the cells through two lasers and determining the exact cell count, state of aggregation and the viability (%) averaged from three measurements.

2.3.6 Passaging and preparation of tumor cells for *in vivo* injections

In order to use cells that were of similar passages, the cells were passaged before the start of the experiments in high quantities and frozen in liquid nitrogen. From these frozen aliquots the cells were thawed and used fresh or passaged maximally twice. Thus, the cells used in the experiments originated from passages that were close to each other. For freezing, the cells were washed with DPBS and removed from the flasks with medium after 5 minutes incubation with 0.5 % trypsin-EDTA. Then, they were centrifuged and taken in freezing medium that consists of DMEM + 10 % FCS and 1 % DMSO and each 1 ml of suspension was put in cryotubes. Then, the tubes were frozen in isopropanol freezing chamber at -80°C which ensures that the cells are

frozen gently and slowly. After two days, the cells could be transferred to liquid nitrogen.

For all *in-vivo* experiments, the tumor cells were thawed (3-5) days before the experiment. On the day before the *in vivo* injection, the cells were washed with DPBS and cultured with fresh medium without antibiotics. On the day of injection, the cells were washed again with DPBS and detached with 0.05 % trypsin-EDTA for 5 minutes at 37°C. The viability of the cells and the number were determined as described previously by Casy-TT® cell counter. For *in vivo* experiments, only cells showing viability higher than 90 % and an aggregation less than 1.3 were used. The required count of the cells for each mouse was calculated and then the cells were again centrifuged at 1500 rpm for 5 minutes and resuspended in DPBS for injection. Finally, the cells ready for injection were kept on ice under sterile conditions until injection.

2.4 Protein biochemical methods

2.4.1 Production of matrix lysates

In order to investigate the extracellular matrix formed by cultured cells, the matrix was isolated based on its insolubility in sodium deoxycholate (DOC). The method had already been described but was slightly modified [237]. In brief, tumor cells were cultured in 48-well plates over a period of 2 days. Then, culture medium was removed and the cells were washed with DPBS. The cells were resuspended in 170 µl DOC lysis buffer per well and pressed three times through a 27 G needle to remove the genomic DNA and transferred into a 1.5 ml reaction tube. After centrifugation at 13000 rpm for 17 minutes at 4°C, the supernatant was transferred to a new reaction tube, which represents the fraction soluble in deoxycholate, the doc sol (deoxycholate soluble, soluble in deoxycholate). The insoluble pellet is the doc insol (deoxycholate insoluble, insoluble in deoxycholate) which was resuspended in 29 µl SDS buffer. Both the isolated doc sol and doc insol fractions were stored at -20°C to be quantified by ELISA and the amount of matrix components corrected to total protein quantified using the BCA assay.

2.4.2 Production of protein lysates for analysis of western blot or ELISA

To obtain protein extracts from the tumors, a small (2 mm) piece was lysed in 300 µl protein lysis buffer and minced with the plunger of a 1 ml syringe. The mixture is then centrifuged at 12000 rpm for 10 min and the supernatant transferred to a new reaction tube. The samples were stored at -80°C until analysis.

2.4.3 Protein concentration by Bradford-assay

Micro BCA™ protein assay kit was used for determination of the protein content in protein lysates. The samples were diluted in Millipore water 1:400-1:1000 depending on the expected protein amount. The standard curve of BSA protein contains the following concentrations: 200, 40, 20, 10, 5, 2.5, 1, 0.5, ng/ml. 150 µl of prepared samples were added to 96 well-plate and then 150 µl of working solution as described in manufacture instructions (BCA protein assay kit, #23225, Thermo scientific). Finally, the plate was incubated for 2 h at 37°C and then according to the manufacturer's instructions, the evaluation was carried out at wave length 562 nm in a microtiter plate

reader. For determination of standard curve and thus protein concentration, the Magellan V6.4 software was used.

2.4.4 ELISA (Enzyme linked immunosorbent assay)

Enzyme linked immunosorbent assay refers to a method that detects and quantifies of soluble proteins possible through the use of specific antibodies against these proteins. Detection of matrix fibronectin was achieved using a sandwich ELISA method in which the primary antibody to the molecule of interest was used in coating buffer to coat the plate overnight/4 °C and 50 µl was used in each well. The next day, after washing three times with PBS-T, the plate was blocked for one hour by blocking solution containing 3 % BSA (Bovine serum albumin) in order to prevent unspecific binding. After that, the plate was washed three times with PBS-T. Samples were diluted with dilution buffer containing 1 % BSA. The dilution factor was a sample-dependent (conditioned media 1:4, matrix 1:2). 50 µl of prepared samples were added to each well. A dilution series of standard protein and an internal control protein was also prepared and added to the plate in order to determine the exact concentration of fibronectin in the samples. The samples and the standards were incubated for 2 h RT to allow for binding to the primary antibody. Then the plate was washed with PBS-T and 50 µl of the secondary antibody against the desired protein was added. After 45 minutes of incubation, the plate was washed to remove the excessive antibody that was not bound to the protein of samples. Since the secondary antibody is conjugated to HRP, the successful binding could be visible by adding 50 µl of TMB substrate solution in each well. After 50 minutes of incubation at room temperature, the reaction was stopped by 50 µl stop solution 5M H₂SO₄. Finally, the plate was analyzed in a Tecan brand microtiter plate reader at the wave length 450 nm and the protein concentration could be calculated by the standard curve using the Magellan V6.4 software.

2.4.5 Human and murine plasma fibronectin ELISA

As clarified previously, the sandwich ELISA method was used for detection both human and murine plasma fibronectin. Anti fibronectin (Sigma-Aldrich, #F3648) from Sigma 1:5000 was used as a primary antibody for both human and murine ELISA. Human plasma fibronectin previously purified from frozen human plasma using gelatin sephrose column was used as a standard. The standard curve of human plasma fibronectin contained the following concentrations: 2000, 1000, 500, 250, 100, 50, 25, 12.5, 6.25, 3.125, 1.56 ng/ml. The following concentration were made from the purchased murine plasma fibronectin (Dunn): 4000, 2000, 1000, 500, 250, 100, 50, 25, 12.5, 6.25, 3.125 ng/ml). Human plasma from a healthy donor was used as an internal control for human plasma fibronectin ELISA and aliquots from a pool of murine plasma obtained from 8 mice was used as an internal standard for murine fibronectin ELISA. The secondary antibody was a HRP-labeled anti-fibronectin (rabbit polyclonal) (at a dilution of 1:2000 for murine fibronectin ELISA and 1:5000 for human fibronectin ELISA).

2.4.6 SDS gel electrophoresis

The separation of proteins based on their molecular weight was performed using SDS sodium dodecyl sulfate polyacrylamide gel electrophoresis. Denaturation of the proteins and their binding with SDS creates a negative charge shell, which covers the charges of the amino acids and thus allows separation in correlation with the molecular weight [238]. To separate a protein solution by SDS gel electrophoresis, a polyacrylamide separating gel is prepared based on the plan in Table 2.4.6. After the

addition of APS (Ammonium persulfate solution) and TEMED (Tetramethyl ethylenediamine), the gel must be poured immediately and covered with isopropanol. After the separating gel has polymerized, the isopropanol is removed, the collecting gel is placed on the separating gel and a comb is carefully inserted without air bubbles into the chamber. Although the collection gel is solid, the gel can be kept wet and stored at 4°C or used immediately. The samples are mixed with 5x loading buffer and denatured at 95°C for 5 minutes. From each sample, 10-20 µl was applied to the gel. The electrophoresis was performed at a voltage of 100V for 60 minutes and then either stained with Coomassie staining solution for 10 minutes and washed with distilled water until the proteins are visible in the gel, or the proteins are transferred to a nitrocellulose membrane.

	Separation gel, 10 ml, 10 %	Stacking/collecting gel, 3 ml 5 %
Deionized water	4.2 ml	1.8 ml
30 % Acrylamid solution	3.3 ml	0.5 ml
1.5 M Tris / HCl pH 8.8	2.5 ml	-
1.0 M Tris / HCl pH 6.8	-	0.8 ml
TEMED	0.007 ml	0.003 ml
10 % APS	0.1 ml	0.03 ml

Table.2.4.6 Pipetting scheme for the preparation of separation and stacking/collection gel

2.4.7 Western blot

The proteins separated by SDS gel electrophoresis are transferred to a nitrocellulose membrane and then proteins can be detected on the membrane with the help of specific antibodies [238]. For the transfer of the proteins from the SDS gel to the nitrocellulose membrane, the semi-dry blotting method was used. For this purpose, four Whatman filter papers and a nitrocellulose membrane were cut to the size of the gel and placed in the transfer buffer. Two filter papers were placed on the anode of the semi-dry-blotter from peqlab, then the nitrocellulose membrane and the SDS gel and finally two filter papers. The sheets must lie on each other without air bubbles and then the cathode, which is located in the cover, is connected. The transmission of the proteins takes place at a constant voltage of 15 V for one hour. The membrane is sometimes cut based on the size of detected protein to allow for parallel blotting. The membranes are blocked with 5 % milk for one hour in order to get rid of unspecific protein binding. Membranes are washed with PBS-T and incubated with the primary antibody overnight at 4°C. The next day, the membrane is washed three times with PBS-T and incubated for one hour with a secondary antibody directed against the primary antibody and coupled with HRP (horseradish peroxidase) which can convert the luminal substrate into an oxidized form producing light. This light can be detected using autoradiography films (x-ray film # RF12 fuji Medical Super Rx, A. Hartenstein). To do that, the membrane is incubated with western blotting substrate (from Pierce), which is mixed 1:1 PBS-T and incubated for 2 minutes and then placed in a film cassette. In the dark room, the film is placed on the membrane and incubated for strong signals for 10-30 seconds and for weak signals for 2-5 minutes. The film is then

developed with AGFA type CP1000 development machine and finally evaluation is carried out using the freeware program ImageJ (Wayne Rasband, NH).

The primary antibodies that were used are:

- Fibronectin, Millipore, #ab2033, 1:5000, rabbit
- GAPDH, Sigma-Aldrich, #G9545, 1:10000, rabbit
- His-tag, Novagen, #70796-3, 1:1000, mouse

The secondary antibodies

- Goat anti-rabbit HRP, Dianova, #111-035-045, 1:10000
- Goat anti-mouse HRP, BioRad, #170-6516, 1:10000

2.4.8 Purification of peptides using a nickel-NTA column

The peptides were produced at the core facility of the Max-Planck Institute for Biochemistry in Martinsried by Dr. Sabine Suppmann and Dr. Stefan Uebel. pUR4 was initially purified from biomass of transfected ClearColitm, which was supplied from Martinsried on dry ice. The isolation was done based on the presence of a His-tag sequence in the peptide (MKHHHHHH-). This His-tag forms a chelating complex with divalent nickel ions. Low imidazole concentrations allow unbound proteins to be washed off from the column, and by increasing the imidazole concentration, the target protein is eluted together with the His tag [239]. To perform this affinity chromatography, the biomass had to be mixed at least 1:1 with binding buffer and lysed on ice ten times for 10 seconds each using ultrasound sonication. Then, the lysate was centrifuged at 20000 rpm (SORVALL® RC-5B PLUS superspeed centrifuge, Thermo Fisher Scientific) for 30 minutes and about 30 ml supernatant is mixed with 1 ml Ni-NTA agarose after washing of Ni-NTA agarose in equilibration buffer. The mixture is rotated overnight at 4°C. The next day, the peptides are detached in the so-called batch process from the column. To do that, the Ni-NTA lysate mixture is centrifuged for 3 minutes at 700 xg and the supernatant is discarded. The nickel column was washed three times with 10 ml wash buffer. Then, the peptides were eluted for 4-5 times with 2 ml elution buffer from the Ni-NTA agarose. The nickel column is regenerated using MES buffer and washed again with Aqua-pro-injection water. For storage, the column is stored in 20 % ethanol at 4°C. To purify the control peptide pUR4scr, 8 M urea had to be added to the binding buffer so that the peptide would not precipitate. The synthetic peptides were also produced so that they have a His-tag and were isolated using the same method. The benefit was the absence of endotoxins and the ability to refold the protein on the column to avoid precipitation. The sequences were as follows:

pUR4: KDQSPLAGESGETEYITEVYGNQQNPVDIDKKLNETGFSGNMVETEDT

The His-tag consisted of MK and 6 histidines on the amino side.

The scrambled peptide was:
EKGYSKPPVGNEGGDQVDEYDTMSQTKLEDEGNTLISPITFENATEQVN.

All peptides were concentrated using 1kD Macrosep columns and the buffer changed to 0.9 % NaCl. After sterile filtration, the quality of the rebuffed peptide was tested on SDS protein gel and the concentration was confirmed by comparison to a standard curve and finally stored in -80°C

2.5 Molecular biology methods

2.5.1 Detection of mycoplasma by PCR

Mycoplasma are the smallest prokaryotes. Their diameter varies between 0.1-2 μm which enables them to pass the sterile filters with pore sizes around 0.22 μm . Contamination of cell cultures with mycoplasma is therefore common, but it is also difficult to detect. Because contamination affects experimental results, it is important to exclude it. To do that, both the supernatant of confluent cells and isolated DNA of these cells are tested for mycoplasma contamination by PCR.

Amounts for one sample:

H ₂ O _d (PCR grade)	15.3 μl	95°C
10x reaction buffer	2.5 μl	
Primer/nucleotide-mix	2.5 μl	
Internal control DNA	2.5 μl	
Taq (5 U/ μl)	0.2 μl	
	Σ 23 μl	

PCR-Program:

3 minutes) x39
95°C	30 s	
55°C	30 s	
72°C	30 s	
4°C	∞	

23 μl master mix was used for each PCR reaction tube and 2 μl was added from the sample, H₂O was used as a negative control, a positive control was added. 10 μl from each PCR product was mixed with 10 μl DNA sample buffer and analyzed on a 1.5 % agarose gel. Mycoplasma contaminated samples and positive control can be detected at 265-268 bp. The internal control shows the correct performance of PCR through the presence of a band at 191 bp.

2.5.2 RNA isolation and the reverse transcription of RNA

For analysis of mRNA expression, cells or tissues were dissolved in RNeasy (1 ml RNeasy / 1×10^7 cells or 1 mg tissue) and lysed. The samples were frozen at -80°C or used directly for RNA isolation. The isolation was done according to the manufacturer's protocol. In short, 0.4-fold volume (HPLC H₂O) of RNeasy was added, mixed, incubated for 5-15 min at room temperature and centrifuged for 15 minutes at 12000 xg. The supernatant was transferred to a new tube and again 0.4-fold volume of 75 % ethanol was added. The samples were incubated 8 min at room temperature and centrifuged for 8 min at 12000 xg). The precipitated RNA was washed with 75 % ethanol and centrifuged for 3 minutes at 12000 xg). Finally, the isolated RNA was dissolved in RNase-free water (about 30 μl) and frozen at -80°C or used directly for cDNA synthesis in order to analyze mRNA by reverse transcription quantitative PCR.

2.5.3 Flow cytometry analysis

Flow cytometry is a technique that can group the cells accurately depending on their size and granularity as well as expression of various proteins using specific antibodies for both cell surface proteins or intracellular proteins. These antibodies are labeled with dyes that can be excited by different lasers and the resulting emission is converted by detectors into dots on a screen (Diva, BD Bioscience). In this work, LSRII from BD Bioscience was used. Tissues were isolated and 1×10^6 cells were suspended in 100 μl FACS buffer and stained with the respective antibodies for 30 minutes at 4°C. 300 μl of FACS buffer was added for washing and samples were centrifuged at 2400 rpm

for 5 minutes. The supernatant was discarded and the pellet was resuspended in 100 μ l FACS buffer and measured immediately using flow cytometry. Each cell is represented as a single point and can be viewed in a dot blot or histogram. Unstained cells or non-specific antibodies coupled with the same fluorescent dye (isotype control) can be used as negative controls. The evaluation of the data was carried out using the DIVA software from BD Bioscience.

- The antibodies that were used for staining are as follows:

- Anti CD45, Pacific Blue, clone 30-F11, dilution 1:400, #103125, Biolegend.
- Anti CD11b, Alexa Fluor 700, clone M1/70, dilution 1:1600, #101222, Biolegend.
- Anti CD11b, FITC, clone M1/70, dilution 1:1600, #101205, Biolegend.
- Anti F4/80, PE, clone BM8, dilution 1:400, #123110, Biolegend.
- Anti Gr1, Alexa Fluor, clone RB6-8C5, dilution 1:1600, #108420, Biolegend.
- Anti Gr1, PE/Cy5, clone RB6-8C5, dilution 1:800, #108409, Biolegend.
- Anti CD49e (integrin α 5) (human), APC, clone NKI-SAM-1, dilution 1:100, #328012, Biolegend.
- Anti-beta 2 microglobulin (human), PE, clone B2M-01, dilution 1:1600, #ab49424, Abcam.

2.6 Histological methods

2.6.1 Preparation of tumor sections

The tumors were isolated and frozen with isopentane and liquid nitrogen and finally stored in -80°C . To make frozen sections of these tumors, a piece of each tumor was embedded using tissue-tek (# 4583, O.C.T. compound, Sakura). As soon as tissue-tek hardens, it becomes white and firm. 5-10 μm thick sections were made with the cryomicrotome (Cryostat CM 3050 of Leica). The chamber temperature was -25°C and the object temperature -12 to -15°C . The tumor slices were transferred to a microscope slide and dried for at least 30 minutes before being either immediately stained or stored at -20°C .

2.6.2 Immunohistochemical staining of frozen sections

The tumor sections were fixed with 4 % PFA (Paraformaldehyde) for 10 minutes at room temperature and then washed with 1x PBS. In order to reduce non-specific background staining of antibodies, the sections were blocked with 5% BSA in PBS for one hour at room temperature. Sections were then washed thrice with PBS and incubated with the primary antibody for one hour at room temperature. After washing for three times for 5 minutes with 1x PBS and staining with the secondary antibody for one hour at room temperature, the sections were washed again thrice with PBS for 5 minutes and dried overnight. This was followed by mounting with Mowiol. In parallel to staining with the secondary antibody, nuclear staining was performed using DAPI 1:10000 (Roth, #6335.1). Finally, the sections were kept at 4°C and the staining viewed and photographed using a fluorescence microscope (ECLIPSE Ti-E, Nikon, Heidelberg university hospital, institute for immunology and serology). The primary antibodies that were used for staining are as following:

- Anti F4/80, e-Bioscience, #14-4801, 1:100, rat
- Anti fibronectin, Millipore, #ab2033, 1:100 rabbit
- Anti murine CD45, BD Pharmingen, #550539 1:100 rat

The secondary antibodies are as following:

- Goat anti rabbit, Alexa fluor 555 Thermo, #A21430 1:500
- Goat anti rat, Alexa fluor 594 Dianova, #112-585-062 1:500

2.7 Statistical evaluations

Statistical analysis of the experiments was done with the Microsoft Office software Excel 2010 and GraphPad Prism (V3, GraphPad Software Inc., San Diego, CA, USA). The statistical differences were evaluated using the two-tailed t-test for independent samples or the non-parametric Mann-Whitney test. Paired data were analysed using paired tests. Data are presented as mean and standard error of the mean (SEM). Significance was determined by a p value < or = 0.05. Wherever relevant the exact p value was provided.

3 RESULTS

3.1 Confirming of the role of fibronectin of cancer cells in tumor growth

The fibronectin produced by cancer cells plays a critical role in tumor growth, possibly through its interaction with the immune cells. Our group had already shown that deleting circulating fibronectin leads to decreased cancer growth [127], and a colleague had data suggesting that deletion of fibronectin in the cancer cells themselves also diminishes cancer growth, and that this effect might be due to a change in the immune response in the tumor [240]. To confirm the previous results of our group and expand on them, the breast cancer MDA-MB 231-B/luc⁺ cell line was used.

3.1.1 Knocking down of fibronectin in MDA cells

Normal human breast cancer MDA-MB231-B/luc⁺ line (MDA-CT) and those in which the endogenous fibronectin was eliminated by RNA interference (MDA-Kd) were cultured *in vitro* [241]. To identify the difference in fibronectin production between these two cell lines in particular the fibronectin of matrix, I used a specific protocol for matrix isolation which depends on its insolubility in sodium deoxycholate. ELISA experiments of matrix fraction (deoxycholate-insoluble fraction) show that the knockdown cells (MDA-Kd) produce significantly less fibronectin than the control cells (MDA-CT: 43±4 vs. MDA-Kd: 30.2±2.2 ng/mg, p<0.01, n=38/31) (Figure 3.1.1). In support of these findings, western blot of conditioned media of MDA-CT and MDA-Kd cells also revealed a significant decrease of fibronectin in MDA-Kd conditioned media compared to the control media (figure3.1.1).

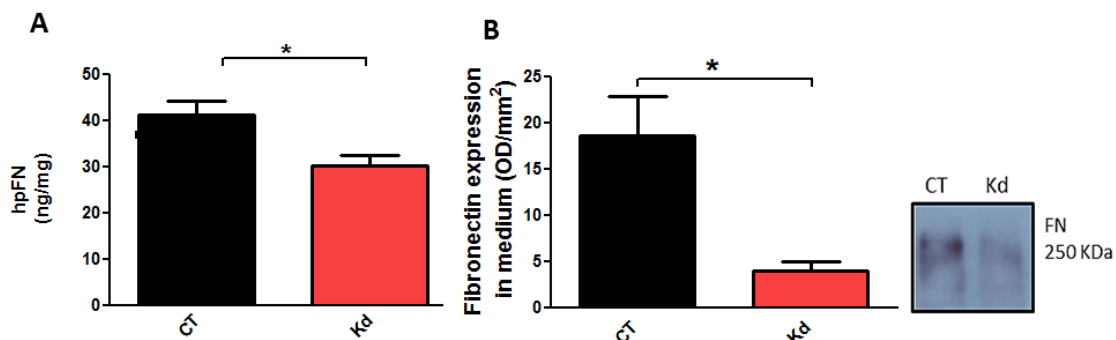


Figure 3.1.1 Fibronectin expression of MDA-MB231 cells. (A) The fibronectin of knockdown tumor cells (MDA-Kd) showed a significant reduction in its expression (n=38/31). (B) Fibronectin was also detected in media by western blotting; densitometry (left) and representative of blots (right) showed a significant decrease in MDA-Kd media compared to MDA-CT media (n=3/3/3).

3.1.2 Induction of local bone metastasis

To evaluate the effect of deletion of cancer cell fibronectin *in vitro* on cancer growth *in vivo*, both the normal MDA-CT line and the MDA-Kd line were injected intratibially into CD1nude control mice.

3.1.3 Analysis of tumor growth

Since the MDA tumor cells have a luciferase construct, tumor growth could be measured after 40 days of intratibial injection by Bioluminescence. Analysis of tumor growth showed a significant reduction in the growth of MDA-Kd cells compared to MDA-CT cells (MDA-CT: $7 \pm 1.1 \times 10^6$ vs. MDA-Kd: $10^6 \pm 3 \times 10^5$ RLU, $p < 0.0001$, $n = 29/19$) (figure 3.1.3)

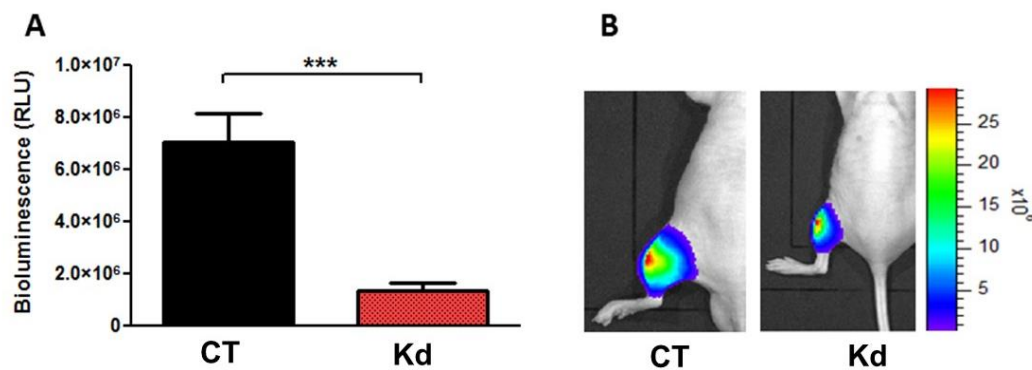


Figure 3.1.3 Tumor growth of MDA-CT and MDA-kd cells. (A) There was a significant decrease in tumor growth of MDA-Kd cells compared to the growth of MDA-CT cells. (B) Bioluminescence image of tumor growth also confirms this reduction and the light emission of luciferase-expressing in tumor cells is represented by colored pixels ($n = 29/19$).

3.1.4 Radiographic analysis of osteolytic lesions

Since the tumor cells also induce osteolysis in tibia after 40 days of tumor injection, it could be visualized by radiography in order to confirm the difference in growth between MDA-CT and MDA-Kd tumors. For the evaluation, the area, the length and width region were measured using the computer program image J.

The analysis showed that the mean area of osteolytic lesion in MDA-CT tumors was $7 \pm 1.02 \text{ mm}^2$. The mean length $5.13 \pm 0.4 \text{ mm}$ and the mean width $1.7 \pm 0.13 \text{ mm}$. A significant decrease in osteolytic lesion area of MDA-Kd tumors was detected (mean: $3 \pm 0.6 \text{ mm}^2$, (mean area CT vs. kd: $p < 0.01$, $n = 20/17$). In addition to the reduction in area, the length of osteolytic lesion of MDA-Kd tumors was also significantly reduced with an average $2 \pm 0.3 \text{ mm}$, ($p < 0.0001$, $n = 20/17$).

RESULTS

A significant decrease in the width of Kd osteolytic lesion was also detected at a mean of $1 \pm 0.0.12$ mm, ($p < 0.0001$, $n = 20/17$) (figure 3.1.4)

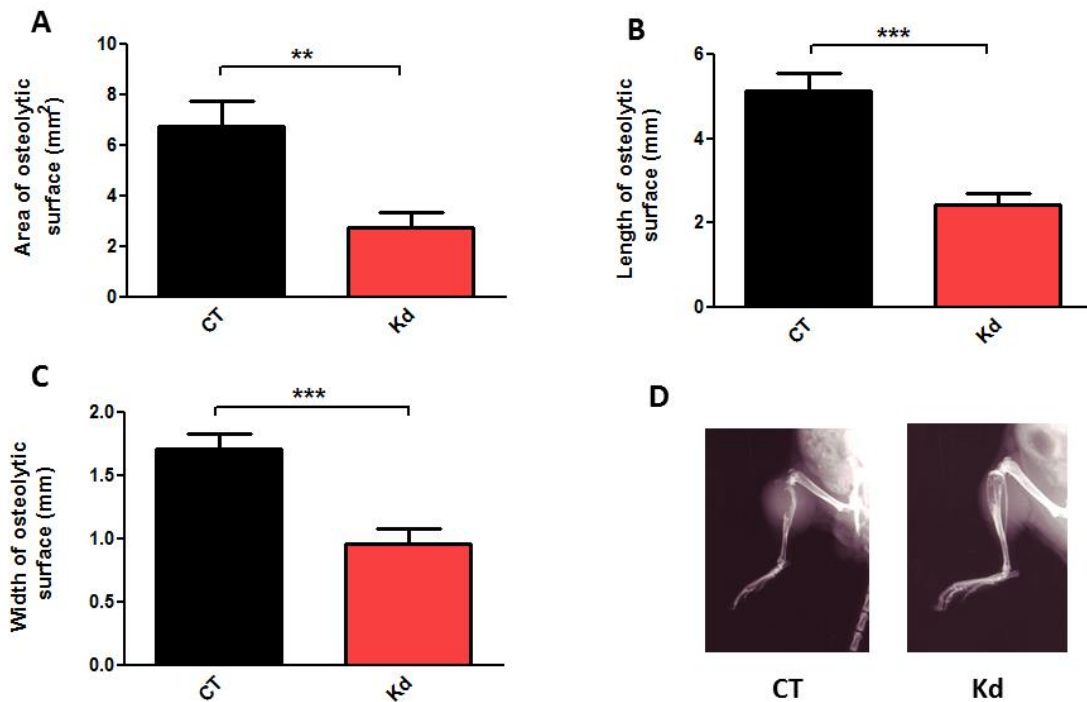


Figure 3.1.4 Size of osteolytic lesions of MDA-CT and MDA-Kd tumors by Radiography. (A, B and C) a radiographic analysis showed a significant reduction in the area, length and width of MDA-Kd tumors compared to the MDA-CT tumors. (D) X-ray images which show the reduction of osteolytic region in Kd tumors and that was consistent with the decreased tumor burden in bioluminescence imaging ($n = 20/17$).

3.1.5 Investigation of immune cells in MDA tumors

Based on the findings of a prior member of the group, Sabrina Kraft [240], we evaluated the immune cells in these tumors by flow cytometer. Only macrophages ($CD11b^- F4/80^+$) in Kd tumors increased compared to CT tumor (CT: 0.8 ± 0.2 vs. Kd: 1.5 ± 0.3 %, $p < 0.0001$, $n = 29/19$) (figure 3.1.5).

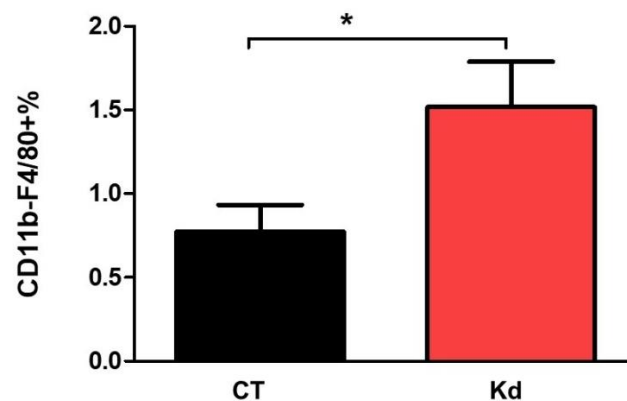


Figure 3.1.5 Immune cells in the MDA-CT and MDA-Kd tumors. The immune cells in the tumor exclusively $CD11b^- F4/80^+$ showed a significant increase in Kd tumors compared to the control tumors ($n = 16/11$).

3.2 Investigation of the effect of fibronectin accumulation inhibitor peptides in MDA human breast cancer model

Fibronectin is an important component of the extracellular matrix and affects tumor progression through different mechanisms. As mentioned before the splicing pattern of its pre-mRNA patterns is deregulated in cancer [190]. Furthermore, fibronectin facilitates invasion by modifying ECM stiffness, affecting metalloproteinase production and protecting the tumor cells from immune system during circulation [109, 115, 223]. The previous work of our group has shown that prevention of fibril formation of fibronectin by pUR4 leads to reduction of collagen accumulation and fibrosis development and improves liver function [242]. Therefore, we asked whether inhibiting fibronectin accumulation by administering pUR4 leads to a decrease or slowing down of tumor growth. We tested this using two cancer cell lines which are murine melanoma cell line B16 and human breast cancer cell line MDA-MB 231/luc⁺.

pUR4 is a polymerization fibronectin inhibitor derived from F1 protein which is the adhesion molecule of streptococcus pyogenes [151]. It contains 49 amino acids and has the following sequence:

KDQSPLAGESGETEYITEVYGNQQNPVDIDKKLPNETGFSGNMVETEDT

Recombinant scrambled peptide is similarly composed of 49 amino acids and has the following sequence:

EKGYSKPPVGNEGGDQVDEYDTMSQTKLEDEGNTLISPITFENATEQVN

3.2.1 Investigation of the effect of recombinant pUR4 and its Scrambled peptide on fibronectin of MDA cells *in vitro*

Recombinant pUR4 and its control peptide were produced, purified and tested *in vitro* on cultured MDA cells. The effect of these recombinant peptides on the matrix was assessed after 72 hours. The fibronectin content was determined by human fibronectin ELISA and recombinant pUR4 diminished significantly fibronectin in the matrix fraction (deoxycholate in-soluble fraction) as shown by ELISA of the matrix (pUR4 treated cells: 19±2 vs. Scrambled peptide treated cells: 31.4±6 ng/mg, p<0.05, n=22/17), (pUR4 treated cells: 19±2 vs. MDA-CT: 43±4 ng/mg, p<0.0001, n=22/38). These results were comparable with the values of matrix measured by ELISA in MDA-Kd cells (MDA-Kd: 30±2 vs. pUR4 treated cells: 19±2 ng/mg, p<0.0001, n=31/22) (figure 3.2.1).

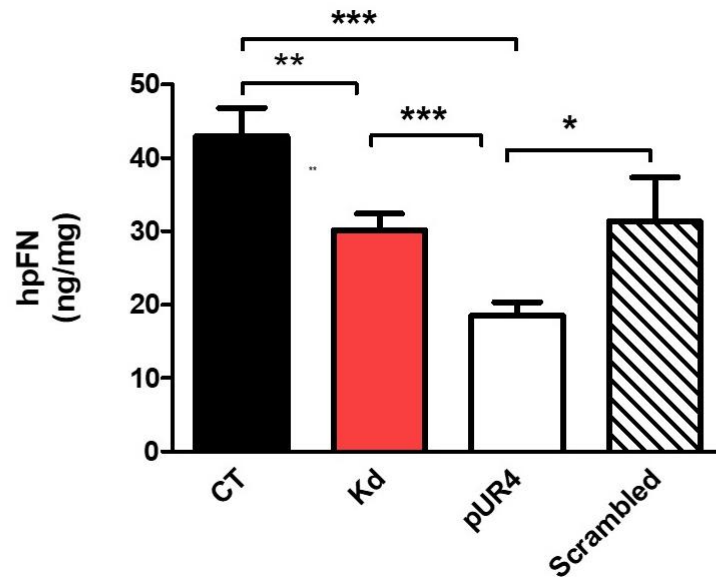


Figure 3.2.1 Recombinant pUR4 decreases matrix accumulation of MDA-CT cells *in vitro*. pUR4 decreases the fibronectin in matrix of MDA cells by ELISA (n=38/31/22/17).

3.2.2 Investigation of the effect of recombinant pUR4 on MDA tumor growth *in vivo*

The next step was to determine whether the preventing of fibronectin polymerization by delivery of pUR4 could diminish the tumor growth in mice. Therefore, an intratibial induction of breast cancer cells was carried out and the *in vivo* experiments were designed as following (figure 3.2.2A):

- The duration of each experiment is 40 days.
- Tumor growth is monitored weekly and also after treatment by bioluminescence.
- On day 28 the mice start receiving 0.5 mg of peptides for ten days.
- Radiography is done before and after treatment

On day 40, the mice are euthanized; tumors are isolated and digested for immune staining.

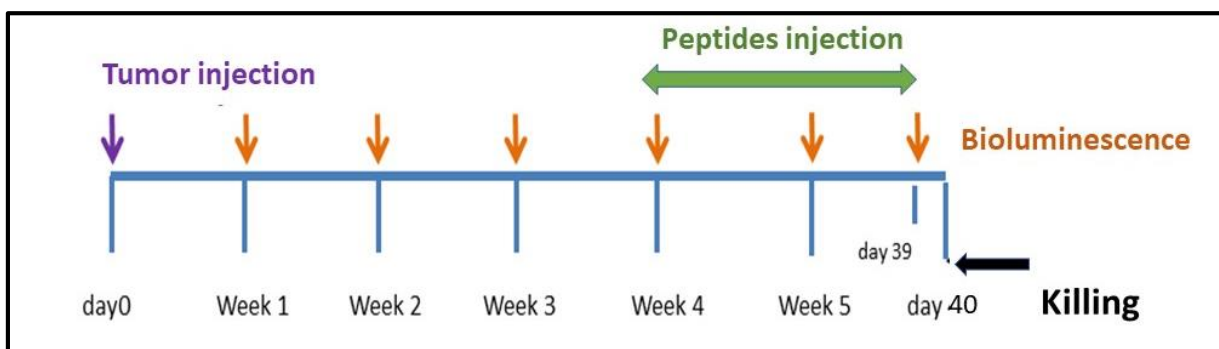


Figure 3.2.2A. Schedule of *in vivo* experiment MDA module.

RESULTS

Analysis of tumor growth by bioluminescence measurement before and after of peptides injection showed that the rate of increase of tumor growth in pUR4 treated mice was significantly lower after treatment compared to Scrambled treated mice and control mice (day 39: CT: $8.364 \times 10^6 \pm 1 \times 10^6$ RLU vs. pUR4: $4.6 \times 10^6 \pm 1.013 \times 10^5$ RLU, $p < 0.05$, $n = 32/20$), (pUR4: $4.549 \times 10^6 \pm 1 \times 10^6$ RLU vs. Scrambled: $9.4 \times 10^6 \pm 2.44 \times 10^6$ RLU, $p < 0.05$, $n = 20/10$) (figure 3.2.2B).

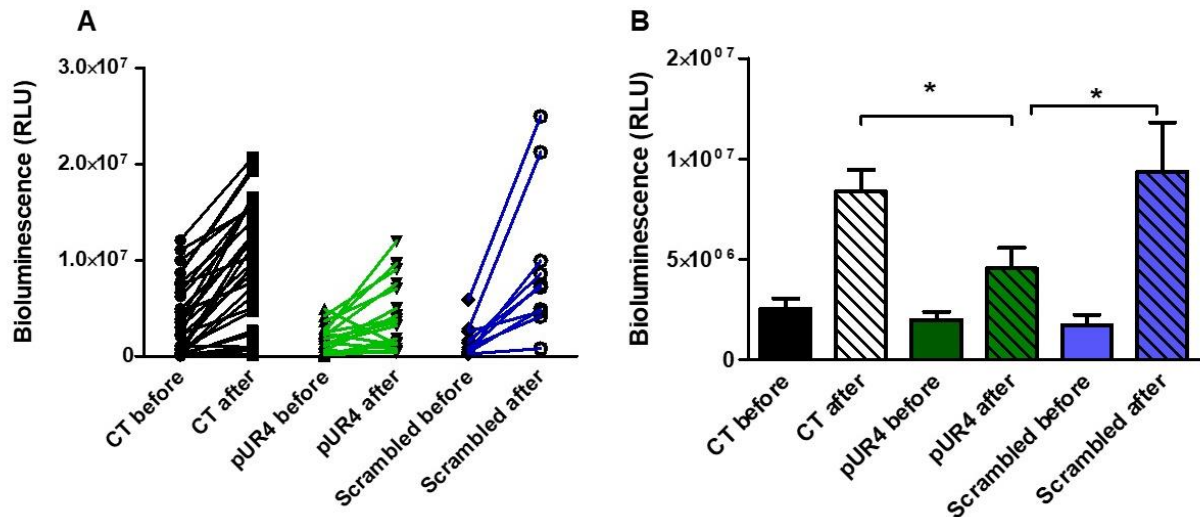


Figure 3.2.2B Tumor growth before and after of recombinant peptides injection. The detected photon emission was significantly reduced in mice in which the pUR4 was applied compared to the control groups (A and B) ($n = 32/20/10$).

3.2.3 Investigation of pUR4 entry into MDA tumors

As shown previously, recombinant pUR4 slowed down of MDA tumor growth. Therefore, the further question was raised whether pUR4 could be detected in tumor lysates in order to confirm its effect on tumor. The administrated pUR4 and Scrambled contain poly histidine tag sequence which forms of six histidine residues at the N-terminus of each peptide, therefore the presence of these peptides in the tumors could be confirmed by detection of this poly-histidine sequence which has the expected mass about 15 kDa. That was done by western blot of protein tumor lysates using anti-polyhistidine-tag antibody. The blots of protein lysates of tumors ensured that the systemically administrated peptides could reach the tumors and perform its effect (figure 3.2.3).

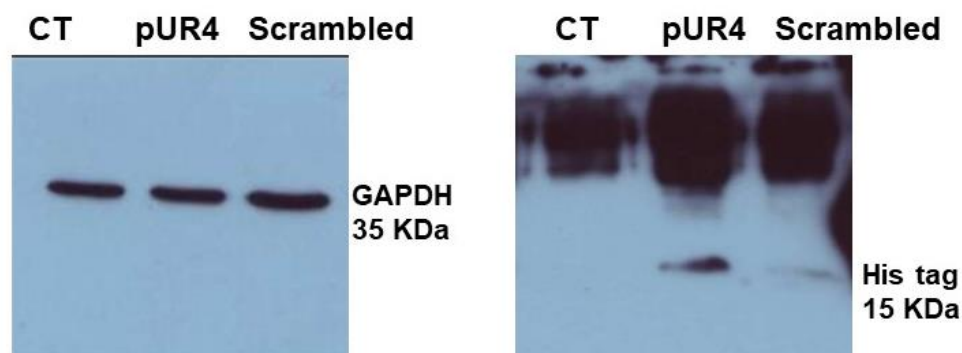


Figure 3.2.3 pUR4 and Scrambled peptides enter the tumor after application. The western blot analysis of the tumor lysates which were treated with peptides showed the His-tag contained in the peptides and as a consequence the respective peptides were in the tumors.

3.2.4 pUR4 decreases fibronectin content of MDA tumors

The fibronectin content of MDA tumors which were treated with recombinant peptides was also assessed by ELISA and corrected to the total protein content. Less fibronectin was significantly detected in recombinant pur4 treated tumors compared to the pUR4scr treated tumors (pur4 treated tumors (pUR4 treated tumors: $234 \pm 32\%$ vs. Scrambled: 403 ± 58 ng/mg, $p < 0.05$, $n = 8/7$). No difference was observed in pUR4 treated tumors compared to the control tumors ($p = ns$, $n = 8/7$) (figure 3.2.4).

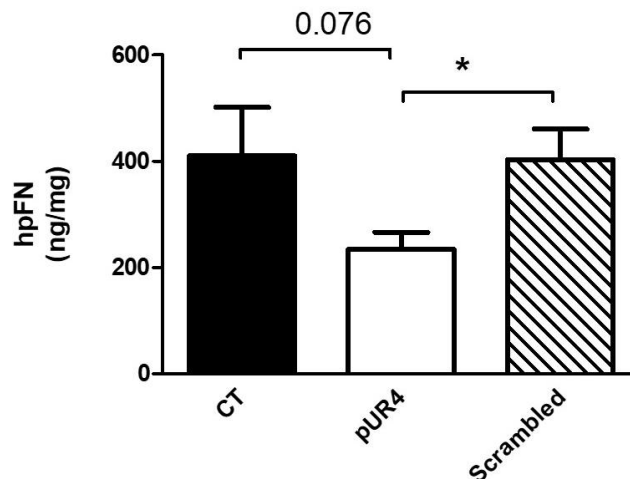


Figure 3.2.4 Fibronectin content in recombinant treated tumors. There was a significant decrease in pUR4 treated tumors compared to Scrambled treated tumors but not to the control tumors ($n = 7/8/7$).

3.2.5 Radiographic analysis of MDA tumors before and after of recombinant peptides injection

X-ray images were taken before and after peptide injection. Due to the significant advantage of pUR4 injection in slowing down of tumor growth that was shown by bioluminescence, it was also important to investigate whether this effect could be confirmed by radiography. The average area, length and width of osteolytic lesions in pUR4 treated mice upon injection were significantly less than the Scrambled treated mice and control mice (area: CT: 7 ± 1.016 mm vs. pUR4: 4 ± 0.7 mm, $p < 0.05$, $n = 20/17$), (area: Scrambled treated group: 8.61 ± 1.365 mm² vs. pUR4 treated group: 4 ± 0.7 mm, $p < 0.05$, $n = 7/17$), (length: CT: 5 ± 0.4 mm vs. pUR4 treated group: 3.3 ± 0.4 mm, $p < 0.01$, $n = 20/17$), (length: Scrambled treated group: 5 ± 0.5 mm vs. pUR4 treated group: 3.3 ± 0.4 mm, $p < 0.05$, $n = 7/17$), (width: CT 1.7 ± 0.13 mm vs. pUR4 treated group: 1.21 ± 0.1 mm, $p < 0.01$, $n = 20/17$), (width: Scrambled treated group: 2 ± 0.2 mm vs. pUR4 treated group: 1.21 ± 0.1 mm, $p < 0.001$, $n = 7/17$) (figure 3.2.5).

RESULTS

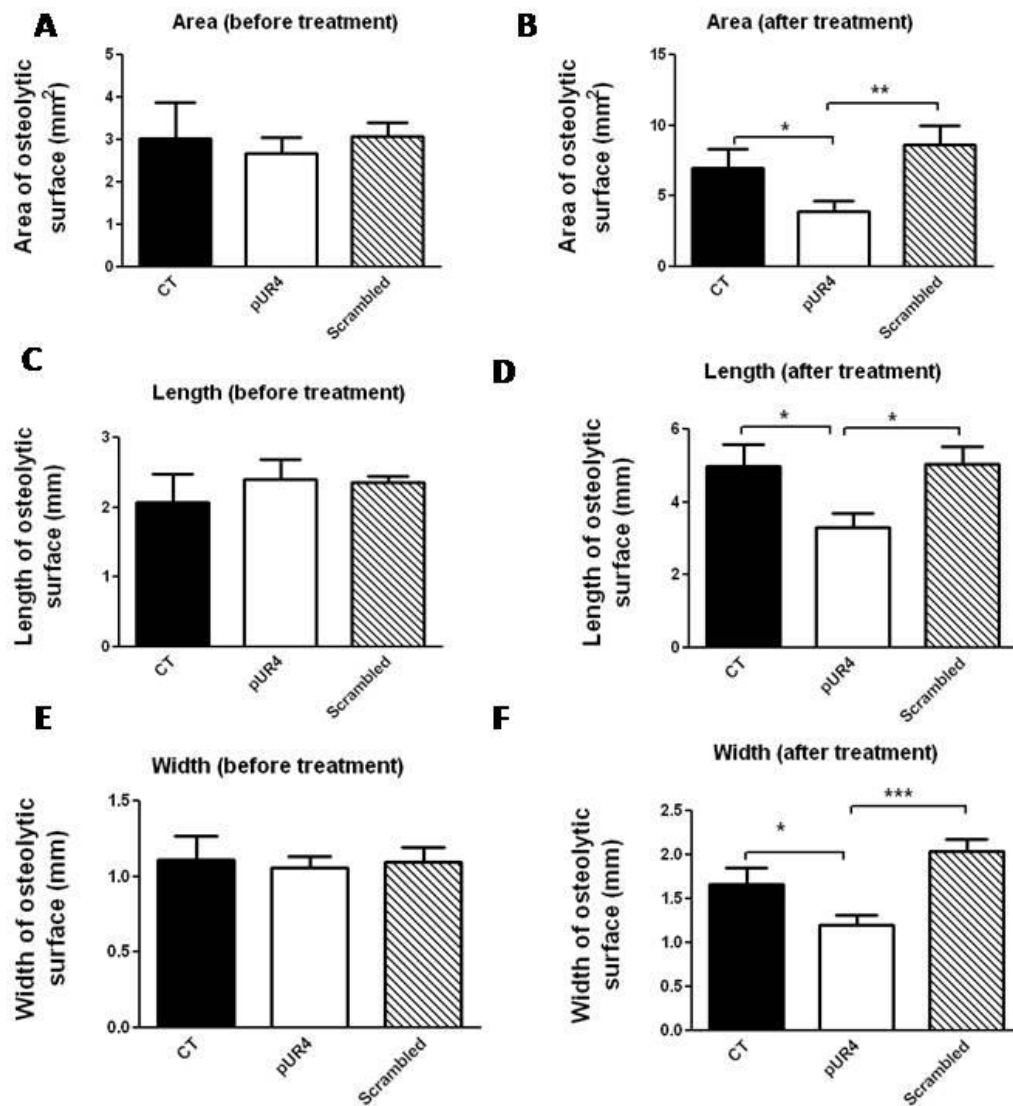


Figure 3.2.5 Radiographic analysis before and after of recombinant peptides application. The average area, length and width of the osteolytic lesions were statistically significantly reduced upon pUR4 treatment compared to the control groups (n=20/17/7).

3.2.6 Investigation of immune cells in MDA tumors treated with recombinant peptides

In order to investigate whether the immune cells are enrolled in slowing down of tumor growth by pUR4 treatment, immune cells in these tumors were analyzed by flow cytometry in parallel with control tumors. There were no significant differences in total immune cells or monocytes ($p=ns$, $n=11/18/8$). The granulocytes and myeloid derived suppressor cells showed a significant decrease in pUR4 and Scrambled treated tumors compared to the control tumors (CD45⁺Gr1⁺ %) (CT: 4.318 ± 1.92 vs. pUR4: 1.111 ± 0.17 %, $p < 0.05$, $n=11/18$), (CD11b⁺Gr1⁺ %) (CT: 4.236 ± 1.9 vs. pUR4: 1.07 ± 0.18 %, $p < 0.05$, $n=11/18$). However, the subpopulation CD11b⁺F4/80⁺ showed a distinctive increase but not significant in pUR4 treated groups compared to the control groups (figure 3.2.6).

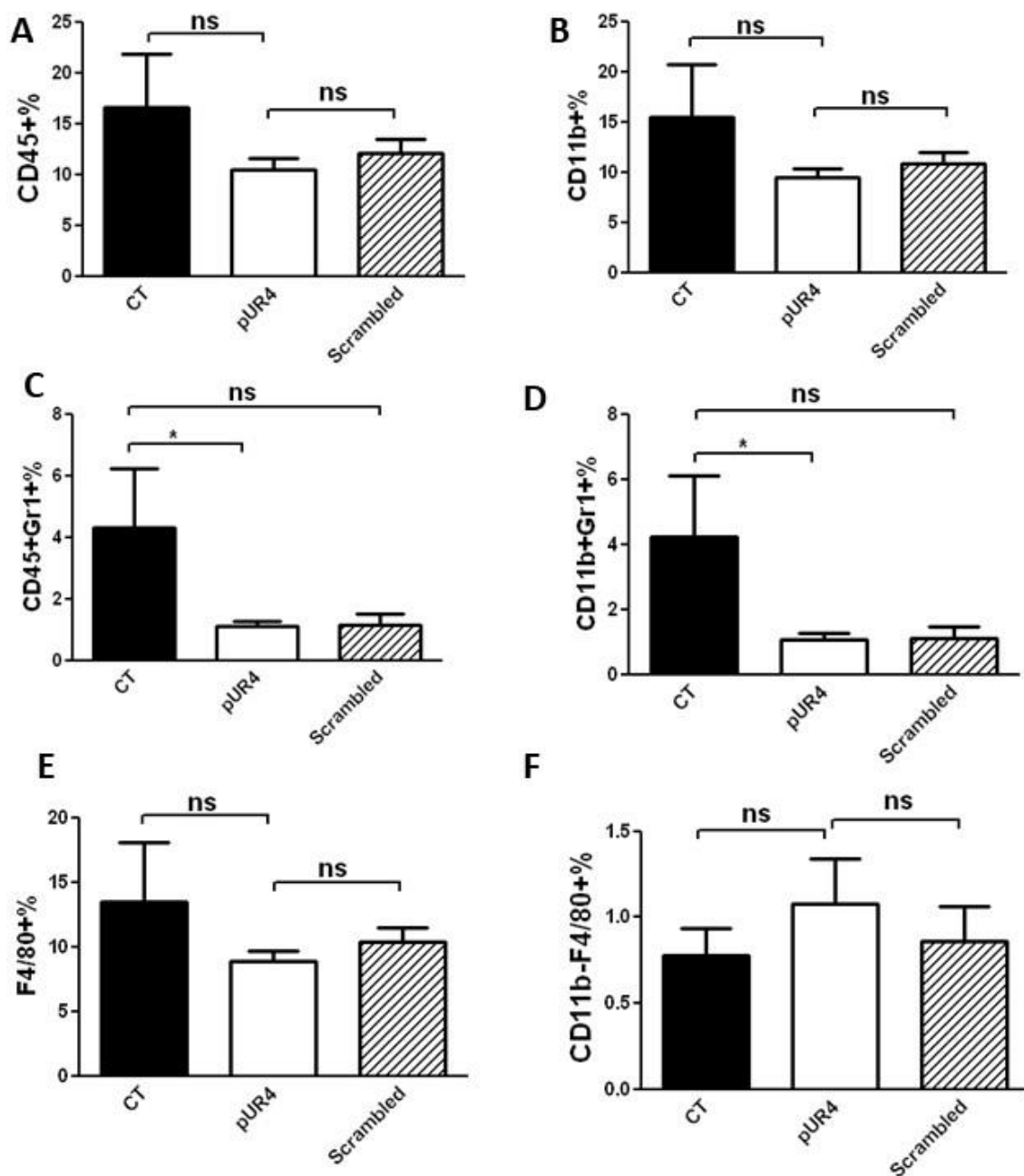


Figure 3.2.6 Analysis of immune cells in MDA tumors treated by recombinant pUR4. There were no significant differences in total immune cells (A), monocytes (B) or macrophages

RESULTS

(E) and (F) of tumors. The granulocytes (C) and myeloid suppressor cells (D) showed a significant decrease in pUR4 and Scrambled treated tumors compared to the control (D) ($p=ns$, $n=11/18/8$).

3.2.7 Investigation of cancer and stromal cells in MDA tumors treated with recombinant peptides

It is widely known that the stromal cells undergo changes in the presence of cancer cells and play a role during initiation, progression and metastasis of cancer. Therefore, it was interesting to determine how pUR4 might affect stromal cells. Their percentage could be evaluated by flow cytometry, however there was no difference in stromal cells between groups ($p=ns$, $n=11/18/8$). That was also confirmed using qPCR to evaluate the relative composition of cancers after depletion from immune cells (using geneticin expression, which quantifies the amount of cancer cells). Thus, recombinant pUR4 affects neither stromal cells nor cancer cells (figure 3.2.7)

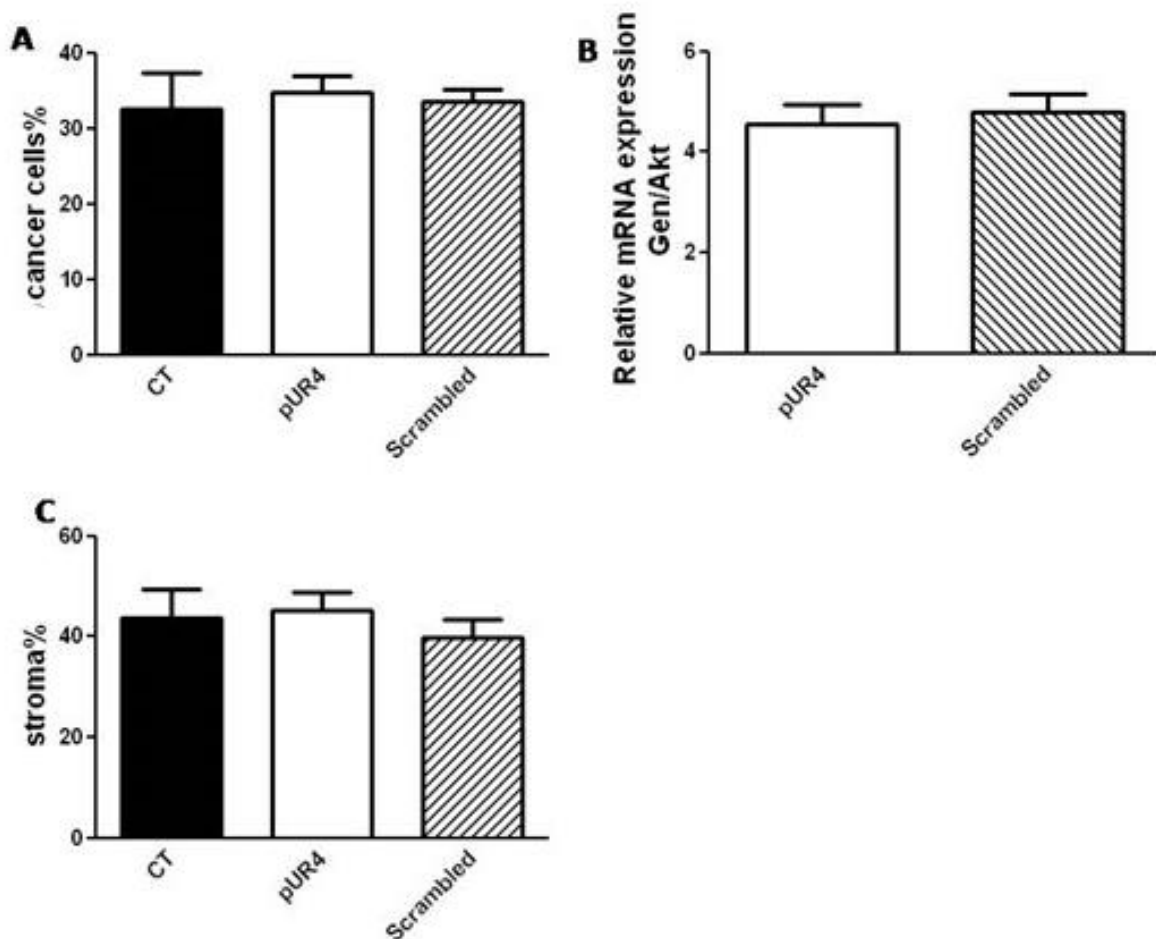


Figure 3.2.7 Analysis of cancer cells and stromal cells in MDA tumors treated by recombinant peptides. No difference was found in cancer cells neither by flow cytometry nor by geneticin mRNA expression. There was also no significant change in stromal cells ($n=11/18/8$).

The previous data indicate that recombinant pUR4 as a fibronectin polymerization inhibitor peptide could diminish fibronectin accumulation of MDA cancer cells *in vitro*,

RESULTS

slowdown of tumor growth *in vivo*, trend to increase of macrophages exclusively the sub-population CD11b⁺F4/80⁺ and to decrease significantly of myeloid derived suppressor cells MDSCs. However, no effect could be obtained on total stroma and cancer cells.

3.3 Evaluation of the effect of synthetic peptides in MDA tumors

In order to investigate whether there is a difference in effect between the recombinant and synthetic pUR4 and also to further understand clearly its mechanism and especially the involvement of immune cells in its activity, pUR4 and its control peptide pUR4scr were synthesized at Max Planck Institute of Biochemistry in Martinsried and tested *in vitro* and *in vivo* on human breast cancer cells.

3.3.1 Investigation of the effect of synthetic pUR4 and its scramble on fibronectin of MDA cells *in vitro*

As shown in the figure, fibronectin ELISA confirmed the effect of pUR4 on fibronectin accumulation in breast cancer cells *in vitro* and the synthetic scramble caused also further reduction in fibronectin content (CT: 462.5±33.84 vs. pUR4: 250.9±25.17 ng/mg, $p < 0.001$, $n = 32/12$); (pUR4: 250.9±25.17 vs. Scrambled: 473.5±51.87 ng/mg, $p < 0.001$, $n = 12/6$) (figure 3.3.1)

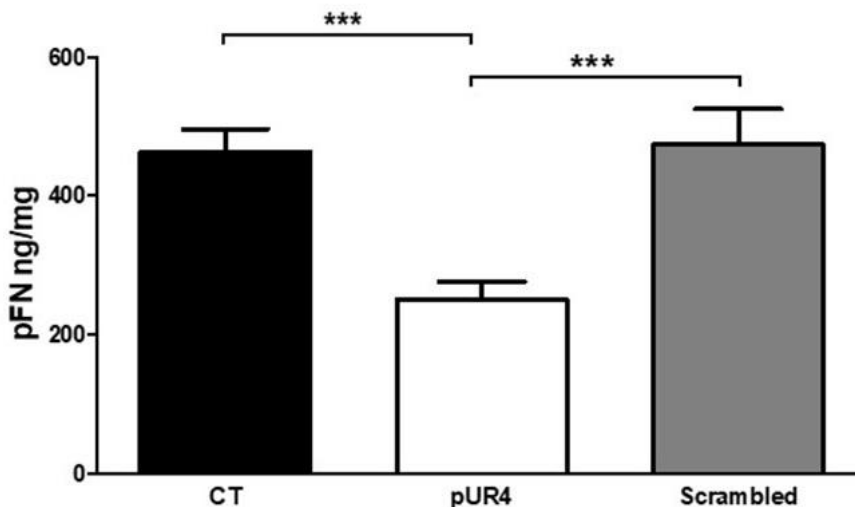


Figure 3.3.1 Synthetic pUR4 decreases fibronectin accumulation of MDA cells *in vitro*. fibronectin quantified in total cell lysate of MDA cells *in vitro* by ELISA after 72 hours induction of pUR4 was significantly less compared to the control ($n = 32/12/6$).

3.3.2 Investigation of the effect of synthetic pUR4 and its scramble peptide in MDA cells *in vivo*

To further investigate the effect of synthetic peptides sequence on tumor growth, MDA tumors which were injected intratibially were treated with these peptides and compared to the control tumors. pUR4 kept slowing down of MDA tumor growth and that was

RESULTS

reproducible compared to the recombinant version (Scrambled: $1 \times 10^7 \pm 1.8 \times 10^6$ RLU vs. pUR4: $6.73 \times 10^6 \pm 1 \times 10^6$ RLU, $p < 0.05$, $n = 16/20$). (figure 3.3.2).

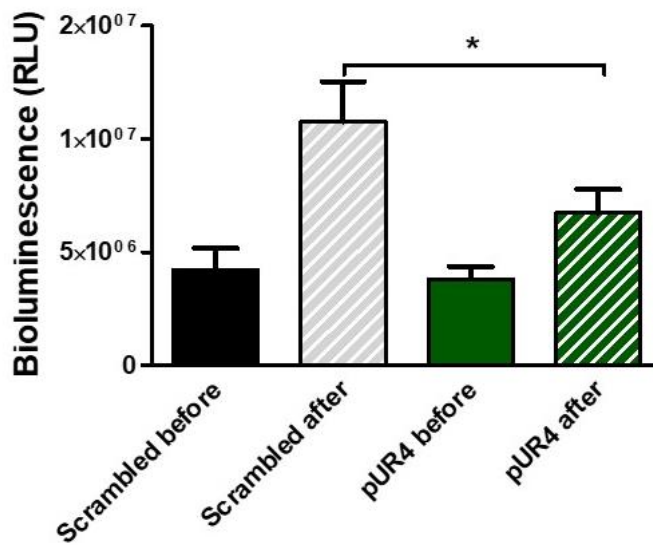


Figure 3.3.2 Analysis of tumor growth before and after of synthetic peptides injection. In comparison with control group, a statistically significant reduction in tumor growth was obtained in mice received of pUR4 and the first modified peptide ($n = 16/20$).

3.3.3 Evaluation of fibronectin content of MDA tumors treated with synthetic peptides

The effect of these peptides on fibronectin of MDA tumors should also directly be observed. Therefore, human fibronectin ELISA of the total protein lysates of treated tumors was done. Treatment by scrambled peptide did not affect the fibronectin content of MDA tumors compared with the control tumors. The tumors which were treated by synthetic pUR4 slightly reduced the fibronectin of MDA tumors compared to the control ones ($p = ns$, $n = 3/3/3$) (figure 3.3.3).

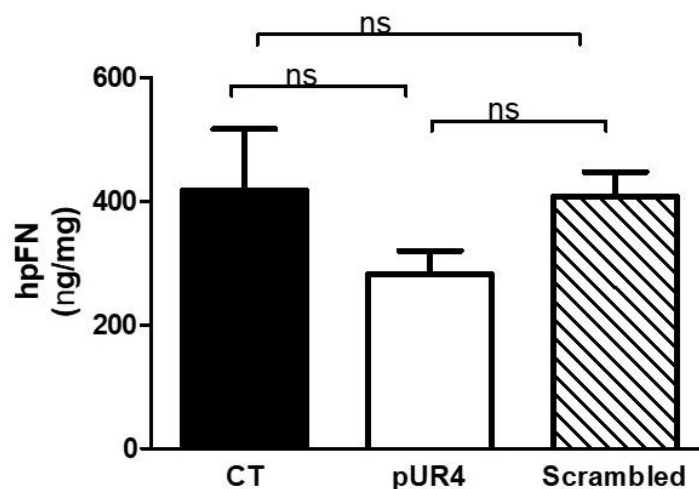


Figure 3.3.3 Fibronectin content in MDA tumors treated with synthetic peptides. ELISA of MDA tumors showed no significant difference among groups ($n = 3/3/3$).

3.3.4 Radiographic analysis of MDA tumors treated with synthetic peptides

In order to find a difference in osteolytic lesions among groups before and after treatment with the synthetic peptides, x ray analysis was done for the MDA tumors as described previously. No difference could be obtained among groups in the area, length and width of osteolytic lesions after the treatment with the synthetic peptides ($p=ns$, $n=15/15/11$) (figure 3.3.4).

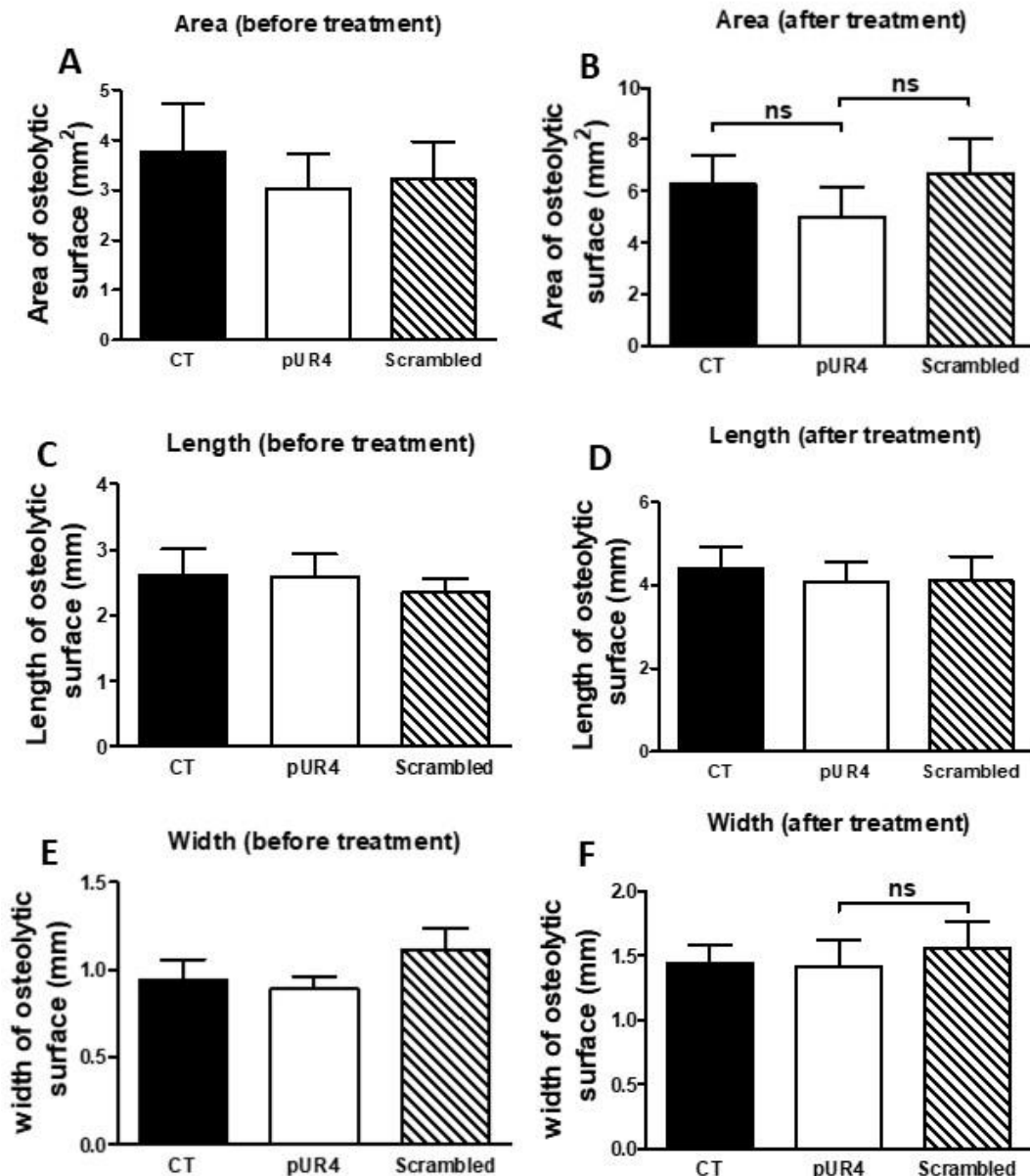


Figure 3.3.4 Radiographic analysis of osteolytic lesions before and after of synthetic peptides injection. The average area of osteolytic lesions was slightly reduced compared to the control group (B) ($n=15/15/11$).

3.3.5 Evaluation of immune cells of MDA tumors treated with synthetic peptides

To better understand the impact of peptides on the immune response of MDA tumors and as a consequence the tumor growth, mice injected intratibial tumors and treated with synthetic peptides were euthanized and immune cells of tumors were analyzed by flow cytometry. Leukocytes, monocytes, granulocytes and myeloid derived suppressor cells showed a little decrease in treated tumors but without significance ($p=ns$, $n=18/20/9$). The macrophages especially the subpopulation $CD11b^-F4/80^+$ showed a slight increase in pUR4 treated group compared to the control group ($p=ns$, $n=18/20$) (figure 3.3.5).

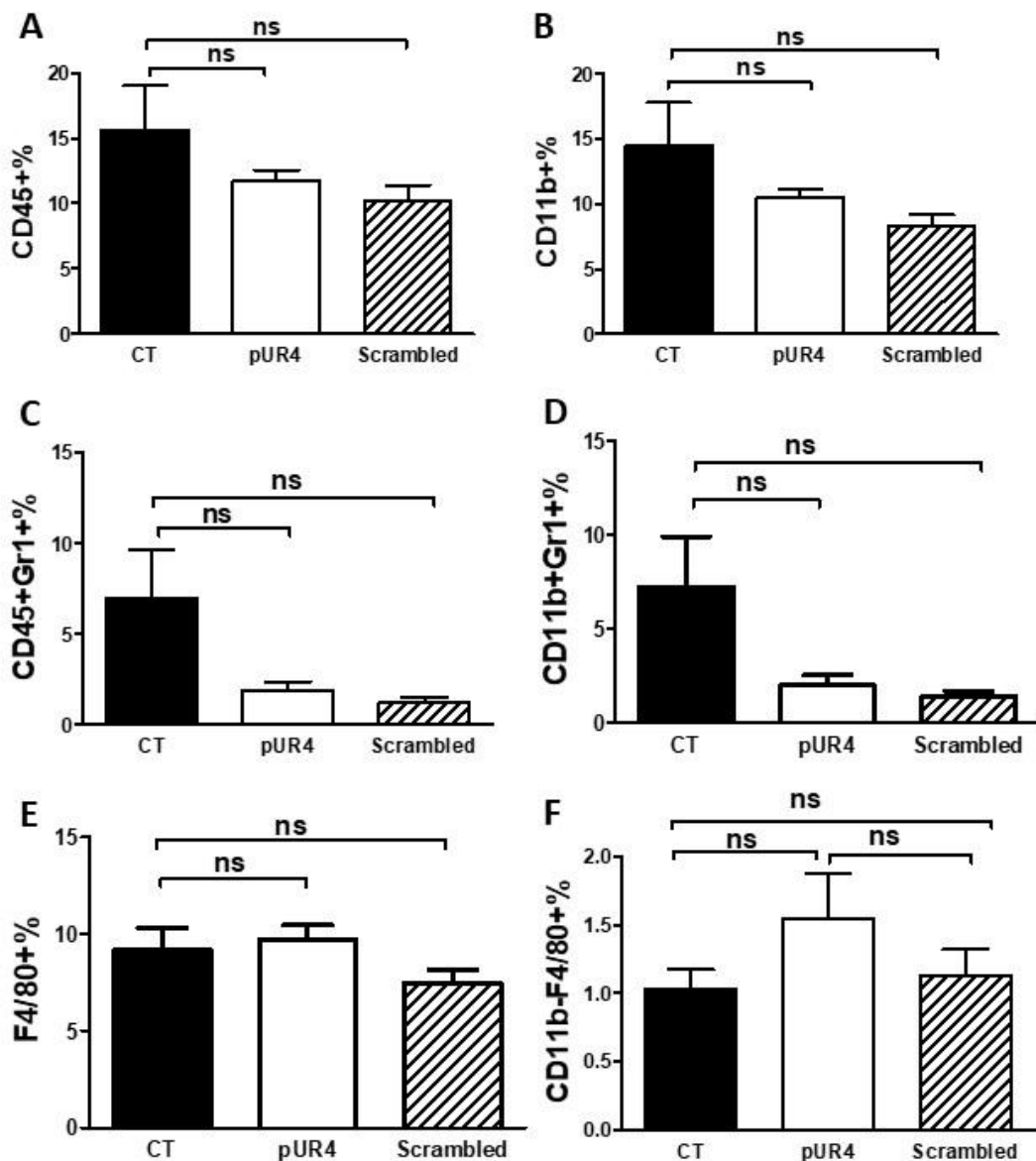


Figure 3.3.5 Analysis of immune cells in MDA tumors treated with synthetic peptides. No significant difference between groups was obtained in immune cells analyzed by a flow cytometry ($n=18/20/9$).

3.3.6 Evaluation of cancer and stromal cells of MDA tumors treated with synthetic peptides

Flow cytometry analysis of digested tumors was also done to investigate the effect of synthetic peptides on the stromal and cancer cells. No difference among groups was detected in stromal cells or cancer cells ($p=ns$, $n=18/20/9$) (figure 3.3.6).

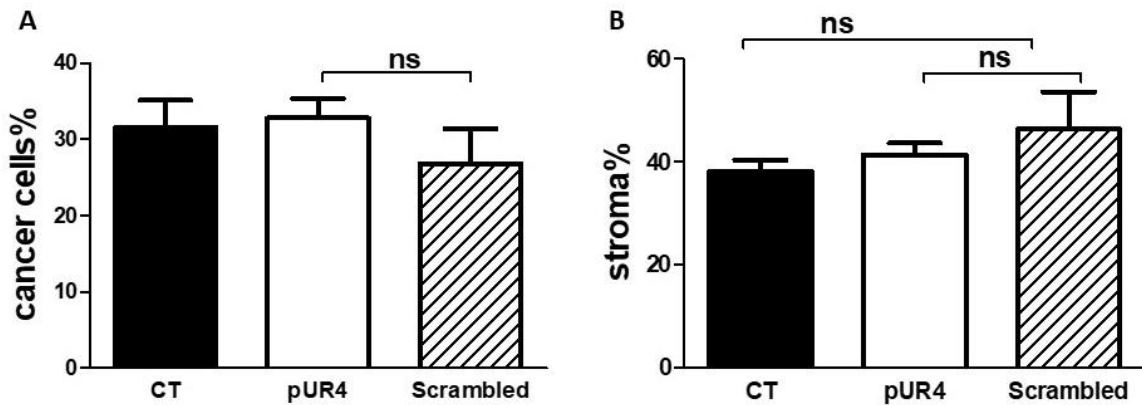


Figure 3.3.6 Analysis of stromal cells and cancer cells in MDA tumors treated with synthetic peptides. No difference was observed between groups in the percentage of stromal or cancer cells as analyzed by flow cytometry (A and B) ($n=18/20/9$).

3.4 Effect of pUR4 in immunocompetent mice

Since the peptides were tested in immune deficient mice where T cells are absent, it was important to further characterize their effect in immunocompetent mice in order to improve our understanding about their mechanism and also to investigate whether T cells are involved in their effect.

3.4.1 Investigation of the effect of recombinant pUR4 and its scramble peptide on fibronectin of B16 melanoma cells *in vitro*

Recombinant pUR4 and its control peptide were tested *in vitro* on cultured B16 melanoma cells that has been isolated from the skin of C57 / BL6 (H-2b) mice. It is a highly invasive skin cancer cell line that can be applied subcutaneously under the epidermis of mice [243]. The effect of these recombinant peptides on the matrix was assessed after 72 hours. The fibronectin content was determined by fibronectin murine ELISA and recombinant pUR4 decreased significantly matrix fibronectin compared to the control groups (CT: 291.3 ± 37.34 vs. pUR4: 185.2 ± 25.24 ng/mg, $p < 0.05$, $n=23/21$) (figure 3.4.1).

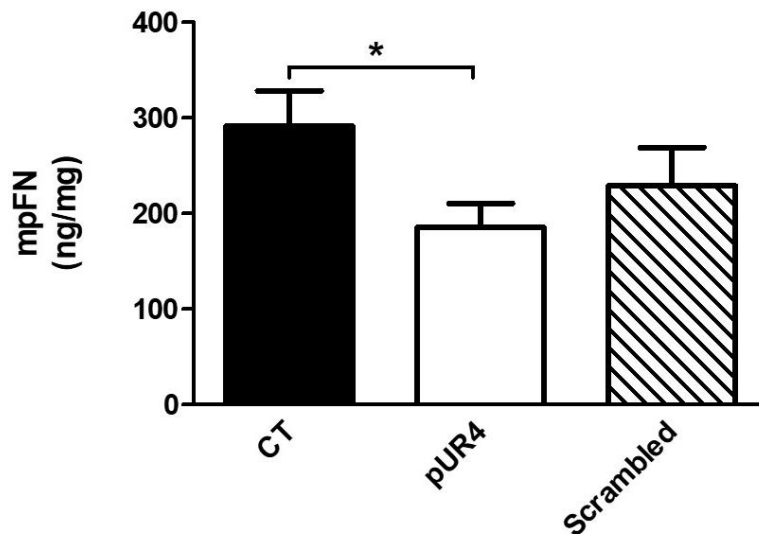


Figure 3.4.1 Recombinant pUR4 decreases matrix accumulation of melanoma cells *in vitro*. pUR4 decreases the fibronectin in melanoma matrix by ELISA (n=23/21/21).

3.4.2 Investigation of the effect of synthetic pUR4 and its scramble peptide on fibronectin of B16 melanoma cells *in vitro*

As the synthetic versions of peptides were tested on MDA cancer module, it was critical also to further characterize their effects on B16 cancer module. The effect of synthetic version of pUR4 and its scramble was also tested *in vitro* on B16 melanoma cells. The fibronectin content of total protein lysates of B16 melanoma cells was assessed by ELISA after 72 hours of peptides induction. No significant difference was observed among groups as shown in figure (3.4.2) (p=ns, n=12/12/12).

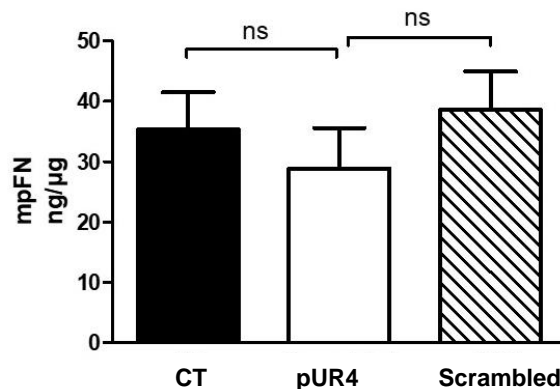


Figure 3.4.2 Effect of synthetic peptides on fibronectin accumulation of B16 melanoma cells *in vitro*. No significant effect was observed on fibronectin accumulation of B16 melanoma cells after 72 hours of synthetic peptides induction as assessed by ELISA (n=12/12/12)

3.4.3 Investigation of the effect of synthetic peptides on B16 tumors growth *in vivo*

To further investigate the effect of pUR4 on melanoma cells *in vivo*, subcutaneous injection of murine B16 melanoma cells was carried out and the *in vivo* experiment was designed as shown in figure (3.4.3A)

At the age of 5 weeks mice were injected subcutaneously with 1×10^6 B16 melanoma cells. Tumor growth was evaluated starting day 4 every other day. On day 8, mice were briefly anesthetized by isoflurane and tumors were measured using calipers. Treatment was then started using peptides (0.5 mg daily) for 5 days.

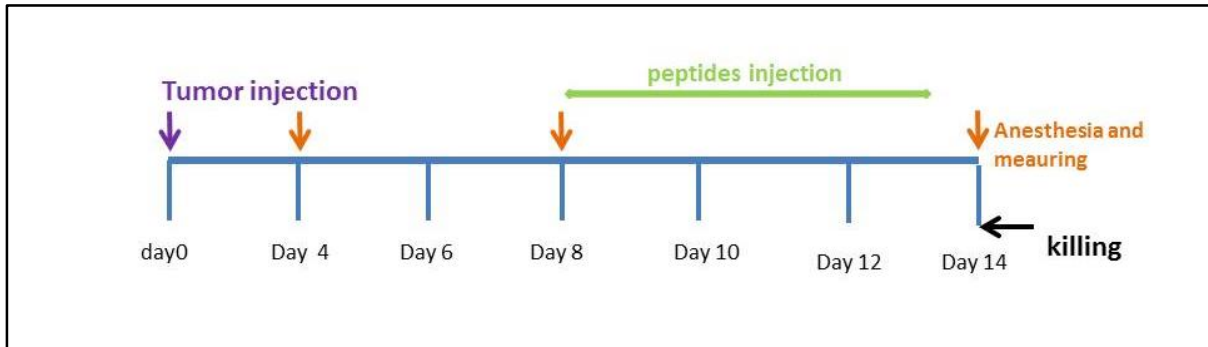


Figure 3.4.3A Schedule of *in vivo* experiment B16 model

After sacrificing the mice, the length, the width and the weight of tumors were determined and compared to the ones of before treatment. The width of pUR4 treated tumors was significantly reduced compared to the scrambled treated group (Scrambled: 0.4 ± 0.03 vs. pUR4: 0.3 ± 0.02 mm, $p < 0.05$, $n = 18/18$) (figure 3.4.3D). Interestingly, there was no effect of synthetic pUR4 on the width of B16 tumors. However, a significant reduction was observed in the weight of pUR4 treated tumors compared to the control and scrambled treated tumors (CT: 124 ± 20 vs. pUR4: 56 ± 11.5 mg, $p < 0.05$, $n = 16/18$), (Scrambled: 111 ± 26 vs. pUR4: 56 ± 11.5 mg, $p < 0.05$, $n = 18/18$) (figure 3.4.3E).

RESULTS

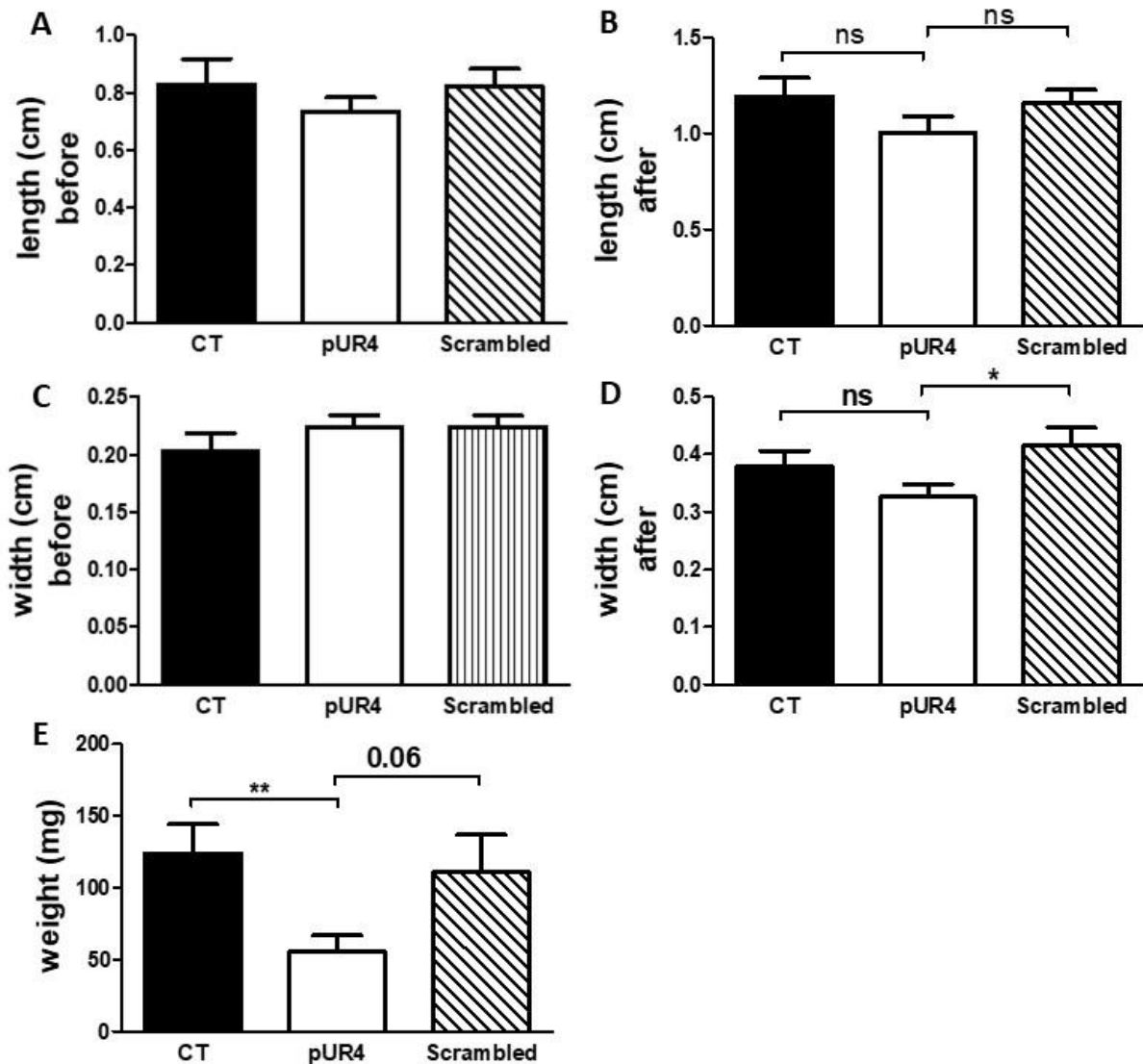


Figure 3.4.3 Tumor length, width and weight of B16 melanoma before and after of synthetic peptides treatment. There was a significant reduction in the width and the weight of pUR4 treated tumors compared to the control tumors (D and E) (n=16/18/18).

3.4.4 Effect of the synthetic pUR4 on the immune cells of B16 tumors

Since the fibronectin affects the immune response, it was important to investigate how pUR4 could affect the immune cells in B16 tumors. Analysis by flow cytometry of digested tumors showed that inhibition of fibronectin polymerization by synthetic pUR4 administration results in a significant difference in leukocytes (CD45⁺: CT: 17.34±1.7 vs. pUR4: 26±1.3 %, p<0.05, n=16/18), monocytes (CD11b⁺: CT: 7±0.6 vs. pUR4: 10±1.2 %, p<0.05, n=16/18), granulocytes (CD45⁺Gr1⁺: CT: 4±0.3 vs. pUR4: 6.7±1.2 %, p<0.05, n=16/18), myeloid derived suppressor cells (CD11b⁺Gr1⁺: CT: 3.45±0.3 vs. pUR4: 5.5±0.9 %, p<0.05, n=16/18), myeloid derived suppressor cells (CD11b⁺Gr1⁺) and macrophages (F4/80⁺: CT: 9.5±0.9 vs. pUR4: 14.4±0.6 %, p<0.0001, n=16/18). Macrophages and especially the sub-population (CD11b⁻F4/80⁺) showed a significant reduction in pUR4 treated tumors compared to scrambled and control treated tumors as well (F4/80⁺: Scrambled: 11.7±0.8 vs. pUR4: 14.4±0.6 %, p<0.00, n=18/18), (CD11b⁻F4/80⁺: CT: 2.8±0.7 vs. pUR4: 5±0.8 %, p<0.05, n=16/18) (Scrambled: 3±0.4 vs. pUR4: 5±0.8%, p<0.05, n=18/18) (figure 3.4.4 E and F).

RESULTS

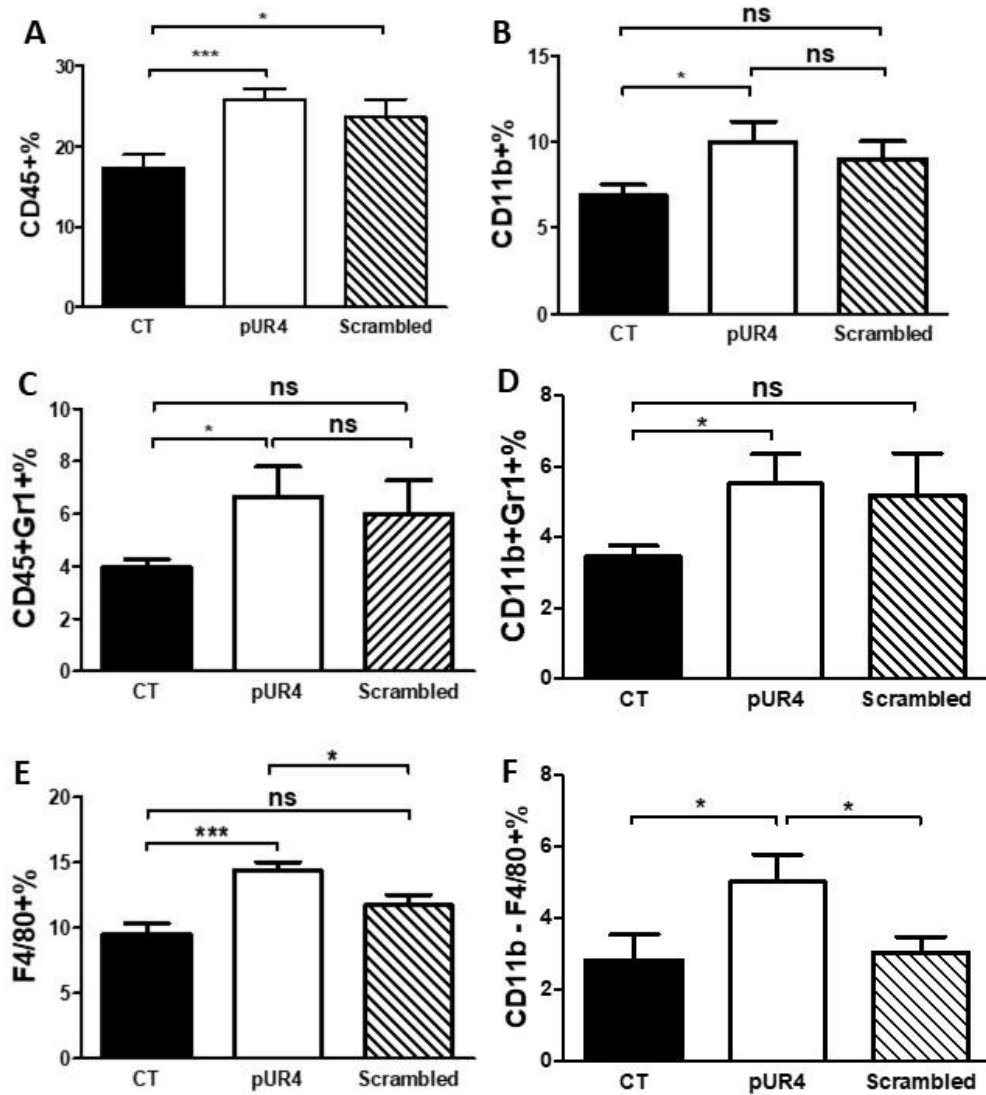


Figure 3.4.4 Effect of synthetic pUR4 on immune cells of B16 tumors. There was a significant increase in the number of leukocytes (CD45⁺) (A), monocytes (CD11b⁺) (B), granulocytes (CD45⁺Gr1⁺) (C), myeloid derived suppressor cells (CD11b⁺Gr1⁺) (D) and macrophages (F4/80⁺ and especially CD11b⁺F4/80⁺) (E and F) in pUR4 treated tumors compared to control tumors (n=16/18/18).

3.4.5 Effect of the synthetic pUR4 on cancer and stromal cells of B16 tumors

Stromal cells play a prominent role in tumor microenvironment. Therefore, it was important to find out the effect of synthetic pUR4 delivery on total stromal cells of B16 tumors. B16 cancer cells were pre-stained using e-flour before injection in order to enable the analysis of fibronectin polymerization inhibitor effect on stromal and cancer cells by flow cytometry. Stromal cells were evaluated from the CD45⁻ cells after excluding of cancer cells. Treatment by pUR4 did not affect cancer cells. A significant decrease was observed in the percentage of stromal cells in pUR4 treated tumors compared to control tumors (CT: 77±2 vs. pUR4: 69±2 %, p<0.01, n=16/18) (figure 3.4.5).

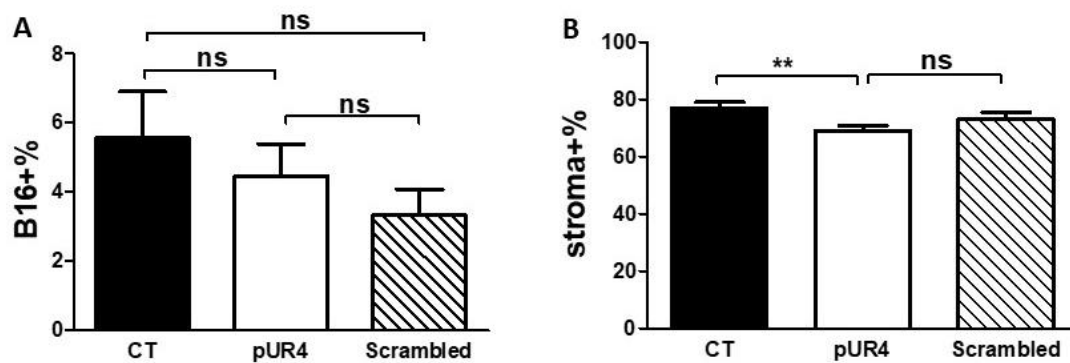


Figure 3.4.5 Effect of synthetic pUR4 on B16 melanoma cells and stromal in B16 tumors. No difference was obtained in cancer cells among groups (p=ns, n=16/18/18) (A). A significant reduction was obtained in stromal cells (which were taken from the live cells after exclusion of immune cells (CD45⁺) and e-flour stained B16 melanoma cells) in pUR4 treated tumors compared to control tumors (n=16/18).

3.5 Evaluation of modified pUR4 effect on MDA cells

Based on the previous functional binding studies of pUR4 [148, 151, 234], new modified peptide was designed and tested on MDA cells. The new modified sequence includes two main motifs which mimics the ones in pUR4 and can interact with ³FNI and ²FNI modules of fibronectin with high affinity.

These synthetic peptides were tested *in vitro* on human breast cancer cells MDA-CT, the unexpected results were that not only pUR4 but also its new modified peptide diminished significantly fibronectin accumulation of MDA-CT cells as quantified by ELISA (CT: 46.8±4.2 vs. modified: 19.12±1.14 ng/mg, p<0.0001, n=36/30), (CT: 46.8±4.2 vs. pUR4: 25±2.4 ng/mg, p<0.05, n=36/19), (pUR4: 25±2.4 vs. modified: 19.12±1.14ng/mg, p<0.001, n=19/30) (figure 3.5).

RESULTS

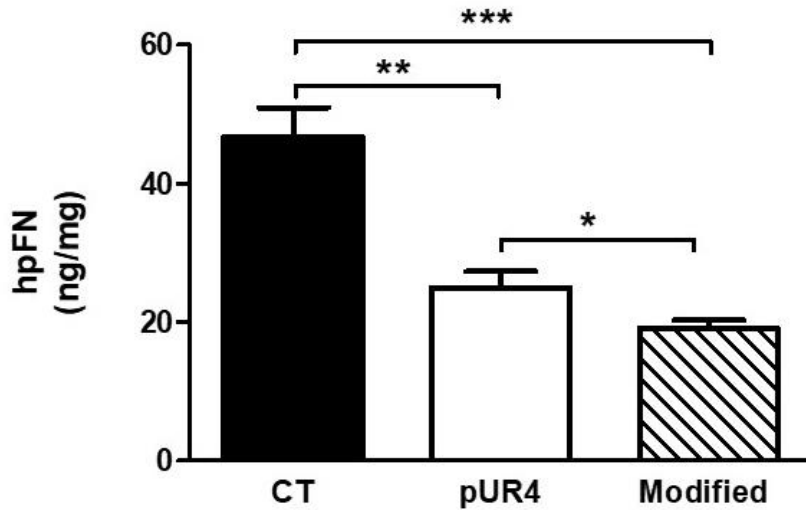
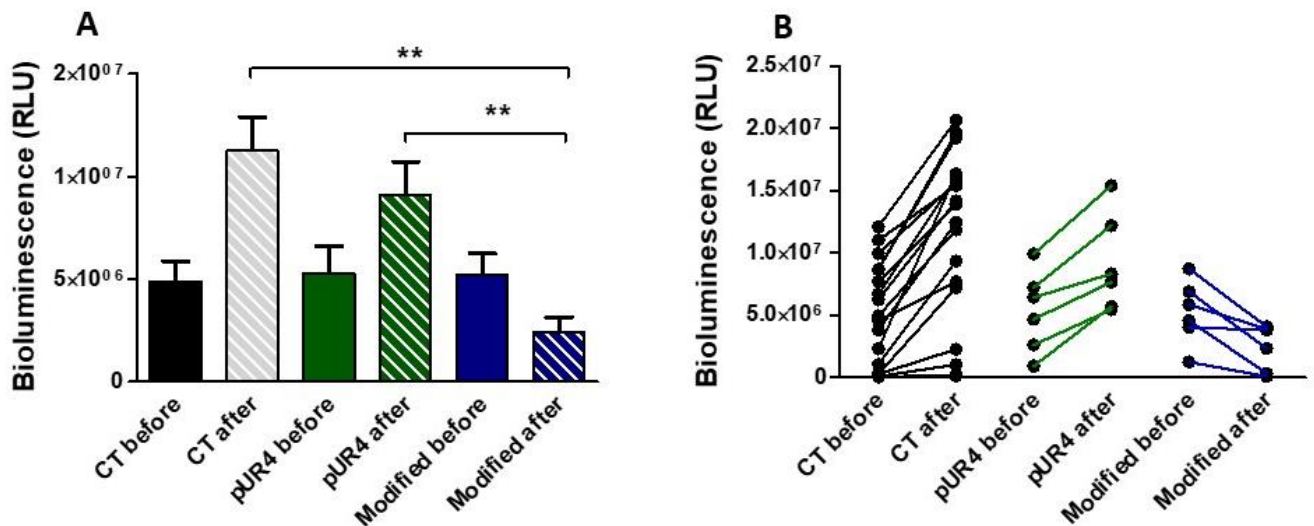


Figure 3.5 The synthetic modified peptide decreases Fibronectin accumulation of MDA cells *in vitro*. Fibronectin assessed in matrix fraction of MDA cells *in vitro* by ELISA after induction of the synthetic modified peptide was significantly less compared to the control (n=36/19/30).

3.5.1 Evaluation of modified synthetic peptides *in vivo*

In vivo experiments using synthetic peptides not only confirmed the results of *in vitro* but also showed that the new synthetic modified peptide causes a decrease in tumor growth. However, the synthetic pUR4 showed the same effect on tumor growth as the recombinant one (pUR4: $9.13 \times 10^6 \pm 1.6 \times 10^6$ RLU vs. modified: $2.4 \times 10^6 \pm 7.5 \times 10^5$ RLU, $P < 0.01$, n=6/6), (CT: $11 \times 10^6 \pm 1.7 \times 10^6$ RLU vs. modified: $2.4 \times 10^6 \pm 7.5 \times 10^5$ RLU, $p < 0.01$, n=17/6) (figure 3.5.1).



RESULTS

Figure 3.5.1 Analysis of tumor growth before and after of synthetic peptides injection. In comparison with control group, a statistically significant reduction in tumor growth was obtained in mice received synthetic modified peptide and slight decrease was detected in pUR4 treated tumors (A and B) (n=17/6/6).

3.5.2 Evaluation of fibronectin content in MDA tumors treated with synthetic modified peptide

In order to find out the effect of the new modified peptide on the fibronectin accumulation in MDA tumors, western blot of the total protein lysates of treated tumors was done in parallel with the total protein lysates of Kd tumors to also further compare the fibronectin content of these tumors with the fibronectin of treated tumors. Treatment by new modified peptide decreased significantly the fibronectin content of MDA tumors compared with the control tumors and was less than the fibronectin content of Kd tumors. The tumors which were treated with synthetic pUR4 also slightly but not significantly decreased the fibronectin of MDA tumors compared to the control ones (figure 3.5.2).

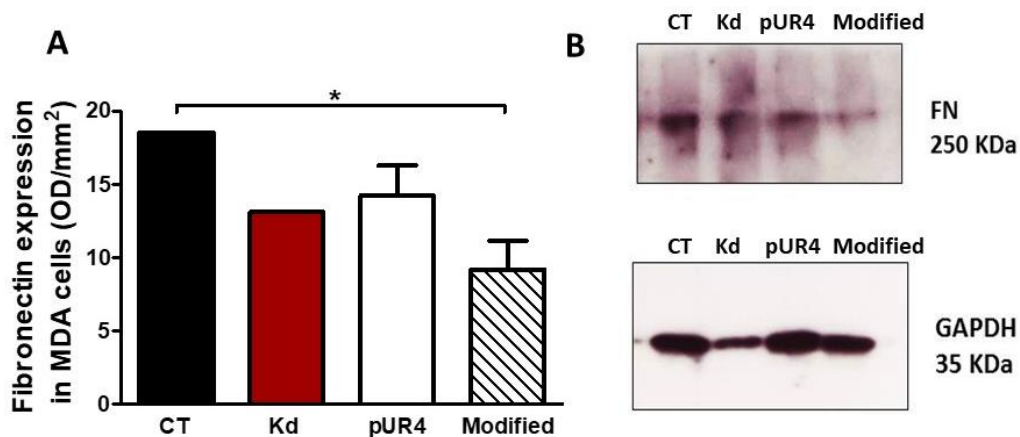


Figure 3.5.2 Fibronectin expression of MDA tumors treated with the second synthetic modified peptides. Fibronectin of MDA tumors which were detected by western blotting; densitometry (A) and representative of blots (B) showed a significant decrease in MDA tumors treated with the second modified peptide compared to the control tumors.

3.5.3 Radiographic analysis of MDA tumors treated with the synthetic modified peptide

Besides to the bioluminescence, radiographic images of the mice were also obtained as an additional evidence of the peptides effect. The analysis showed that the average area and width of osteolytic lesions in-mice injected with the synthetic peptides were slightly reduced compared to the control group but without significance (p=ns, n=15/5/5) (figure 3.5.3).

RESULTS

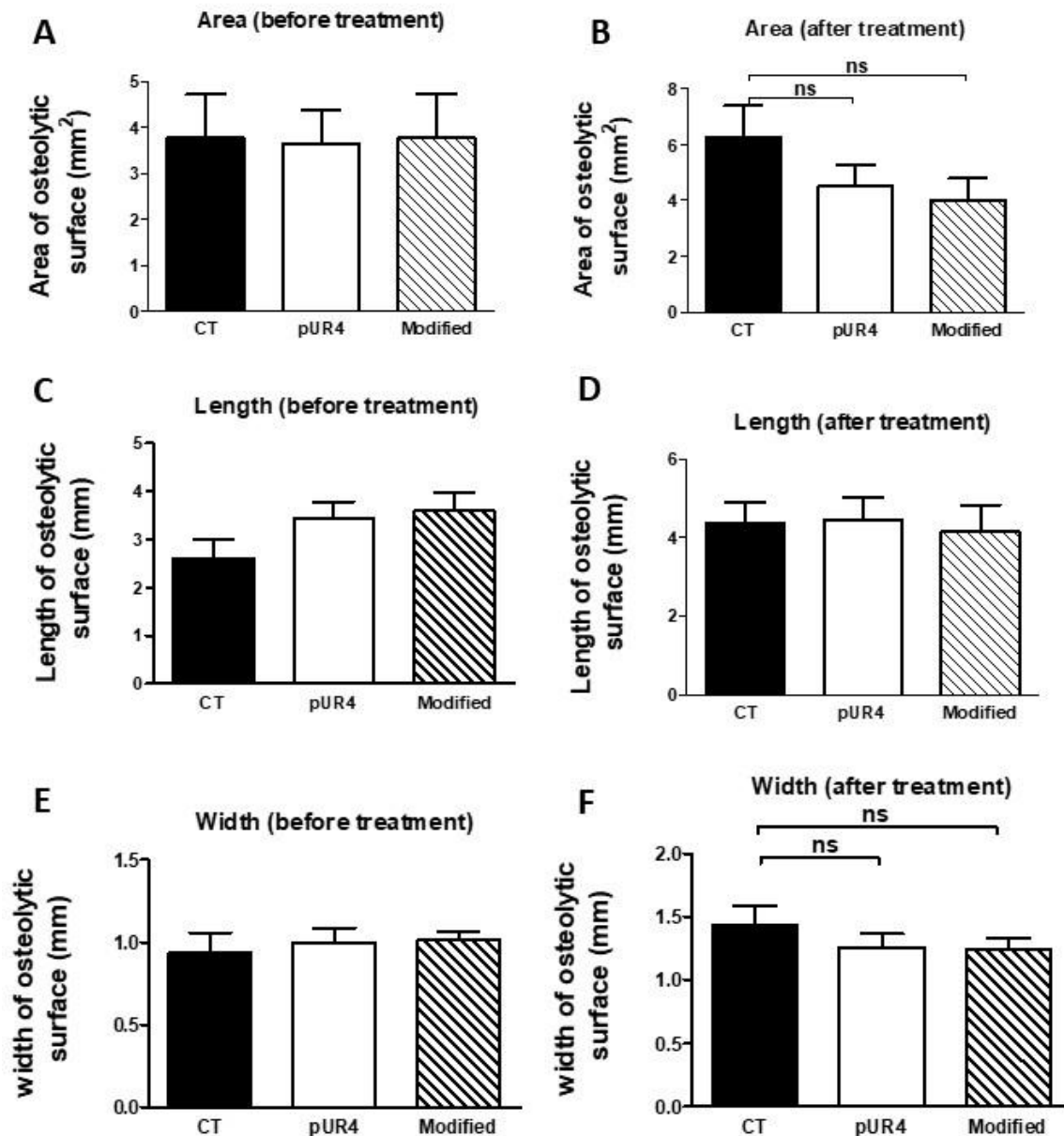


Figure 3.5.3 Radiographic analysis of osteolytic lesions before and after of synthetic modified peptide injection. The average area and width of osteolytic lesions was slightly reduced compared to the control group (B and F) ($p=ns$, $n=15/5/5$).

3.5.4 Characterization of immune cells in MDA tumors treated with the synthetic modified peptide

The immune cells of these tumors were also further analyzed by flow cytometry and no significant reduction was detected in leukocytes, monocytes of treated groups compared to the control group ($p=ns$, $n=18/6/6$). Since the granulocytes and myeloid derived suppressor cells strongly expanded in cancer, it was also critical to characterize them and they were slightly decreased in treated tumors but without significance compared to the control group ($p=ns$, $n=18/6/6$). The macrophages showed non-significant reduction but the sub-population $CD11b^+F4/80^+$ which tended to be increased after recombinant pUR4 treatment exclusively showed a significant

RESULTS

increase in treated groups compared to the control group (CT: 1 ± 0.14 % vs. modified: 2.7 ± 0.4 %, $p < 0.0001$, $n = 18/6$), (CT: 1.033 ± 0.14 % vs. pUR4: 1.8 ± 0.4 %, $p < 0.05$, $n = 18/6$) (Figure 3.5.4).

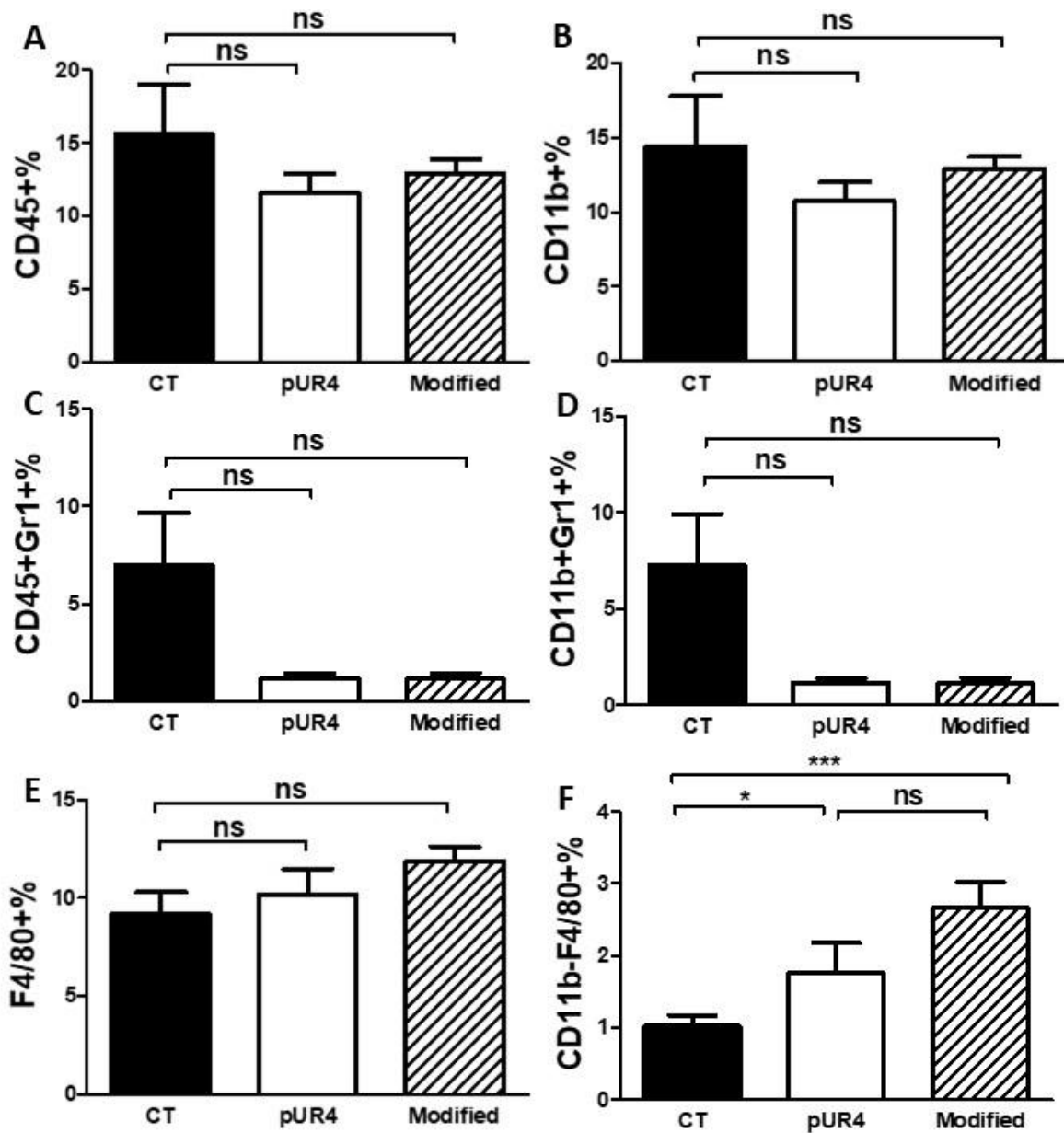


Figure 3.5.4 Analysis of immune cells in MDA tumors treated with the synthetic modified peptide. There was no difference in leukocytes (CD45⁺) (A), monocytes (CD11b⁺) (B), granulocytes (CD45⁺Gr1⁺) (C), or myeloid suppressor cells (CD11b⁺Gr1⁺) (D). A significant increase was observed in macrophages and exclusively the sub-population (CD11b⁻F4/80⁺) (F) ($n = 18/6/6$).

3.5.5 Characterization of cancer and stromal cells in MDA tumors treated with the modified synthetic peptides

Total cancer cells were also quantified in these digested tumors and a slight reduction in modified peptide treated group was obtained compared to the pUR4 treated group ($p=ns$, $n=6/6$). It was also surprising that the stromal cells modified peptide treated tumors were significantly increased compared to the control tumors (CT: $38\pm 2.3\%$ vs. modified: $50\pm 7\%$, $p<0.05$, $n=18/6$) (figure 3.5.5).

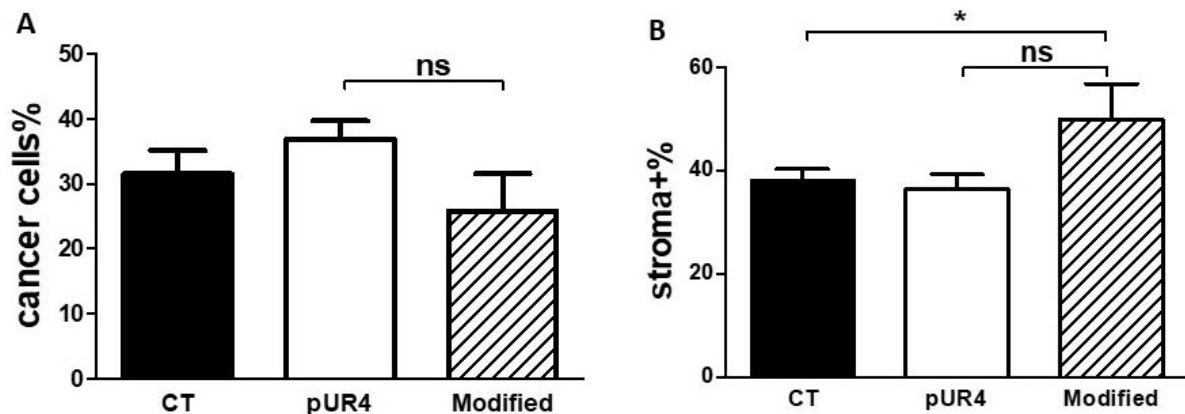


Figure 3.5.5 Analysis of cancer and stromal cells in MDA tumors treated with the synthetic modified peptide. No difference was observed in cancer cells among groups (A) and a significant increase in stromal cells (B) was observed by flow cytometry in modified treated tumors compared to the control ones ($n=18/6/6$).

3.6 Investigation of the effect of modified peptide in B16 melanoma cells

Based on the effect of the synthetic modified peptide in decreasing of MDA tumor growth, it was interesting to investigate its effect in another cancer model which is B16 melanoma cells. The schedule of the *in vivo* experiment is the same one shown in figure (3.4.3A).

3.6.1 Investigation of the effect of synthetic modified peptide on fibronectin of B16 melanoma cells *in vivo*

1 million B16 melanoma cells were injected into immune competent mice in order to further investigate the effect of T cells presence on development of treated tumors. Tumor growth is monitored by daily examination and peptides were injected daily for 5 days after 7 days of tumor cells injection. Subsequently, the mice were euthanized and the tumors were removed. The tumor size was determined by a caliper and the tumor weight using a sensitive scale. There was a reduction in tumor weight in the pUR4 and modified peptide treated mice compared to the controls ($p<0.05$, $n=13/13/13/13$) (figure 3.6.1E). The width and length of pUR4 and modified peptide treated tumors did not show any significant difference compared to the control and scramble treated tumors ($p=ns$, $n=13/13/13$) (figure 3.6.1B and D).

RESULTS

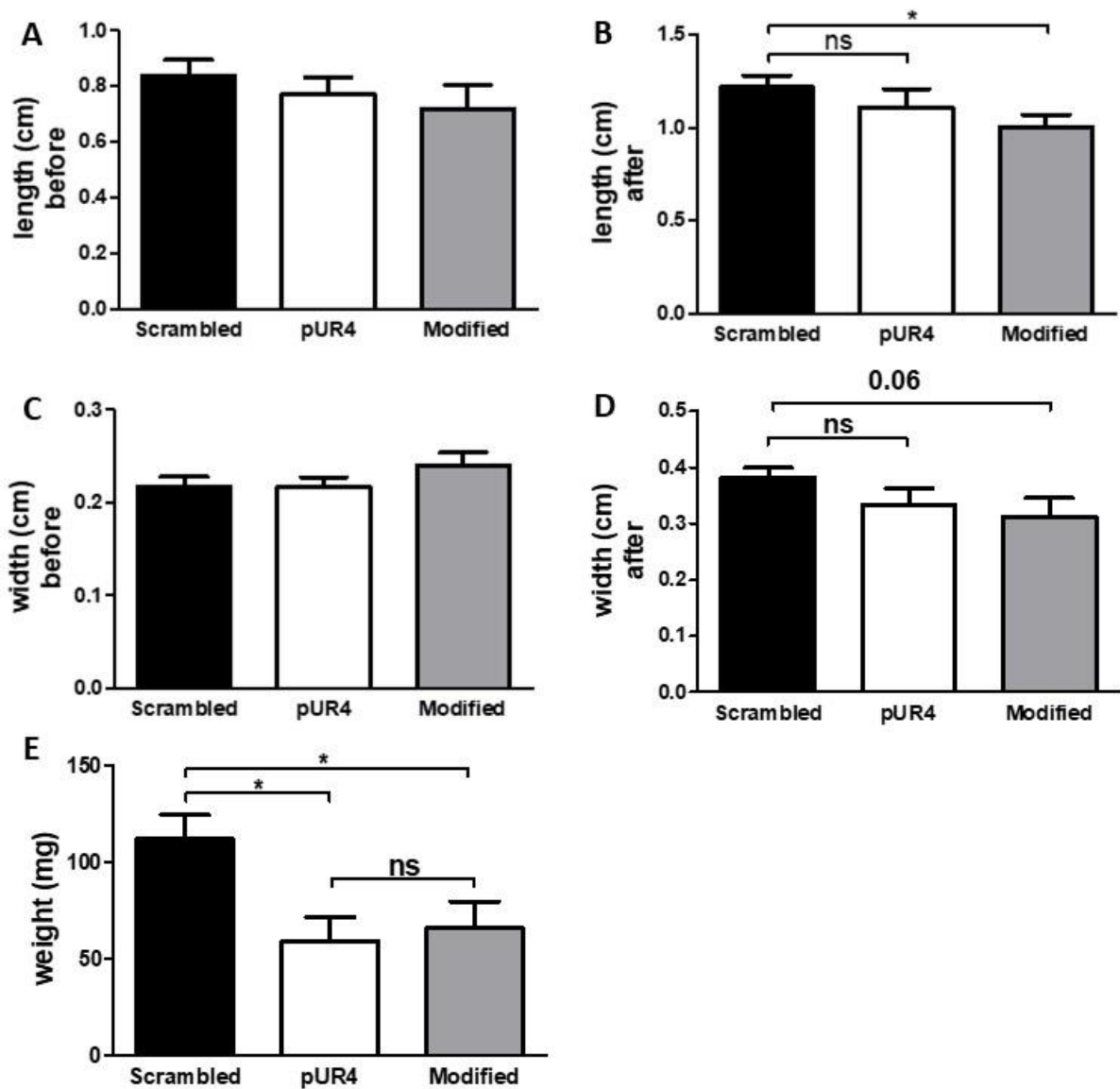


Figure 3.6.1 Tumor length, width and weight of B16 melanoma before and after of modified peptide treatment in immune competent mice. After 12 days of melanoma injection including peptides treatment for the last 5 days, there was a significant reduction in tumor weight (E). No difference was obtained in the length and width of treated tumors compared to the control ones (B and D) (n=13/13/13).

3.6.2 Effect of the synthetic modified peptide on the immune cells of B16 tumors in immune competent mice

In order to investigate whether the immune cells are responsible for diminished tumor growth, the tumors were analyzed by flow cytometry after digestion. A significant increase in leukocytes (CD45⁺: CT: 15.2±2.5 vs. pUR4: 24.7±1.7 %, p<0.05, n=8/8), monocytes (CD11b⁺: 7±1 vs. pUR4: 9.5±0.6 %, p<0.05, n=8/8) and macrophages (F4/80⁺: CT: 8±1.3 vs. pUR4: 13.2±0.6 %, p<0.05, n=8/8) were detected in pUR4 treated tumors compared to the control ones (figure 3.6.2A, B and E). In modified peptide treated tumors, granulocytes (CD45⁺Gr1⁺) and myeloid derived suppressor cells (CD11b⁺Gr1⁺) were significantly decreased compared to control and pUR4 groups (CD45⁺Gr1⁺: CT: 4.4±0.6 vs. modified peptide: 2.6±0.4 %, p<0.05, n=8/8), (CD45⁺Gr1⁺: pUR4: 4.4±0.3 vs. modified peptide: 2.6±0.4 %, p<0.05, n=8/8),

RESULTS

(CD11b⁺Gr1⁺: CT: 4.4±0.6 vs. modified peptide: 2.6±0.4 %, p<0.05, n=8/8), (CD11b⁺Gr1⁺: pUR4: 4.4±0.3 vs. modified peptide: 2.6±0.4%, p<0.05, n=8/8) (figure 3.6.2C and D). A significant increase was observed in macrophages subpopulation with pUR4 (CD11b⁺F4/80⁺) (pUR4: 4±0.5 vs. modified peptide: 1.7±0.3 %, p<0.001, n=8/8) in modified peptide tumors compared to pUR4 treated tumors (figure 3.6.2F).

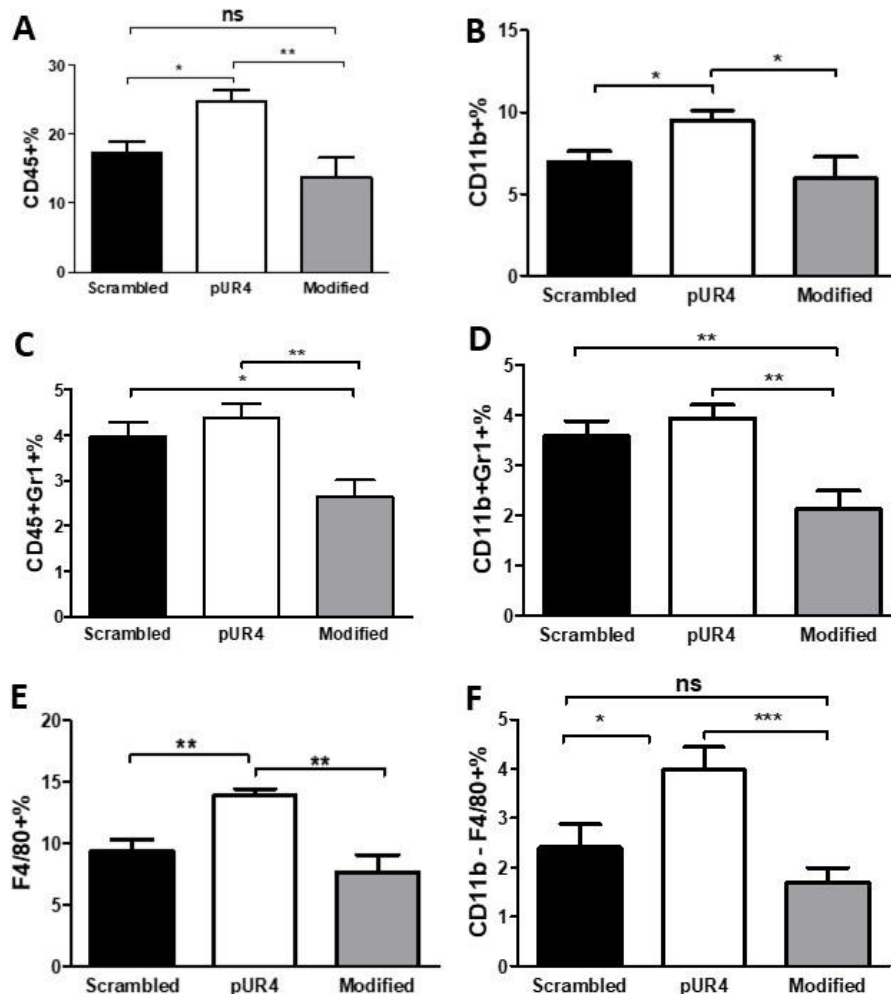


Figure 3.6.2 Immune cells in B16 tumors treated with synthetic modified peptide in immune competent mice. In B16 tumors, there was a significant increase in the number of leukocytes (CD45⁺) (A), monocytes (CD11b⁺) (B) and macrophages (F4/80⁺) (E) in pUR4 treated tumors compared to the control ones. A significant decrease was also detected in the percentage of granulocytes and myeloid derived suppressor cells in synthetic modified peptide treated tumors compared to the control ones (C and D) (n=8/8/8).

3.6.3 Effect of the synthetic modified peptide on B16 melanoma cells and stromal cells of B16 tumors in immune competent mice

It was important to characterize these populations after treatment in B16 tumors. Since the B16 cells were previously stained with e-flour which could be seen in Alexa 647 channel, they could be differentiated by FACs analysis. No significant difference was obtained in B16 cancer cells and stromal cells among groups (p=ns, n=8/8/8/8). No significant difference was obtained in B16 cancer cells among groups (figure 3.6.3A and B).

RESULTS

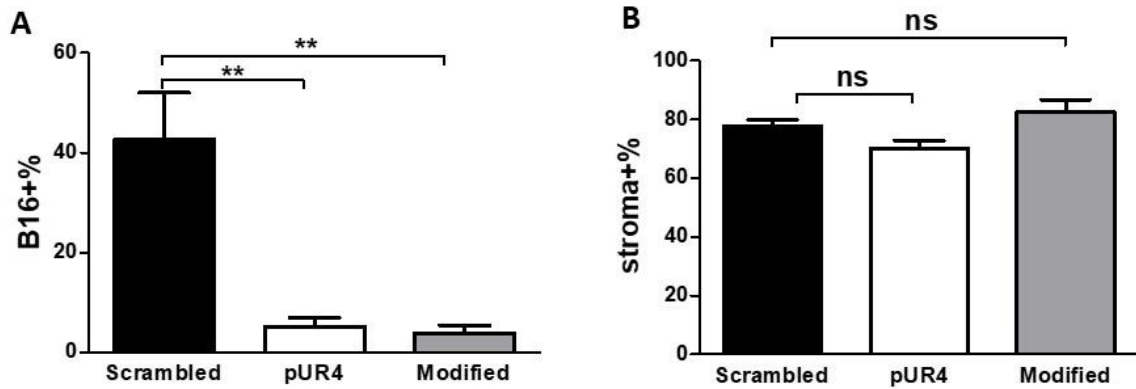


Figure 3.6.3 B16 melanoma cells and stromal cells in B16 tumors of immune competent mice treated with synthetic peptides. No significant difference was obtained among groups in B16 cancer cells and stromal cells (n=8/8/8).

3.7 Investigation of the fractions of the modified synthetic peptide *in vitro*

The previous data indicate that the modified peptide acting as a fibronectin polymerization inhibitor peptide could diminish fibronectin accumulation of MDA cancer cells *in vitro* and decreased tumor growth *in vivo* without affecting the immune response which was seen with pUR4. Therefore, it was interesting to find out which part of molecule is responsible for these effects. To achieve that, the modified peptide was divided into 3 individual peptides, synthesized in parallel with the original sequence of pUR4 and its scrambled peptide and tested *in vitro* on MDA cells for 72 hours.

Fibronectin content of matrix was assessed by ELISA and as shown in the figure, the peptide B which represents internal sequence of modified peptide diminished significantly fibronectin accumulation compared with the control cells and that was more than peptide A and peptide C (CT: 73.33 ± 11 vs. peptide A: 46 ± 8.152 ng/mg, $p < 0.05$, $n = 14/21$), (CT: 73.33 ± 11 vs. peptide B: 38.2 ± 4.5 ng/mg, $p < 0.01$, $n = 14/24$), (CT: 73.33 ± 11 vs. peptide C: 49 ± 3.8 ng/mg, $p < 0.05$, $n = 14/18$). Treatment of the cells with 1mM tri-fluoroacetate was done in parallel as a control and its toxic effect killed the cells and reduced significantly the fibronectin more than the other groups compared with the control cells (CT: 73.33 ± 11 vs. TFA: 26 ± 8.2 ng/mg, $p < 0.01$, $n = 14/11$) (figure 3.7A).

RESULTS

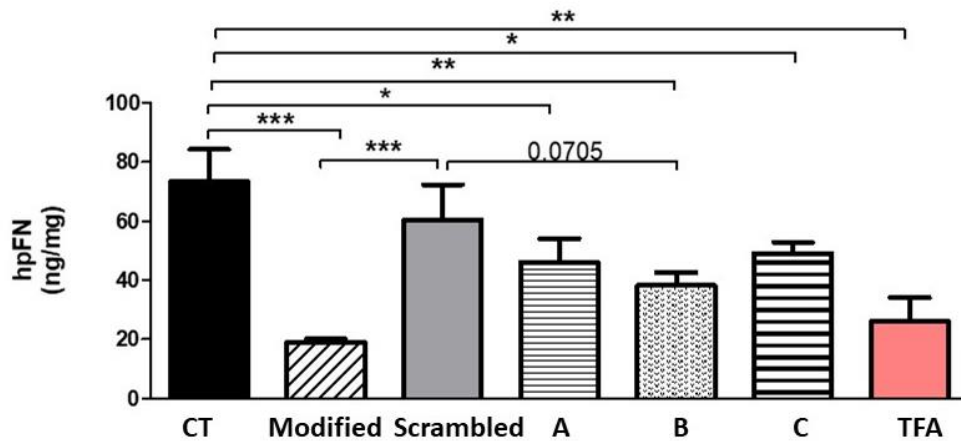


Figure 3.7A investigation the effect of the fractions of synthetic modified peptide on fibronectin accumulation of human breast cancer cells *in vitro*. The middle fraction (fraction B) of the synthetic modified peptide was the best one in the inhibition of fibronectin accumulation of human breast cancer cells.

The synthetic modified peptide has functional domains in comparison to those of pUR4. It includes the SGF fragment which mimics the sequence in pUR4 that interacts with ³FNI. The sequence DEEDQT in the synthetic modified peptide also mimics EDT which was confirmed to interact with ²FNI with high affinity [244-246]. Depending on the literature mentioned previously, pUR4 and its modified peptide especially the fraction B were further fractionated, modified and 3 new peptides were designed and tested *in vitro* on MDA cells.

Human fibronectin ELISA was assessed for total protein lysates after 72 hours of peptides induction. Peptide (1) was the best one in an inhibition of fibronectin accumulation of human breast cancer cells compared to the control cells (CT: 462.5±33.84 vs. peptide (1): 350.9±46 ng/mg, p<0.05, n=32/18) (figure 3.7B).

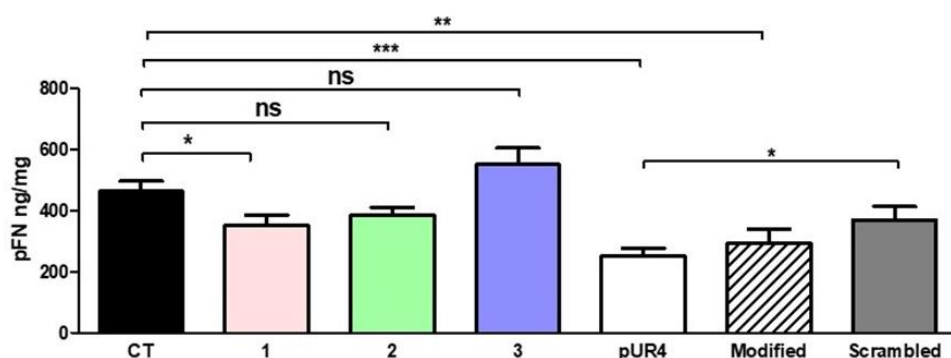


Figure 3.7B investigation the effect of the synthetic modified short peptides on fibronectin accumulation of human breast cancer cells *in vitro*. The sequence (1) reduced significantly the fibronectin accumulation of human breast cancer cells compared with control as shown by ELISA of the total protein lysates (n=32/18/18/18/12/14/15).

3.8 Cytokines expression of MDA tumors

Most recent findings confirm the involvement of the inflammatory cytokines in tumor progression but at the same time it is so complex and need to be further characterized. Therefore, it was important to explore the link between their expression and the different cancer groups to increase our understanding of peptides mechanisms in order to be introduced as a new approach for cancer treatment. Since the peptides could alter the immune response in tumors which normally leads to the change of cytokines expression, it is interesting also to assess the cytokines expression in treated tumors. Arginase-1 has a tumor growth promoting effect in which it supports the M2 macrophages. Firstly, I detected the expression of Arg-1 in CD11b⁺ cells which were isolated from MDA-CT and MDA-Kd tumors and 5 tumors in each group were pooled together. Arg-1 expression was reduced in Kd tumors compared to the control tumors. The expression of this cytokine was also assessed in total treated tumors and a significant decrease was observed in recombinant pUR4 treated tumors compared to the control (CT: $2 \pm 0.8 \times 10^{-3}$ vs. pUR4: $0.004 \pm 0.002 \times 10^{-3}$, $p < 0.05$, $n = 2/3$) and a slight decrease but without significance was obtained in the synthetic pUR4 and modified treated tumors compared to the control ($p = ns$, $n = 3/3/2$) (figure 3.8)

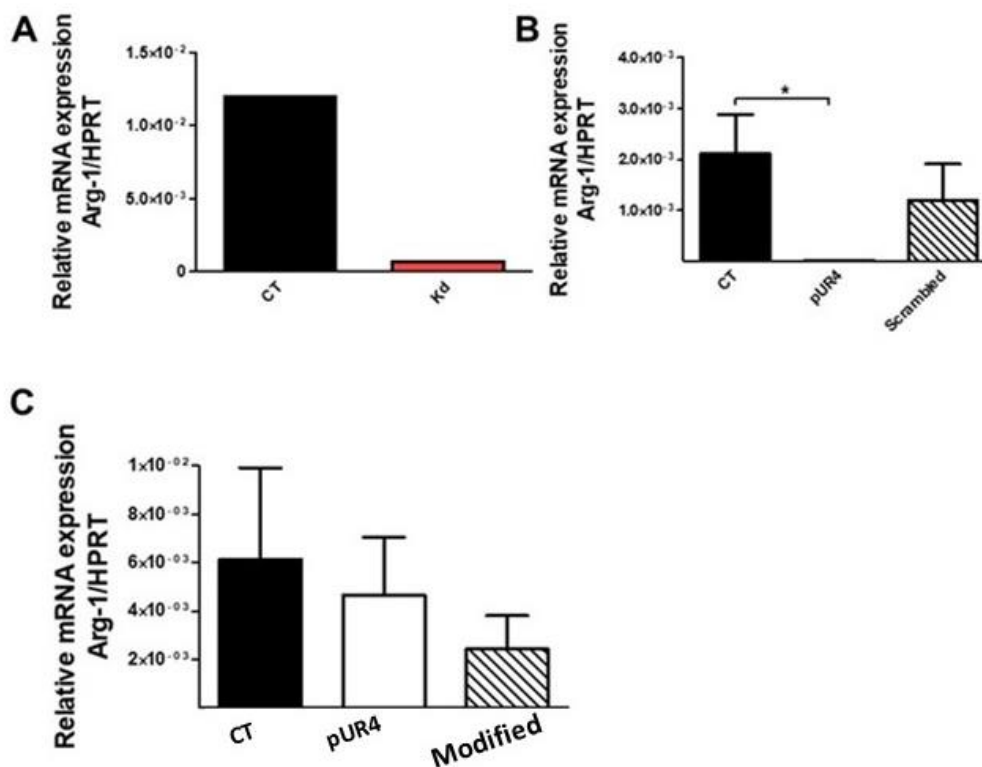
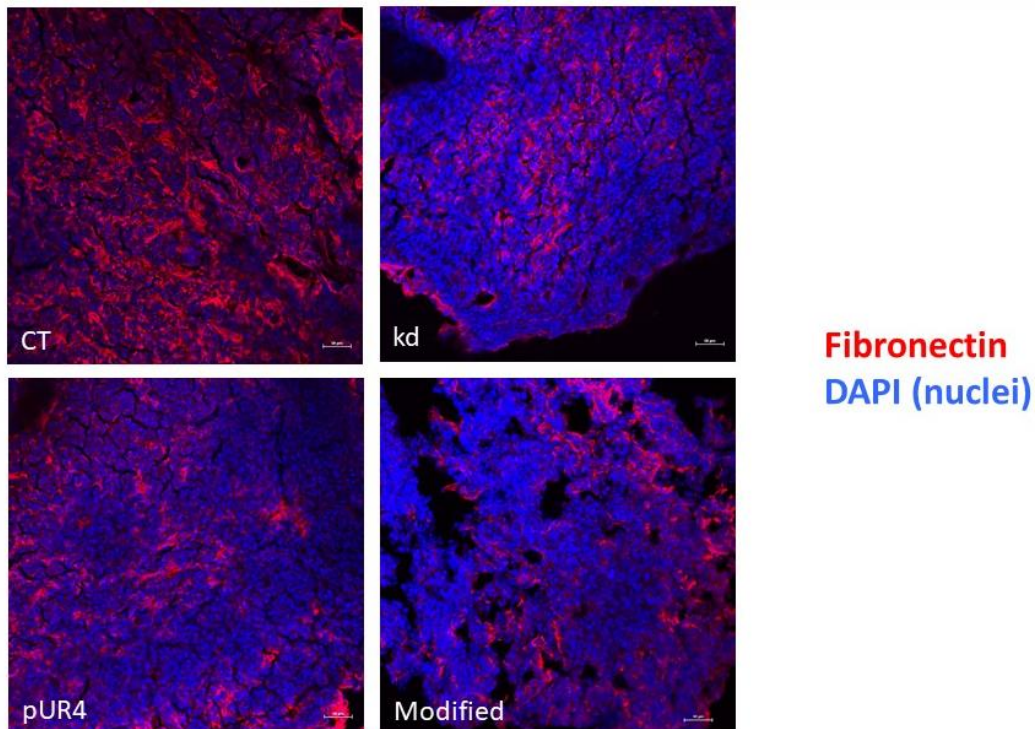


Figure 3.8 Analysis of Arg-1 expressions in MDA tumors. A decrease in its expression was detected in CD11b⁺ cells of Kd tumors compared to control tumors (A). A significant reduction was detected in recombinant pUR4 tumors (B) ($n = 2/3$). A slight decrease in the tumors treated with the synthetic modified peptide without significance (C) ($n = 3/3/2$).

3.9 Immunohistochemical staining of MDA tumors

Immunohistochemical staining of frozen sections of MDA tumors for fibronectin confirmed the results of ELISA as shown in the figure (3.9A) (fibronectin in red). Since the flow cytometry results were not clear enough to outline how the tested peptides could affect the non-malignant part of tumor microenvironment and especially the leukocytes and macrophages, it was necessary to investigate these populations in the frozen MDA sections of different tested groups by immunohistochemical staining. As shown in the figure (3.9A) by immune fluorescence, the administration of pUR4 and the synthetic modified peptide reduced the fibronectin content of tumors and that was consistent with the diminished fibronectin content of kd tumors where the endogenous fibronectin of cancer cells was knocked down. On the other hand, immunohistochemical analysis of frozen sections of tumors for leukocytes (CD45⁺ cells) clarified better the role of injected peptides in the immune response of tumors as the evaluation of these cells in pUR4 treated tumors revealed a significant increase compared with the Scrambled treated tumors and that was also consistent with the leukocytes values in kd tumors compared to control tumors (CT: 273±29 vs. kd: 760±34 cells per mm², p<0.0001, n=3 tumors/group, at least 3 sections in each group), (pUR4: 624 ±42 vs. Scrambled: 429±65.6 cells per mm², p <0.05, n=3 tumors/group, at least 3 sections in each group). The frozen sections of MDA tumors were also stained for macrophages (F4/80⁺ cells) and the kd tumors, pUR4 and synthetic modified treated tumors showed a significant increase in macrophages compared to the control tumors (CT: 532±27.3 vs. kd: 815±36 cells per mm², p<0.0001, n=3 tumors/group, at least 3 sections in each group), (CT: 532±27.3 vs. modified: 857.7±90.04 cells per mm², p<0.0001, n=3 tumors/group, at least 3 sections in each group), (CT: 532±27.3 vs. pUR4: 987±40.6 cells per mm², p <0.0001, n=3 tumors/group, at least 3 sections in each group), (kd: 814.8±36 vs. pUR4: 987±40.6 cells per mm², p<0.01, n=3 tumors/group, at least 3 sections in each group) (figure 3.9A).



RESULTS

Figure 3.9 A Immunohistochemical staining of MDA tumors for fibronectin (fibronectin in red). The treatment with pUR4 and the synthetic modified peptide resulted in a decrease in fibronectin content in the tumor as shown by immune fluorescence (n= 3/group and at least 3 sections for each tumor, bar=50 μ m)

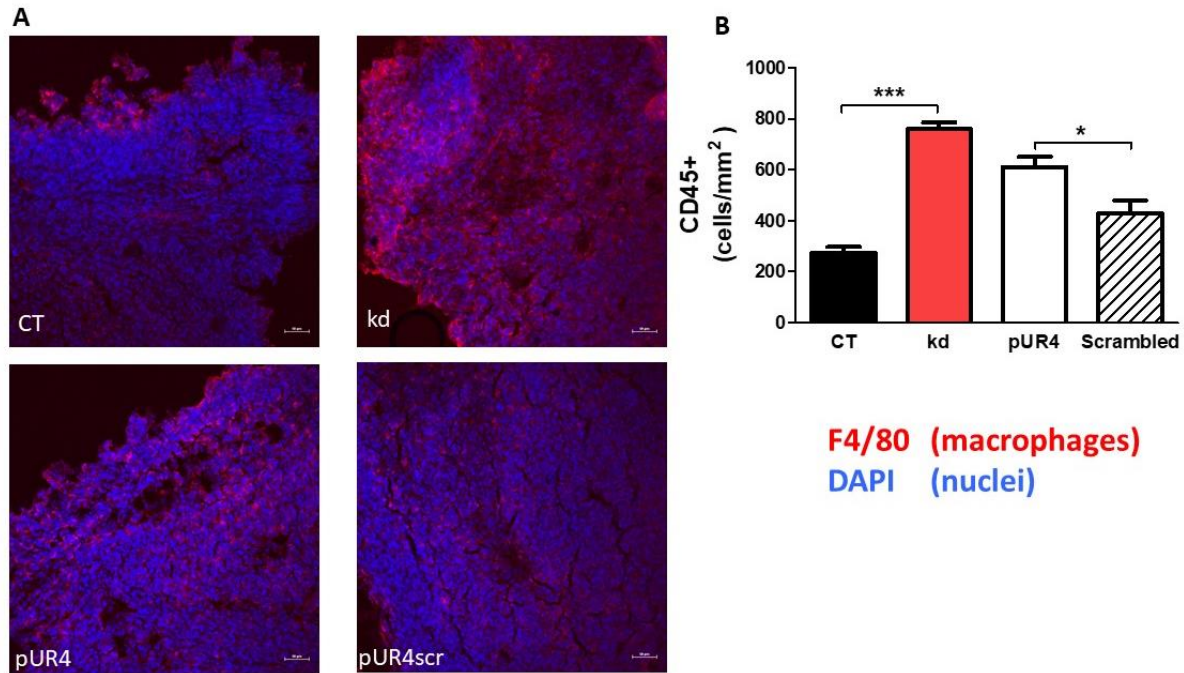
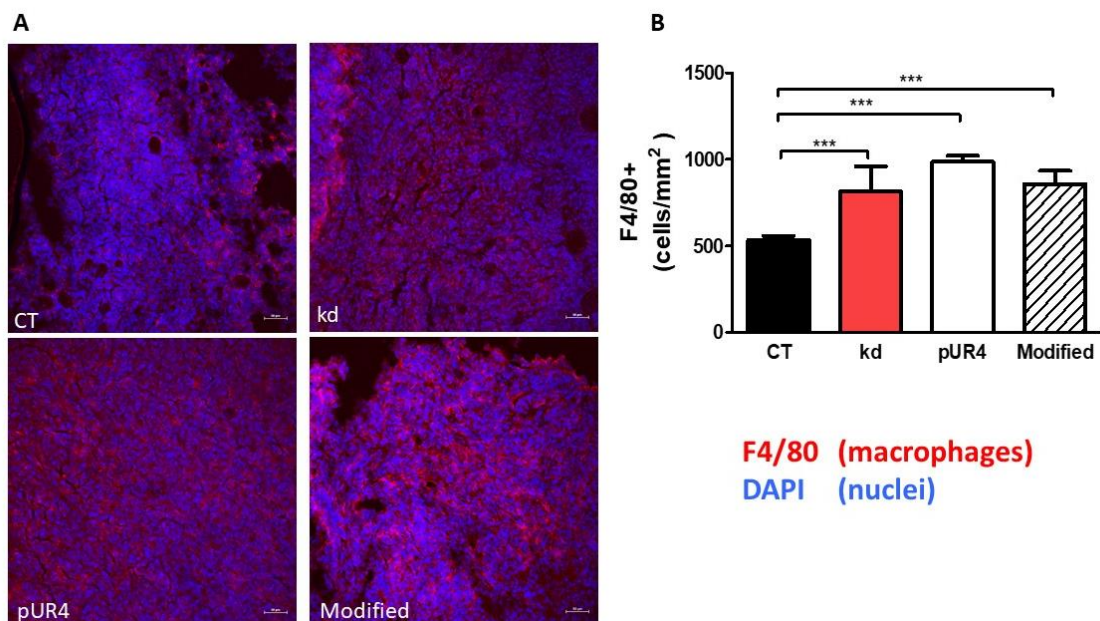


Figure 3.9B Immunohistochemical staining of MDA tumors for fibronectin (fibronectin in red). The treatment with pUR4 and the synthetic modified peptide resulted in a decrease in fibronectin content in the tumor as shown by immune fluorescence (n= 3 / group and at least 3 sections for each tumor, bar=50 μ m).

Figure 3.9C Evaluation of macrophages in MDA sections by immune fluorescence. Analysis of stained MDA sections for F4/80⁺ cells revealed a significant increase in Kd, pUR4 and synthetic modified treated tumors compared to the controls. A summary of the data is



RESULTS

shown in (B) as number of cells/mm² and the representative images of the groups are shown in A (bar=50μm).

4 DISCUSSION

4.1 Effect of tumor-cell-fibronectin on tumor growth

4.1.1 Knock down of fibronectin in MDA-MB-231 cells

The successful knock down (Kd) of fibronectin by RNA interference in breast cancer cell line has already been performed in our group and I was able to confirm this by ELISA of matrix fibronectin in Kd cells where it was diminished by 30% compared to the control cells. The low degree of deletion of fibronectin in Kd cells could be due to the fact that the cells were transfected more than 10 years ago and that some cells lost the promoter and thus, they were still able to produce fibronectin. However, the *in vivo* experiments in which these Kd cells were injected intratibially into immune deficient nude mice confirmed a decrease in cancer growth when using Kd cells. This was consistent with previous findings of our group, group, and is at least in part due to a decrease in angiogenesis due to the diminution of fibronectin in the tumor [240, 241, 247]

4.1.1.1 Effect on the growth of MDA-MB-231B / luc + - breast cancer cells

Loss of endogenous fibronectin production by the tumor cells was confirmed by ELISA *in vitro* and the effect of this loss evaluated *in vivo* using the intratibial model of cancer lesion induction. The decrease in growth in this model is consistent with the results previously obtained in our group and the work of Anja von Au [127], where she showed that the deletion of circulating fibronectin led to a decrease in cancer growth due to diminished VEGF and blood vessel formation. Because of the high concentration of fibronectin found in several tumors, it was interesting to investigate the role of fibronectin in tumors. Tumor growth of Kd tumor cells in CT mice was significantly diminished compared to CT tumor cells in Alb-cKO mice in which circulating fibronectin was deleted using the albumin promoter attached to cre-recombinase in fibronectin floxed mice. The growth of MDA-CT tumor cells in Alb-cKO mice was also significantly less than the growth of both cells in CT mice but the growth of MDA-Kd cells was even more pronounced. This suggests that despite the decrease of fibronectin to the same degree in loss of circulating fibronectin and loss of cancer fibronectin there is an additional factor that limits the growth in Kd tumors. Possibly the immune cell composition.

In work from our lab, Stephanie Rossnagl and Sabrina Kraft had found that the production of EDA-containing fibronectin leads to a change in the behavior of myeloid cells expressing CD11b against tumors [220]. Since the MDA-breast cancer cell line produces mostly EDA-fibronectin as was shown by Anja von Au, it is possible that the absence of EDA fibronectin also affects the immune cells in the tumors. Since the immune response in the tumors can have an important impact on their growth, we analyzed the characteristics of the immune cells using the two cell lines producing fibronectin (CT) and the one lacking it (Kd) by flow cytometry. There was an increase in immune cells of myeloid lineage, with an increase in CD11b⁺F4/80⁺ of almost 50% in the MDA-kd tumors. The effect of loss of endogenous fibronectin on the immune cells was also confirmed by immunohistochemistry of frozen MDA sections which showed a significant increase in immune cells (CD45⁺ cells) and this increase was due to the significant increase of macrophages (F4/80⁺ cells) in the MDA-kd tumors by

immune histochemistry confirming the findings generated by flow cytometry. It should be noted that macrophages can be generated from CD11b⁺ cells [248]. This suggests that EDA-fibronectin might also play a role within the tumor itself in modulating the immune cell differentiation. Therefore, it seems that the loss of endogenous fibronectin of cancer cells leads to increase infiltration of immune cells into the tumor and that this effect contributes to a decrease in cancer growth. These findings are in line with the previous findings of our group.

4.2 Modulation of fibronectin of cancer cells using a bacterial peptide

As described previously, fibronectin has a variety of roles in several steps of tumor development. It mediates cell adhesion, migration, and proliferation. It is responsible for angiogenesis of tumors and affects metastasis formation [127]. Based on the previous finding in our group that the inhibition of fibronectin accumulation by application of a small peptide can improve liver function and reduce liver fibrosis [242], we decided to evaluate the effect of this peptide in cancer. The hypothesis is that the decrease in fibronectin accumulation will lead firstly to decreased growth as was seen with the deletion of circulating fibronectin and also to an increase in the immune reaction against cancer as was suggested by the absence of EDA-fibronectin in osteoblasts in the bone marrow and the increase in immune cells in Kd tumors. As described previously, pUR4 represents part of an adhesion molecule (part of the functional upstream domain (FUD) of F1 adhesin molecule) of *Streptococcus pyogenes*. It consists of 49 amino acids. It belongs to a class of adhesions termed MSCRAMMS (Microbial Surface Components Recognizing Adhesive Matrix Molecules) which are known to bind specifically to fibronectin. because of pUR4 ability to prevent fibronectin polymerization, it was widely used as a tool in many biomedical studies to investigate the involvement of fibronectin in several processes such as vascular remodeling and angiogenesis [225, 249, 250]. It was reported that the F1 domains can bind to the soluble and matrix fibronectin suggesting that binding sites are expressed in both forms of fibronectin [251, 252] by means of integrin $\alpha 5\beta 1$ which has a function in fibronectin assembly and $\alpha v\beta 3$ integrin which is involved in the formation of focal contacts that are required for the assembly of fibronectin fibrils [253]. Several forms were evaluated: recombinant, synthetic and individually modified peptides in two cancer models which are human breast cancer cells MDA cells and melanoma murine cancer cells B16.

4.2.1 pUR4 inhibits fibronectin accumulation of human breast cancer cells *in vitro* and reduces cancer growth *in vivo*

The extracellular matrix has a complex and a dynamic structure that it is deposited, remodelled and degraded in order to maintain the tissue homeostasis. Many of previous studies have already reported the role of dysregulation of extracellular matrix in cancer development. The extracellular matrix consists of several of molecules, however because of its many functions, our group focuses on fibronectin. Although collagen seems to be involved in a variety of pathological processes, the presence of fibronectin is needed for the collagen accumulation [254] and that was confirmed *in vitro* and *in vivo* by our group. Furthermore, our group has already shown that the deletion of circulating fibronectin which is produced by liver cells leads to suppression of angiogenesis by decreasing VEGF concentrations and thus diminishing tumor

growth using the breast cancer MDA cells [127]. Based on the previous findings, the question arose whether the modulation of fibronectin could lead to smaller breast cancer tumors. Because fibronectin plays a crucial role in many steps of cancer development, it was interesting to find out whether reducing of fibronectin content in tumors can affect significantly the tumor growth. Treatment of human breast cancer cells for 72 hours with pUR4 *in vitro* reduced the fibronectin of matrix as assessed by ELISA. These data were consistent with the previous *in vitro* data showing that inhibition of fibronectin polymerization decreases the accumulation of fibronectin in the ECM [210, 225, 242], and suggest that pUR4 might have an effect on breast cancer growth. The *in vivo* findings confirmed the inhibitory role of pUR4 on fibronectin accumulation which led to a slowing of the growth of MDA tumors. These results were comparable with the effect of knocking down of endogenous fibronectin on tumor growth. This was similar to what was already confirmed by our group in a liver fibrosis model [242]. Importantly, the immune response against cancer cells was also changed. The macrophages which play a fundamental role in the tumor microenvironment either by supporting a proinflammatory response and diminishing its growth (M1 cells) or by inhibiting the immune response and thus indirectly promoting cancer growth (M2) [255-257]. The immune cells mostly consisting of macrophages were increased in tumors of mice treated with pUR4. This could be due to increased leukocytes infiltration through the vessel wall [225]. However, no effect could be observed on the cancer and stromal cells. On the protein levels, pUR4 diminished the total fibronectin content of tumors compared to the control tumors. All of the previous findings confirm the importance of fibronectin polymerization and accumulation in the development of cancer. Therefore, targeting fibronectin could be a key for improving cancer treatment.

4.2.2 pUR4 diminishes tumor growth of murine B16 melanomas

B16 murine melanoma cells are commonly used for studying tumor growth because they share similarities with the human melanoma [258]. These cells represent a good model for studying the immune response, because it has already been shown that myeloid suppressor cells (CD11b⁺Gr-1⁺ cells) promote proliferation in the B16 melanoma cells [259]. These cells often [260] interact with T cells, therefore they offered the opportunity to study the role of T cells, in particular T cell suppression induced by myeloid suppressor cells. We used immunocompetent mice in order to determine the effect of the peptides on myeloid-T-cell-mediated immune response. Melanoma cells were injected subcutaneously into the left flank of the mouse and after 7 days of melanoma injection in immune competent mice in order to allow the tumors to reach a measurable size, tumor size was measured. The synthetic peptides affected the tumor growth of MDA in immune deficient mice and B16 in immune competent mice. The flow cytometry analysis of immune cells of tumors however replicated some of the changes seen in MDA tumors treated with pUR4 and in MDA-Kd tumors. It is clear that an effect on immune cells is seen in the absence of fibronectin in tumors after treatment with pUR4. Whether this can be exploited in the fight against cancer is not clear.

As shown in figure (4.2.2), binding studies performed by others had already shown that none of the synthesized N- and C-terminal peptides were able to inhibit fibronectin polymerization to a degree similar to the pUR4 with its 49 Amino acids. Binding affinity studies confirmed that loss of the 7 N-terminal amino acids eradicates the inhibitory effect. Furthermore, the lack of only 6 amino acids on the C-terminal also resulted in a 100-fold decrease in inhibition. Interestingly, the 7 N-terminal amino acids did not have

any inhibitory effect. Therefore, it seems that the sequence within pUR4 is important for inhibiting fibronectin fibril formation [151, 234]

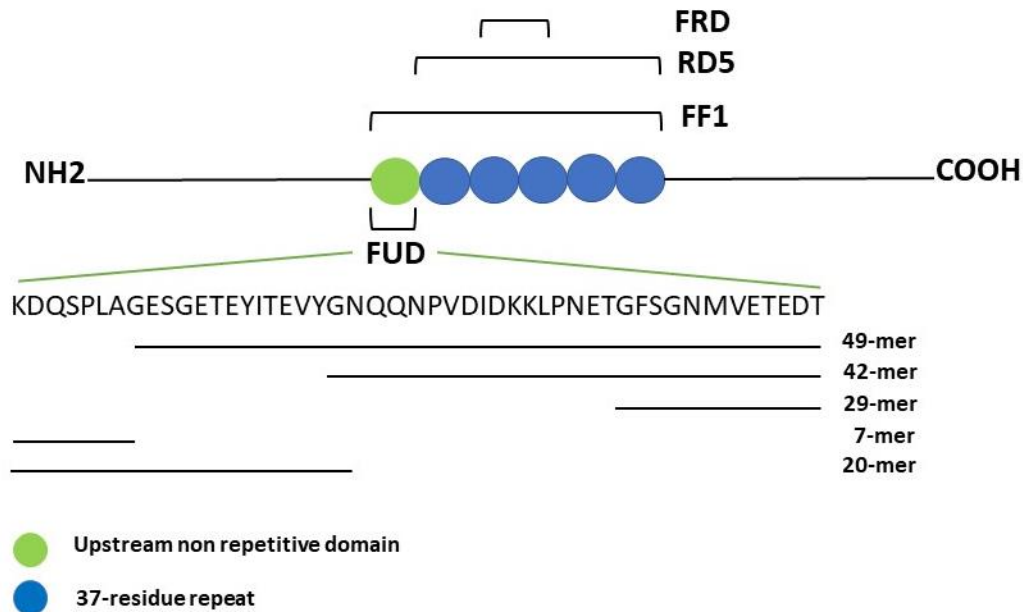


Figure 4.2.2. Schematic representation fibronectin binding F1 domains of streptococcus pyogenes and individual FUD derived peptides [151]. Representation of F1 adhesion molecule and its functional domains besides to the truncated sequences of the functional upstream domain (FUD). Reproduced and modified from [151]

It has been reported that deletion of fibronectin from cultured cells leads to loss collagen fibrils [261]. Furthermore, the fibronectin-collagen interactions prevent the collagen degradation [262]. Therefore, the decrease in fibronectin probably also diminishes collagen accumulation. It could be shown that as collagen accumulates, it contributes to the stiffness and progression of cancer [118]. It is possible that preventing fibronectin and indirectly collagen accumulation also contributed to the suppression of cancer growth in tumors treated with pUR4. This highlights the importance as well as the complexity of matrix in cancer.

4.2.3 The effect of the modification of pUR4 *in vivo* and *in vitro*

pUR4 both in recombinant and synthetic form prevented fibronectin accumulation *in vitro* and *in vivo*. We decided to modify this sequence in order to become an even stronger effect and if possible, stimulate the immune response against cancer.

It was previously reported that all of the fibronectin-binding MSCRAMMS include the VETEDT sequence and analysis of different sequences of pUR4 showed that this last six amino acids sequence of pUR4 is crucial for the high binding affinity to fibronectin [252, 263]. The general conclusion that has been characterized from the binding studies that presence of 7-N terminal amino acids, the 6-C-terminal amino acids and the entire sequence are fundamental for the optimal inhibitory activity [151]. Regarding the binding interactions, the optimal blocking of fibrinogenesis requires the binding of pUR4 to the N-terminal type I modules of fibronectin [264], which means that pUR4 mimics the binding sites on cell surface to the five N-terminal type I modules of

fibronectin [151]. On the other hand, pUR4 was compared with STAFF-5 and STATT-5 peptides. They are crystal structures that depend on fibronectin-binding protein from *Staphylococcus aureus* and they could bind to ²FNI-³FNI and ⁴FNI-⁵FNI, respectively, with high affinity [244, 265]. The interactions of crystal structures (STAFF-5 and STATT-5) which were found with fibronectin modules were used for the pUR4 sequence [244]. pUR4 was set depending on the EDT sequence at its C terminus for ²FNI interaction and compared with the STATT-5 sequence. It was shown that MVETEDT of pUR4 was more preferable than HTTVEDT sequence of STATT-5 for ²FNI binding [246]. The same comparison was done for ³FNI interactions and the ETGFSG had more favorable energy for this binding depending on the IVTGAV sequence of STATT-5. Furthermore, all bacterial fibronectin-binding proteins include GEXGE motif that was shown by NMR spectroscopy to bind to ⁸⁻⁹FNI modules [213, 266]. It was also confirmed that collagen type I interacts with ⁸⁻⁹FNI modules by this motif and pUR4 contains GESGE sequence which its involvement in collagen binding was also confirmed [211, 213]. Therefore, pUR4 was recommended as a strong inhibitor of assembly because it has binding sites to ²FNI, ³FNI, ⁸⁻⁹FNI as well as collagen type I. The second modified peptide has also functional domains in comparison to those of pUR4 and the crystal structures that were mentioned before. It includes the SGF fragment which mimics the sequence in pUR4 that interacts with ³FNI. The sequence DEEDQT in the second modified peptide mimics also EDT which was confirmed to interact with ²FNI with high affinity. In the *in vitro* experiments evaluating these modifications, we found an effect on fibronectin accumulation. This was also associated with a decrease in cancer growth both in the MDA and in the melanoma models. However, the effect *in vivo* was not improved over the effect of pUR4 on growth in the immune competent model using B16 melanoma cells. Even though the modified peptide decreased the growth of MDA *in vivo* possibly more than pUR4, this could be due to the low number of replicates we had in this model. The modified peptide did not affect the macrophages in the B16 model, which suggests that the effect is due to the inhibition of fibronectin. Thus, the change in immune cells in the pUR4 treated mice could be irrelevant for the change in growth of cancer.

The modified sequence was then divided into three individual peptides and synthesized to find out which part is responsible for the inhibition of matrix accumulation. The fraction of the modified peptides was tested *in vitro* on MDA cells and the fibronectin content was quantified by ELISA. The data showed that the internal sequence “peptide B” which contains the ³FNI and ²FNI binding sequence was the best one in inhibition of fibronectin accumulation. This part was further divided into three parts, but none of these short peptides was better than the pUR4 or the modified peptide in decreasing fibronectin accumulation. Thus, while these modifications offer promise for the development of a potent matrix inhibitor to take advantage of in the therapy of cancer, they fail to offer measurable advantages on matrix accumulation over pUR4 or the modified peptide.

4.3 Changes in the expression of cytokines profile of tumors

The cytokines produced by immune cells and their involvement in tumor progression has been well described [267]. Arginase-1 which is produced by M2 macrophages was assessed in the immune cells isolated from MDA-tumors and its expression showed a significant decrease in CD11b+ cells isolated from MDA-Kd tumors compared to the control tumors MDA-CT. These findings were compatible with the reduced tumor growth seen in MDA-Kd tumors because high expression of this molecule is associated

DISCUSSION

with an inhibition of the immune response against cancer and ultimately increased cancer growth [268]. These results suggest that the macrophages in the MDA-Kd tumors have an immune modulatory phenotype which is associated with the production of tumor-growth-inhibiting molecules including iNOS and IFN- γ [260]. I could not confirm a change in iNOS mRNA expression of the isolated myeloid cells from tumors because of its very low expression and the availability of only a small amount of mRNA. Arginase-1 expression was also evaluated in the control tumors treated with the pUR4 peptide. Its expression in pUR4-treated tumors was significantly reduced compared to the control tumors and these findings are consistent with the slow growth of the tumors treated with this peptide. This also suggests that the effect of pUR4 on tumor growth is similar to that of elimination of endogenous fibronectin produced by tumor cells.

Based on the change in arginase-1 mRNA expression in Kd and pUR4-treated tumors, it seems that macrophages that inhibit tumor growth are dominant in these tumors. This also suggests that inhibition of tumor fibronectin production or accumulation could increase the immune cell response against cancer. The effect of the modified peptide on decreasing cancer growth in the absence of a change in macrophages could be an indicator, that only matrix modification is relevant and that the change in the immune cells is without major relevance. Alternatively, the change in percentage could be only a side effect with the major effect mediated by a change in the behavior of the cells present, for example by changing arginase-1 expression.

In summary, these data suggest that decreasing the amount of fibronectin in two cancer models diminishes cancer growth. This could be in part due to a change in the behavior of the immune cells that infiltrate the tumor. Further studies are needed to establish a causal relationship between the inhibition of matrix accumulation and the change in macrophage behavior. Even though several modifications failed to result in a more pronounced inhibition of cancer growth, this work offers the basis for inhibiting matrix accumulation in the development of new therapeutic classes against cancer.

5 SUMMARY

An emerging field in cancer research consists of the study of the role of extracellular matrix proteins. The participation of fibronectin in different stages of tumorigenesis by different mechanisms has already been confirmed in numerous studies. Therefore, the potential of use of fibronectin modulation as a therapeutic approach in cancer might be promising. In this work, the effect of peptides that target fibronectin accumulation was tested in two different cancer models.

pUR4 is a bacterial peptide which that prevents fibronectin fibril formation. Because fibronectin is required for collagen accumulation, this leads to a decrease in collagen. The recombinant version of pUR4 was tested *in vitro* and *in vivo* in human breast cancer cell line MDA and murine B16 melanoma cells. This peptide was then synthesized and modified in order to better understand its effect on the immune response against tumors and to investigate whether an improvement can be achieved by various modifications.

The fibronectin polymerization inhibitor pUR4 diminished fibronectin accumulation by MDA cancer cells *in vitro* and was able to reduce tumor growth *in vivo*. However, growth proceeded nevertheless albeit at a slower rate. This was associated with an increase in a subpopulation of immune cells compatible with macrophages (CD11b-F4/80+) and a decrease in the mRNA expression of arginase in myeloid cells isolated from the treated tumors. The suppression of growth was confirmed using a second model of melanoma in immune competent mice.

Several modifications were introduced and a new peptide was synthesized, but its effect on fibronectin accumulation *in vitro* was not more pronounced than pUR4. *In vivo*, the modification diminished cancer growth further compared to pUR4 in the immune deficient MDA model, but this could not be confirmed in the immune competent melanoma B16 model suggesting it is due to the small sample size in the MDA model, or that it is not a universal effect. Interestingly, we could not detect a change in the macrophages with the modified peptide despite the decrease in cancer growth. Attempts at characterizing the best sequence within the modified peptide led to short peptides that diminish fibronectin accumulation *in vitro*, but none was better than pUR4.

The data indicate that pUR4 suppresses fibronectin accumulation and leads to a decrease in cancer growth. An accompanying change in the mRNA expression in the macrophages could contribute to this effect, but causality was not evaluated in this work. In summary, matrix manipulation offers new possibilities in suppressing cancer growth.

6 REFERENCES

1. Cancer research UK. *Worldwide cancer statistics*. 2018, January,30; Available from: <https://www.cancerresearchuk.org/health-professional/cancer-statistics/worldwide-cancer#heading-Zero>.
2. Forman, D., et al., *The global and regional burden of cancer*. 2014. **2014**: p. 16-54.
3. Xu, C., et al., *Hepatitis B virus-induced hepatocellular carcinoma*. *Cancer Lett*, 2014. **345**(2): p. 216-22.
4. zur Hausen, H., *Papillomavirus infections--a major cause of human cancers*. *Biochim Biophys Acta*, 1996. **1288**(2): p. F55-78.
5. Forsyth, C.B., et al., *Alcohol stimulates activation of Snail, epidermal growth factor receptor signaling, and biomarkers of epithelial-mesenchymal transition in colon and breast cancer cells*. *Alcohol Clin Exp Res*, 2010. **34**(1): p. 19-31.
6. Meadows, G.G. and H. Zhang, *Effects of Alcohol on Tumor Growth, Metastasis, Immune Response, and Host Survival*. *Alcohol Res*, 2015. **37**(2): p. 311-22.
7. Ratna, A. and P. Mandrekar, *Alcohol and Cancer: Mechanisms and Therapies*. *Biomolecules*, 2017. **7**(3).
8. Gawełek, E., B. Drozdowska, and A. Fuchs, *Radon as a risk factor of lung cancer*. *Przegl Epidemiol*, 2017. **71**(1): p. 90-98.
9. Soehnge, H., A. Ouhtit, and O.N. Ananthaswamy, *Mechanisms of induction of skin cancer by UV radiation*. *Front Biosci*, 1997. **2**: p. d538-51.
10. Allott, E.H. and S.D. Hursting, *Obesity and cancer: mechanistic insights from transdisciplinary studies*. *Endocr Relat Cancer*, 2015. **22**(6): p. R365-86.
11. Surman, M. and M.E. Janik, *Stress and its molecular consequences in cancer progression*. *Postepy Hig Med Dosw (Online)*, 2017. **71**(0): p. 485-499.
12. Nilsson, M.B., et al., *Stress hormones regulate interleukin-6 expression by human ovarian carcinoma cells through a Src-dependent mechanism*. *J Biol Chem*, 2007. **282**(41): p. 29919-26.
13. Costanzo, E.S., et al., *Psychosocial factors and interleukin-6 among women with advanced ovarian cancer*. *Cancer*, 2005. **104**(2): p. 305-13.
14. Masur, K., et al., *Norepinephrine-induced migration of SW 480 colon carcinoma cells is inhibited by beta-blockers*. *Cancer Res*, 2001. **61**(7): p. 2866-9.
15. Sood, A.K., et al., *Stress hormone-mediated invasion of ovarian cancer cells*. *Clin Cancer Res*, 2006. **12**(2): p. 369-75.
16. Yang, E.V., et al., *Norepinephrine up-regulates the expression of vascular endothelial growth factor, matrix metalloproteinase (MMP)-2, and MMP-9 in nasopharyngeal carcinoma tumor cells*. *Cancer Res*, 2006. **66**(21): p. 10357-64.
17. Knudson, A.G., *Two genetic hits (more or less) to cancer*. *Nat Rev Cancer*, 2001. **1**(2): p. 157-62.
18. Marbaniang, C. and L. Kma, *Dysregulation of Glucose Metabolism by Oncogenes and Tumor Suppressors in Cancer Cells*. *Asian Pac J Cancer Prev*, 2018. **19**(9): p. 2377-2390.
19. Abreu Velez, A.M. and M.S. Howard, *Tumor-suppressor Genes, Cell Cycle Regulatory Checkpoints, and the Skin*. *N Am J Med Sci*, 2015. **7**(5): p. 176-88.
20. Elmore, S., *Apoptosis: a review of programmed cell death*. *Toxicol Pathol*, 2007. **35**(4): p. 495-516.

21. Bernal, A. and L. Tusell, *Telomeres: Implications for Cancer Development*. Int J Mol Sci, 2018. **19**(1).
22. Hanahan, D. and R.A. Weinberg, *Hallmarks of cancer: the next generation*. Cell, 2011. **144**(5): p. 646-74.
23. Hanahan, D. and R.A. Weinberg, *The hallmarks of cancer*. Cell, 2000. **100**(1): p. 57-70.
24. Suzuki, H.I., et al., *MicroRNA regulons in tumor microenvironment*. Oncogene, 2015. **34**(24): p. 3085-94.
25. Lawrence, T. and D.W. Gilroy, *Chronic inflammation: a failure of resolution?* Int J Exp Pathol, 2007. **88**(2): p. 85-94.
26. Mantovani, A., et al., *Cancer-related inflammation*. Nature, 2008. **454**(7203): p. 436-44.
27. Tlsty, T.D. and L.M. Coussens, *Tumor stroma and regulation of cancer development*. Annu Rev Pathol, 2006. **1**: p. 119-50.
28. Ruffell, B., et al., *Leukocyte composition of human breast cancer*. Proc Natl Acad Sci U S A, 2012. **109**(8): p. 2796-801.
29. Balkwill, F., K.A. Charles, and A. Mantovani, *Smoldering and polarized inflammation in the initiation and promotion of malignant disease*. Cancer Cell, 2005. **7**(3): p. 211-7.
30. Bhowmick, N.A., E.G. Neilson, and H.L. Moses, *Stromal fibroblasts in cancer initiation and progression*. Nature, 2004. **432**(7015): p. 332-7.
31. Lu, P., et al., *Extracellular matrix degradation and remodeling in development and disease*. Cold Spring Harb Perspect Biol, 2011. **3**(12).
32. Mohamed, M.M. and B.F. Sloane, *Cysteine cathepsins: multifunctional enzymes in cancer*. Nat Rev Cancer, 2006. **6**(10): p. 764-75.
33. Pontiggia, O., et al., *The tumor microenvironment modulates tamoxifen resistance in breast cancer: a role for soluble stromal factors and fibronectin through beta 1 integrin*. Breast Cancer Res Treat, 2012. **133**(2): p. 459-71.
34. Gialeli, C., A.D. Theocharis, and N.K. Karamanos, *Roles of matrix metalloproteinases in cancer progression and their pharmacological targeting*. Febs j, 2011. **278**(1): p. 16-27.
35. Kessenbrock, K., V. Plaks, and Z. Werb, *Matrix metalloproteinases: regulators of the tumor microenvironment*. Cell, 2010. **141**(1): p. 52-67.
36. Giannelli, G., et al., *Induction of cell migration by matrix metalloprotease-2 cleavage of laminin-5*. Science, 1997. **277**(5323): p. 225-8.
37. Yokoyama, Y., et al., *Matrilysin (MMP-7) is a novel broadly expressed tumor antigen recognized by antigen-specific T cells*. Clin Cancer Res, 2008. **14**(17): p. 5503-11.
38. Hanahan, D. and L.M. Coussens, *Accessories to the crime: functions of cells recruited to the tumor microenvironment*. Cancer Cell, 2012. **21**(3): p. 309-22.
39. Poh, A.R. and M. Ernst, *Targeting Macrophages in Cancer: From Bench to Bedside*. Front Oncol, 2018. **8**: p. 49.
40. Bingle, L., N.J. Brown, and C.E. Lewis, *The role of tumour-associated macrophages in tumour progression: implications for new anticancer therapies*. J Pathol, 2002. **196**(3): p. 254-65.
41. Lewis, C.E. and J.O.D. McGee, *The Macrophage*. 1992, Oxford; New York: IRL Press at Oxford University Press.
42. Konur, A., et al., *Three-dimensional co-culture of human monocytes and macrophages with tumor cells: analysis of macrophage differentiation and activation*. Int J Cancer, 1996. **66**(5): p. 645-52.
43. Mizuno, R., et al., *The Role of Tumor-Associated Neutrophils in Colorectal Cancer*. Int J Mol Sci, 2019. **20**(3).

44. Hagemann, T., et al., *Macrophages induce invasiveness of epithelial cancer cells via NF-kappa B and JNK*. J Immunol, 2005. **175**(2): p. 1197-205.
45. Yang, L. and Y. Zhang, *Tumor-associated macrophages: from basic research to clinical application*. J Hematol Oncol, 2017. **10**(1): p. 58.
46. Lu, T., et al., *Tumor-infiltrating myeloid cells induce tumor cell resistance to cytotoxic T cells in mice*. J Clin Invest, 2011. **121**(10): p. 4015-29.
47. Kuang, D.M., et al., *Activated monocytes in peritumoral stroma of hepatocellular carcinoma foster immune privilege and disease progression through PD-L1*. J Exp Med, 2009. **206**(6): p. 1327-37.
48. Smith, H.A. and Y. Kang, *The metastasis-promoting roles of tumor-associated immune cells*. J Mol Med (Berl), 2013. **91**(4): p. 411-29.
49. Seftor, R.E., et al., *maspin suppresses the invasive phenotype of human breast carcinoma*. Cancer Res, 1998. **58**(24): p. 5681-5.
50. Jossion, S., et al., *Tumor-stroma co-evolution in prostate cancer progression and metastasis*. Semin Cell Dev Biol, 2010. **21**(1): p. 26-32.
51. Corzo, C.A., et al., *HIF-1alpha regulates function and differentiation of myeloid-derived suppressor cells in the tumor microenvironment*. J Exp Med, 2010. **207**(11): p. 2439-53.
52. Liechtenstein, T., et al., *A highly efficient tumor-infiltrating MDSC differentiation system for discovery of anti-neoplastic targets, which circumvents the need for tumor establishment in mice*. Oncotarget, 2014. **5**(17): p. 7843-57.
53. Rodriguez, P.C., D.G. Quiceno, and A.C. Ochoa, *L-arginine availability regulates T-lymphocyte cell-cycle progression*. Blood, 2007. **109**(4): p. 1568-73.
54. Kumar, V., et al., *The Nature of Myeloid-Derived Suppressor Cells in the Tumor Microenvironment*. Trends Immunol, 2016. **37**(3): p. 208-220.
55. Youn, J.I., et al., *Subsets of myeloid-derived suppressor cells in tumor-bearing mice*. J Immunol, 2008. **181**(8): p. 5791-802.
56. Movahedi, K., et al., *Identification of discrete tumor-induced myeloid-derived suppressor cell subpopulations with distinct T cell-suppressive activity*. Blood, 2008. **111**(8): p. 4233-44.
57. Peranzoni, E., et al., *Myeloid-derived suppressor cell heterogeneity and subset definition*. Curr Opin Immunol, 2010. **22**(2): p. 238-44.
58. Fridman, W.H., et al., *The immune contexture in human tumours: impact on clinical outcome*. Nat Rev Cancer, 2012. **12**(4): p. 298-306.
59. Sharpe, A.H., et al., *The function of programmed cell death 1 and its ligands in regulating autoimmunity and infection*. Nat Immunol, 2007. **8**(3): p. 239-45.
60. Coussens, L.M., L. Zitvogel, and A.K. Palucka, *Neutralizing tumor-promoting chronic inflammation: a magic bullet?* Science, 2013. **339**(6117): p. 286-91.
61. Speiser, D.E., et al., *T cell differentiation in chronic infection and cancer: functional adaptation or exhaustion?* Nat Rev Immunol, 2014. **14**(11): p. 768-74.
62. de Visser, K.E., A. Eichten, and L.M. Coussens, *Paradoxical roles of the immune system during cancer development*. Nat Rev Cancer, 2006. **6**(1): p. 24-37.
63. Ondondo, B., et al., *Home sweet home: the tumor microenvironment as a haven for regulatory T cells*. Front Immunol, 2013. **4**: p. 197.
64. Bauer, C.A., et al., *Dynamic Treg interactions with intratumoral APCs promote local CTL dysfunction*. J Clin Invest, 2014. **124**(6): p. 2425-40.
65. Jarnicki, A.G., et al., *Suppression of antitumor immunity by IL-10 and TGF-beta-producing T cells infiltrating the growing tumor: influence of tumor*

- environment on the induction of CD4+ and CD8+ regulatory T cells.* J Immunol, 2006. **177**(2): p. 896-904.
66. Aspod, C., et al., *Breast cancer instructs dendritic cells to prime interleukin 13-secreting CD4+ T cells that facilitate tumor development.* J Exp Med, 2007. **204**(5): p. 1037-47.
 67. DeNardo, D.G., et al., *CD4(+) T cells regulate pulmonary metastasis of mammary carcinomas by enhancing protumor properties of macrophages.* Cancer Cell, 2009. **16**(2): p. 91-102.
 68. Parker, D.C., *T cell-dependent B cell activation.* Annu Rev Immunol, 1993. **11**: p. 331-60.
 69. Nelson, B.H., *CD20+ B cells: the other tumor-infiltrating lymphocytes.* J Immunol, 2010. **185**(9): p. 4977-82.
 70. Pio, R., L. Corrales, and J.D. Lambris, *The role of complement in tumor growth.* Adv Exp Med Biol, 2014. **772**: p. 229-62.
 71. Shalapour, S., et al., *Immunosuppressive plasma cells impede T-cell-dependent immunogenic chemotherapy.* Nature, 2015. **521**(7550): p. 94-8.
 72. Tsou, P., et al., *The Emerging Role of B Cells in Tumor Immunity.* Cancer Res, 2016. **76**(19): p. 5597-5601.
 73. Shiga, K., et al., *Cancer-Associated Fibroblasts: Their Characteristics and Their Roles in Tumor Growth.* Cancers (Basel), 2015. **7**(4): p. 2443-58.
 74. Orimo, A. and R.A. Weinberg, *Heterogeneity of stromal fibroblasts in tumors.* Cancer Biol Ther, 2007. **6**(4): p. 618-9.
 75. Sugimoto, H., et al., *Identification of fibroblast heterogeneity in the tumor microenvironment.* Cancer Biol Ther, 2006. **5**(12): p. 1640-6.
 76. Yamamura, Y., et al., *Akt-Girdin signaling in cancer-associated fibroblasts contributes to tumor progression.* Cancer Res, 2015. **75**(5): p. 813-23.
 77. Kalluri, R. and M. Zeisberg, *Fibroblasts in cancer.* Nat Rev Cancer, 2006. **6**(5): p. 392-401.
 78. Loeffler, M., et al., *Targeting tumor-associated fibroblasts improves cancer chemotherapy by increasing intratumoral drug uptake.* J Clin Invest, 2006. **116**(7): p. 1955-62.
 79. Knauper, V., et al., *Activation of progelatinase B (proMMP-9) by active collagenase-3 (MMP-13).* Eur J Biochem, 1997. **248**(2): p. 369-73.
 80. Stuelten, C.H., et al., *Breast cancer cells induce stromal fibroblasts to express MMP-9 via secretion of TNF-alpha and TGF-beta.* J Cell Sci, 2005. **118**(Pt 10): p. 2143-53.
 81. Crawford, Y., et al., *PDGF-C mediates the angiogenic and tumorigenic properties of fibroblasts associated with tumors refractory to anti-VEGF treatment.* Cancer Cell, 2009. **15**(1): p. 21-34.
 82. Pietras, K. and A. Ostman, *Hallmarks of cancer: interactions with the tumor stroma.* Exp Cell Res, 2010. **316**(8): p. 1324-31.
 83. Rasanen, K. and A. Vaheri, *Activation of fibroblasts in cancer stroma.* Exp Cell Res, 2010. **316**(17): p. 2713-22.
 84. Vong, S. and R. Kalluri, *The role of stromal myofibroblast and extracellular matrix in tumor angiogenesis.* Genes Cancer, 2011. **2**(12): p. 1139-45.
 85. Chaffer, C.L. and R.A. Weinberg, *A perspective on cancer cell metastasis.* Science, 2011. **331**(6024): p. 1559-64.
 86. Stover, D.G., B. Bierie, and H.L. Moses, *A delicate balance: TGF-beta and the tumor microenvironment.* J Cell Biochem, 2007. **101**(4): p. 851-61.
 87. Balliet, R.M., et al., *Mitochondrial oxidative stress in cancer-associated fibroblasts drives lactate production, promoting breast cancer tumor growth:*

- understanding the aging and cancer connection*. Cell Cycle, 2011. **10**(23): p. 4065-73.
88. Ertel, A., et al., *Is cancer a metabolic rebellion against host aging? In the quest for immortality, tumor cells try to save themselves by boosting mitochondrial metabolism*. Cell Cycle, 2012. **11**(2): p. 253-63.
 89. Rattigan, Y.I., et al., *Lactate is a mediator of metabolic cooperation between stromal carcinoma associated fibroblasts and glycolytic tumor cells in the tumor microenvironment*. Exp Cell Res, 2012. **318**(4): p. 326-35.
 90. Sotgia, F., et al., *Caveolin-1 and cancer metabolism in the tumor microenvironment: markers, models, and mechanisms*. Annu Rev Pathol, 2012. **7**: p. 423-67.
 91. Ribeiro, A.L. and O.K. Okamoto, *Combined effects of pericytes in the tumor microenvironment*. Stem Cells Int, 2015. **2015**: p. 868475.
 92. Armulik, A., A. Abramsson, and C. Betsholtz, *Endothelial/pericyte interactions*. Circ Res, 2005. **97**(6): p. 512-23.
 93. Gerhardt, H. and C. Betsholtz, *Endothelial-pericyte interactions in angiogenesis*. Cell Tissue Res, 2003. **314**(1): p. 15-23.
 94. Stapor, P.C., et al., *Pericyte dynamics during angiogenesis: new insights from new identities*. J Vasc Res, 2014. **51**(3): p. 163-74.
 95. Farrington-Rock, C., et al., *Chondrogenic and adipogenic potential of microvascular pericytes*. Circulation, 2004. **110**(15): p. 2226-32.
 96. Crisan, M., et al., *Perivascular multipotent progenitor cells in human organs*. Ann N Y Acad Sci, 2009. **1176**: p. 118-23.
 97. Theocharis, A.D., et al., *Extracellular matrix structure*. Adv Drug Deliv Rev, 2016. **97**: p. 4-27.
 98. Abedin, M. and N. King, *Diverse evolutionary paths to cell adhesion*. Trends Cell Biol, 2010. **20**(12): p. 734-42.
 99. Pupa, S.M., et al., *New insights into the role of extracellular matrix during tumor onset and progression*. J Cell Physiol, 2002. **192**(3): p. 259-67.
 100. Steeg, P.S., *Tumor metastasis: mechanistic insights and clinical challenges*. Nat Med, 2006. **12**(8): p. 895-904.
 101. van Zijl, F., G. Krupitza, and W. Mikulits, *Initial steps of metastasis: cell invasion and endothelial transmigration*. Mutat Res, 2011. **728**(1-2): p. 23-34.
 102. Chambers, A.F., A.C. Groom, and I.C. MacDonald, *Dissemination and growth of cancer cells in metastatic sites*. Nat Rev Cancer, 2002. **2**(8): p. 563-72.
 103. Saxena, M. and G. Christofori, *Rebuilding cancer metastasis in the mouse*. Mol Oncol, 2013. **7**(2): p. 283-96.
 104. Kalluri, R. and R.A. Weinberg, *The basics of epithelial-mesenchymal transition*. J Clin Invest, 2009. **119**(6): p. 1420-8.
 105. Wei, S.C., L. Fattet, and J. Yang, *The forces behind EMT and tumor metastasis*. Cell Cycle, 2015. **14**(15): p. 2387-8.
 106. Jin, H., et al., *Snail is critical for tumor growth and metastasis of ovarian carcinoma*. Int J Cancer, 2010. **126**(9): p. 2102-11.
 107. Olmeda, D., et al., *SNAI1 is required for tumor growth and lymph node metastasis of human breast carcinoma MDA-MB-231 cells*. Cancer Res, 2007. **67**(24): p. 11721-31.
 108. Garg, M., *Epithelial-mesenchymal transition - activating transcription factors - multifunctional regulators in cancer*. World J Stem Cells, 2013. **5**(4): p. 188-95.
 109. Lamouille, S., J. Xu, and R. Derynck, *Molecular mechanisms of epithelial-mesenchymal transition*. Nat Rev Mol Cell Biol, 2014. **15**(3): p. 178-96.

110. Kudo-Saito, C., et al., *Cancer metastasis is accelerated through immunosuppression during Snail-induced EMT of cancer cells*. *Cancer Cell*, 2009. **15**(3): p. 195-206.
111. Friedl, P. and K. Wolf, *Tumour-cell invasion and migration: diversity and escape mechanisms*. *Nat Rev Cancer*, 2003. **3**(5): p. 362-74.
112. Alizadeh, A.M., S. Shiri, and S. Farsinejad, *Metastasis review: from bench to bedside*. *Tumour Biol*, 2014. **35**(9): p. 8483-523.
113. Guan, X., *Cancer metastases: challenges and opportunities*. *Acta Pharm Sin B*, 2015. **5**(5): p. 402-18.
114. Bissell, M.J. and W.C. Hines, *Why don't we get more cancer? A proposed role of the microenvironment in restraining cancer progression*. *Nat Med*, 2011. **17**(3): p. 320-9.
115. Lauwaet, T., et al., *Molecular mechanisms of invasion by cancer cells, leukocytes and microorganisms*. *Microbes Infect*, 2000. **2**(8): p. 923-31.
116. Spano, D., et al., *Molecular networks that regulate cancer metastasis*. *Semin Cancer Biol*, 2012. **22**(3): p. 234-49.
117. Condeelis, J. and J.E. Segall, *Intravital imaging of cell movement in tumours*. *Nat Rev Cancer*, 2003. **3**(12): p. 921-30.
118. Levental, K.R., et al., *Matrix crosslinking forces tumor progression by enhancing integrin signaling*. *Cell*, 2009. **139**(5): p. 891-906.
119. Gupta, G.P. and J. Massague, *Cancer metastasis: building a framework*. *Cell*, 2006. **127**(4): p. 679-95.
120. Giampieri, S., et al., *Localized and reversible TGFbeta signalling switches breast cancer cells from cohesive to single cell motility*. *Nat Cell Biol*, 2009. **11**(11): p. 1287-96.
121. Carmeliet, P. and R.K. Jain, *Principles and mechanisms of vessel normalization for cancer and other angiogenic diseases*. *Nat Rev Drug Discov*, 2011. **10**(6): p. 417-27.
122. Gupta, G.P., et al., *Mediators of vascular remodelling co-opted for sequential steps in lung metastasis*. *Nature*, 2007. **446**(7137): p. 765-70.
123. Nagrath, S., et al., *Isolation of rare circulating tumour cells in cancer patients by microchip technology*. *Nature*, 2007. **450**(7173): p. 1235-9.
124. Bos, P.D., et al., *Genes that mediate breast cancer metastasis to the brain*. *Nature*, 2009. **459**(7249): p. 1005-9.
125. Julien, S., et al., *Selectin ligand sialyl-Lewis x antigen drives metastasis of hormone-dependent breast cancers*. *Cancer Res*, 2011. **71**(24): p. 7683-93.
126. Leong, H.S., et al., *Invadopodia are required for cancer cell extravasation and are a therapeutic target for metastasis*. *Cell Rep*, 2014. **8**(5): p. 1558-70.
127. von Au, A., et al., *Circulating fibronectin controls tumor growth*. *Neoplasia*, 2013. **15**(8): p. 925-38.
128. Valastyan, S. and R.A. Weinberg, *Tumor metastasis: molecular insights and evolving paradigms*. *Cell*, 2011. **147**(2): p. 275-92.
129. Schreiber, T.D., et al., *The integrin alpha9beta1 on hematopoietic stem and progenitor cells: involvement in cell adhesion, proliferation and differentiation*. *Haematologica*, 2009. **94**(11): p. 1493-501.
130. Mathot, L. and J. Steninger, *Behavior of seeds and soil in the mechanism of metastasis: a deeper understanding*. *Cancer Sci*, 2012. **103**(4): p. 626-31.
131. Hart, I.R. and I.J. Fidler, *Role of organ selectivity in the determination of metastatic patterns of B16 melanoma*. *Cancer Res*, 1980. **40**(7): p. 2281-7.
132. Tabaries, S., et al., *Claudin-2 is selectively enriched in and promotes the formation of breast cancer liver metastases through engagement of integrin complexes*. *Oncogene*, 2011. **30**(11): p. 1318-28.

133. Minn, A.J., et al., *Genes that mediate breast cancer metastasis to lung*. Nature, 2005. **436**(7050): p. 518-24.
134. Kang, Y., et al., *A multigenic program mediating breast cancer metastasis to bone*. Cancer Cell, 2003. **3**(6): p. 537-49.
135. Hiratsuka, S., et al., *C-X-C receptor type 4 promotes metastasis by activating p38 mitogen-activated protein kinase in myeloid differentiation antigen (Gr-1)-positive cells*. Proc Natl Acad Sci U S A, 2011. **108**(1): p. 302-7.
136. McAllister, S.S., et al., *Systemic endocrine instigation of indolent tumor growth requires osteopontin*. Cell, 2008. **133**(6): p. 994-1005.
137. Bergers, G. and L.E. Benjamin, *Tumorigenesis and the angiogenic switch*. Nat Rev Cancer, 2003. **3**(6): p. 401-10.
138. Varghese, H.J., et al., *Activated ras regulates the proliferation/apoptosis balance and early survival of developing micrometastases*. Cancer Res, 2002. **62**(3): p. 887-91.
139. Folkman, J., *Role of angiogenesis in tumor growth and metastasis*. Semin Oncol, 2002. **29**(6 Suppl 16): p. 15-8.
140. Garat, C., et al., *Soluble and insoluble fibronectin increases alveolar epithelial wound healing in vitro*. Am J Physiol, 1996. **271**(5 Pt 1): p. L844-53.
141. Potts, J.R. and I.D. Campbell, *Fibronectin structure and assembly*. Curr Opin Cell Biol, 1994. **6**(5): p. 648-55.
142. Erickson, H.P., *Stretching fibronectin*. J Muscle Res Cell Motil, 2002. **23**(5-6): p. 575-80.
143. Mao, Y. and J.E. Schwarzbauer, *Fibronectin fibrillogenesis, a cell-mediated matrix assembly process*. Matrix Biol, 2005. **24**(6): p. 389-99.
144. Pankov, R. and K.M. Yamada, *Fibronectin at a glance*. J Cell Sci, 2002. **115**(Pt 20): p. 3861-3.
145. Singh, P., C. Carraher, and J.E. Schwarzbauer, *Assembly of fibronectin extracellular matrix*. Annu Rev Cell Dev Biol, 2010. **26**: p. 397-419.
146. Geiger, B., et al., *Transmembrane crosstalk between the extracellular matrix--cytoskeleton crosstalk*. Nat Rev Mol Cell Biol, 2001. **2**(11): p. 793-805.
147. Takahashi, S., et al., *The RGD motif in fibronectin is essential for development but dispensable for fibril assembly*. J Cell Biol, 2007. **178**(1): p. 167-78.
148. Tomasini-Johansson, B.R., D.S. Annis, and D.F. Mosher, *The N-terminal 70-kDa fragment of fibronectin binds to cell surface fibronectin assembly sites in the absence of intact fibronectin*. Matrix Biol, 2006. **25**(5): p. 282-93.
149. Cho, J. and D.F. Mosher, *Characterization of fibronectin assembly by platelets adherent to adsorbed laminin-111*. J Thromb Haemost, 2006. **4**(5): p. 943-51.
150. McKeown-Longo, P.J. and D.F. Mosher, *Interaction of the 70,000-mol-wt amino-terminal fragment of fibronectin with the matrix-assembly receptor of fibroblasts*. J Cell Biol, 1985. **100**(2): p. 364-74.
151. Tomasini-Johansson, B.R., et al., *A 49-residue peptide from adhesin F1 of Streptococcus pyogenes inhibits fibronectin matrix assembly*. J Biol Chem, 2001. **276**(26): p. 23430-9.
152. Sottile, J., et al., *Five type I modules of fibronectin form a functional unit that binds to fibroblasts and Staphylococcus aureus*. J Biol Chem, 1991. **266**(20): p. 12840-3.
153. Curnis, F., et al., *Spontaneous formation of L-isoaspartate and gain of function in fibronectin*. J Biol Chem, 2006. **281**(47): p. 36466-76.
154. Schor, S.L., et al., *Motogenic activity of IGD-containing synthetic peptides*. J Cell Sci, 1999. **112** (Pt 22): p. 3879-88.

155. Maurer, L.M., D.S. Annis, and D.F. Mosher, *IGD motifs, which are required for migration stimulatory activity of fibronectin type I modules, do not mediate binding in matrix assembly*. PLoS One, 2012. **7**(2): p. e30615.
156. Schwarzbauer, J.E., *Alternative splicing of fibronectin: three variants, three functions*. Bioessays, 1991. **13**(10): p. 527-33.
157. Gutman, A. and A.R. Kornblihtt, *Identification of a third region of cell-specific alternative splicing in human fibronectin mRNA*. Proc Natl Acad Sci U S A, 1987. **84**(20): p. 7179-82.
158. Kumra, H., et al., *Roles of fibronectin isoforms in neonatal vascular development and matrix integrity*. PLoS Biol, 2018. **16**(7): p. e2004812.
159. Vibe-Pedersen, K., A.R. Kornblihtt, and F.E. Baralle, *Expression of a human alpha-globin/fibronectin gene hybrid generates two mRNAs by alternative splicing*. Embo j, 1984. **3**(11): p. 2511-6.
160. Bergijk, E.C., et al., *Cloning of the mouse fibronectin V-region and variation of its splicing pattern in experimental immune complex glomerulonephritis*. J Pathol, 1996. **178**(4): p. 462-8.
161. Kornblihtt, A.R., et al., *Primary structure of human fibronectin: differential splicing may generate at least 10 polypeptides from a single gene*. Embo j, 1985. **4**(7): p. 1755-9.
162. French-Constant, C., *Alternative splicing of fibronectin--many different proteins but few different functions*. Exp Cell Res, 1995. **221**(2): p. 261-71.
163. Kosmehl, H., A. Berndt, and D. Katenkamp, *Molecular variants of fibronectin and laminin: structure, physiological occurrence and histopathological aspects*. Virchows Arch, 1996. **429**(6): p. 311-22.
164. Borsi, L., et al., *Monoclonal antibodies in the analysis of fibronectin isoforms generated by alternative splicing of mRNA precursors in normal and transformed human cells*. J Cell Biol, 1987. **104**(3): p. 595-600.
165. Zardi, L., et al., *Transformed human cells produce a new fibronectin isoform by preferential alternative splicing of a previously unobserved exon*. Embo j, 1987. **6**(8): p. 2337-42.
166. White, E.S., F.E. Baralle, and A.F. Muro, *New insights into form and function of fibronectin splice variants*. J Pathol, 2008. **216**(1): p. 1-14.
167. White, E.S. and A.F. Muro, *Fibronectin splice variants: understanding their multiple roles in health and disease using engineered mouse models*. IUBMB Life, 2011. **63**(7): p. 538-46.
168. Xia, P. and L.A. Culp, *Adhesion activity in fibronectin's alternatively spliced domain EDa (EIIIA) and its neighboring type III repeats: oncogene-dependent regulation*. Exp Cell Res, 1994. **213**(1): p. 253-65.
169. Manabe, R., N. Oh-e, and K. Sekiguchi, *Alternatively spliced EDA segment regulates fibronectin-dependent cell cycle progression and mitogenic signal transduction*. J Biol Chem, 1999. **274**(9): p. 5919-24.
170. Muro, A.F., et al., *Regulated splicing of the fibronectin EDA exon is essential for proper skin wound healing and normal lifespan*. J Cell Biol, 2003. **162**(1): p. 149-60.
171. Serini, G., et al., *The fibronectin domain ED-A is crucial for myofibroblastic phenotype induction by transforming growth factor-beta1*. J Cell Biol, 1998. **142**(3): p. 873-81.
172. Pulakazhi Venu, V.K., et al., *Fibronectin extra domain A stabilises atherosclerotic plaques in apolipoprotein E and in LDL-receptor-deficient mice*. Thromb Haemost, 2015. **114**(1): p. 186-97.
173. Hackl, N.J., et al., *Circulating fibronectin isoforms predict the degree of fibrosis in chronic hepatitis C*. Scand J Gastroenterol, 2010. **45**(3): p. 349-56.

174. Muro, A.F., et al., *An essential role for fibronectin extra type III domain A in pulmonary fibrosis*. Am J Respir Crit Care Med, 2008. **177**(6): p. 638-45.
175. Wang, J.P. and A. Hielscher, *Fibronectin: How Its Aberrant Expression in Tumors May Improve Therapeutic Targeting*. J Cancer, 2017. **8**(4): p. 674-682.
176. Glukhova, M.A., et al., *Expression of fibronectin variants in vascular and visceral smooth muscle cells in development*. Dev Biol, 1990. **141**(1): p. 193-202.
177. Rybak, J.N., et al., *The extra-domain A of fibronectin is a vascular marker of solid tumors and metastases*. Cancer Res, 2007. **67**(22): p. 10948-57.
178. Kawaguchi, T. and K. Nakamura, *[Cancer metastasis and blood vessels]*. Gan To Kagaku Ryoho, 1983. **10**(7): p. 1569-76.
179. Matsumoto, E., et al., *Expression of fibronectin isoforms in human breast tissue: production of extra domain A+/extra domain B+ by cancer cells and extra domain A+ by stromal cells*. Jpn J Cancer Res, 1999. **90**(3): p. 320-5.
180. Ou, J., et al., *Endothelial cell-derived fibronectin extra domain A promotes colorectal cancer metastasis via inducing epithelial-mesenchymal transition*. Carcinogenesis, 2014. **35**(7): p. 1661-70.
181. Sun, X., et al., *The EDA-containing cellular fibronectin induces epithelial-mesenchymal transition in lung cancer cells through integrin alpha9beta1-mediated activation of PI3-K/AKT and Erk1/2*. Carcinogenesis, 2014. **35**(1): p. 184-91.
182. Frey, K., et al., *Different patterns of fibronectin and tenascin-C splice variants expression in primary and metastatic melanoma lesions*. Exp Dermatol, 2011. **20**(8): p. 685-8.
183. Manabe, R., et al., *Modulation of cell-adhesive activity of fibronectin by the alternatively spliced EDA segment*. J Cell Biol, 1997. **139**(1): p. 295-307.
184. Johansson, S., et al., *Fibronectin-integrin interactions*. Front Biosci, 1997. **2**: p. d126-46.
185. Fattorusso, R., et al., *NMR structure of the human oncofoetal fibronectin ED-B domain, a specific marker for angiogenesis*. Structure, 1999. **7**(4): p. 381-90.
186. Trachsel, E., et al., *A human mAb specific to oncofetal fibronectin selectively targets chronic skin inflammation in vivo*. J Invest Dermatol, 2007. **127**(4): p. 881-6.
187. Khan, Z.A., et al., *EDB fibronectin and angiogenesis -- a novel mechanistic pathway*. Angiogenesis, 2005. **8**(3): p. 183-96.
188. Kawelke, N., et al., *Isoform of fibronectin mediates bone loss in patients with primary biliary cirrhosis by suppressing bone formation*. J Bone Miner Res, 2008. **23**(8): p. 1278-86.
189. Sens, C., et al., *An O-Glycosylation of Fibronectin Mediates Hepatic Osteodystrophy Through alpha4beta1 Integrin*. J Bone Miner Res, 2017. **32**(1): p. 70-81.
190. French-Constant, C. and R.O. Hynes, *Alternative splicing of fibronectin is temporally and spatially regulated in the chicken embryo*. Development, 1989. **106**(2): p. 375-88.
191. Paganì, F., et al., *Tissue-specific splicing pattern of fibronectin messenger RNA precursor during development and aging in rat*. J Cell Biol, 1991. **113**(5): p. 1223-9.
192. Castellani, P., et al., *The fibronectin isoform containing the ED-B oncofetal domain: a marker of angiogenesis*. Int J Cancer, 1994. **59**(5): p. 612-8.

193. Astrof, S., D. Crowley, and R.O. Hynes, *Multiple cardiovascular defects caused by the absence of alternatively spliced segments of fibronectin*. Dev Biol, 2007. **311**(1): p. 11-24.
194. Pujuguet, P., et al., *Expression of fibronectin ED-A+ and ED-B+ isoforms by human and experimental colorectal cancer. Contribution of cancer cells and tumor-associated myofibroblasts*. Am J Pathol, 1996. **148**(2): p. 579-92.
195. Sauer, S., et al., *Expression of the oncofetal ED-B-containing fibronectin isoform in hematologic tumors enables ED-B-targeted 131I-L19SIP radioimmunotherapy in Hodgkin lymphoma patients*. Blood, 2009. **113**(10): p. 2265-74.
196. Schwarzbauer, J.E., C.S. Spencer, and C.L. Wilson, *Selective secretion of alternatively spliced fibronectin variants*. J Cell Biol, 1989. **109**(6 Pt 2): p. 3445-53.
197. Wilson, C.L. and J.E. Schwarzbauer, *The alternatively spliced V region contributes to the differential incorporation of plasma and cellular fibronectins into fibrin clots*. J Cell Biol, 1992. **119**(4): p. 923-33.
198. Krolo, M., et al., *Fibronectin expression in the developing human spinal cord, nerves, and ganglia*. Croat Med J, 1998. **39**(4): p. 386-91.
199. George, E.L., et al., *Defects in mesoderm, neural tube and vascular development in mouse embryos lacking fibronectin*. Development, 1993. **119**(4): p. 1079-91.
200. Plow, E.F., et al., *Ligand binding to integrins*. J Biol Chem, 2000. **275**(29): p. 21785-8.
201. Leiss, M., et al., *The role of integrin binding sites in fibronectin matrix assembly in vivo*. Curr Opin Cell Biol, 2008. **20**(5): p. 502-7.
202. Katagiri, Y.U., et al., *Non-RGD domains of osteopontin promote cell adhesion without involving alpha v integrins*. J Cell Biochem, 1996. **62**(1): p. 123-31.
203. Sakamoto, H., et al., *Cell-type specific recognition of RGD- and non-RGD-containing cell binding domains in fibrillin-1*. J Biol Chem, 1996. **271**(9): p. 4916-22.
204. Aota, S., M. Nomizu, and K.M. Yamada, *The short amino acid sequence Pro-His-Ser-Arg-Asn in human fibronectin enhances cell-adhesive function*. J Biol Chem, 1994. **269**(40): p. 24756-61.
205. Guan, J.L. and R.O. Hynes, *Lymphoid cells recognize an alternatively spliced segment of fibronectin via the integrin receptor alpha 4 beta 1*. Cell, 1990. **60**(1): p. 53-61.
206. Shinde, A.V., et al., *Identification of the peptide sequences within the E111A (EDA) segment of fibronectin that mediate integrin alpha9beta1-dependent cellular activities*. J Biol Chem, 2008. **283**(5): p. 2858-70.
207. Midwood, K.S., L.V. Williams, and J.E. Schwarzbauer, *Tissue repair and the dynamics of the extracellular matrix*. Int J Biochem Cell Biol, 2004. **36**(6): p. 1031-7.
208. Morgan, M.R., M.J. Humphries, and M.D. Bass, *Synergistic control of cell adhesion by integrins and syndecans*. Nat Rev Mol Cell Biol, 2007. **8**(12): p. 957-69.
209. Rostagno, A., et al., *Further characterization of the NH2-terminal fibrin-binding site on fibronectin*. J Biol Chem, 1994. **269**(50): p. 31938-45.
210. Sottile, J., et al., *Fibronectin-dependent collagen I deposition modulates the cell response to fibronectin*. Am J Physiol Cell Physiol, 2007. **293**(6): p. C1934-46.

211. Erat, M.C., et al., *Identification and structural analysis of type I collagen sites in complex with fibronectin fragments*. Proc Natl Acad Sci U S A, 2009. **106**(11): p. 4195-200.
212. Erat, M.C., et al., *Structural analysis of collagen type I interactions with human fibronectin reveals a cooperative binding mode*. J Biol Chem, 2013. **288**(24): p. 17441-50.
213. Ma, W., et al., *Bivalent ligation of the collagen-binding modules of fibronectin by SFS, a non-anchored bacterial protein of Streptococcus equi*. J Biol Chem, 2015. **290**(8): p. 4866-76.
214. Jo, J.S., et al., *Homologous fibronectin enhances healing of excised wounds in rats*. J Korean Med Sci, 1991. **6**(3): p. 197-205.
215. Matuskova, J., et al., *Decreased plasma fibronectin leads to delayed thrombus growth in injured arterioles*. Arterioscler Thromb Vasc Biol, 2006. **26**(6): p. 1391-6.
216. Nam, J.M., et al., *Breast cancer cells in three-dimensional culture display an enhanced radioresponse after coordinate targeting of integrin alpha5beta1 and fibronectin*. Cancer Res, 2010. **70**(13): p. 5238-48.
217. Han, S.W. and J. Roman, *Fibronectin induces cell proliferation and inhibits apoptosis in human bronchial epithelial cells: pro-oncogenic effects mediated by PI3-kinase and NF-kappa B*. Oncogene, 2006. **25**(31): p. 4341-9.
218. Ou, J., et al., *Fibronectin extra domain A (EDA) sustains CD133(+)/CD44(+) subpopulation of colorectal cancer cells*. Stem Cell Res, 2013. **11**(2): p. 820-33.
219. Sengupta, S., et al., *Short hairpin RNA-mediated fibronectin knockdown delays tumor growth in a mouse glioma model*. Neoplasia, 2010. **12**(10): p. 837-47.
220. Rosnagl, S., et al., *EDA-Fibronectin Originating from Osteoblasts Inhibits the Immune Response against Cancer*. PLoS Biol, 2016. **14**(9): p. e1002562.
221. Xiang, L., et al., *The extra domain A of fibronectin increases VEGF-C expression in colorectal carcinoma involving the PI3K/AKT signaling pathway*. PLoS One, 2012. **7**(4): p. e35378.
222. Werb, Z., et al., *Signal transduction through the fibronectin receptor induces collagenase and stromelysin gene expression*. J Cell Biol, 1989. **109**(2): p. 877-89.
223. Gay, L.J. and B. Felding-Habermann, *Contribution of platelets to tumour metastasis*. Nat Rev Cancer, 2011. **11**(2): p. 123-34.
224. Knowles, L.M., G. Malik, and J. Pilch, *Plasma Fibronectin Promotes Tumor Cell Survival and Invasion through Regulation of Tie2*. J Cancer, 2013. **4**(5): p. 383-90.
225. Chiang, H.Y., et al., *Fibronectin is an important regulator of flow-induced vascular remodeling*. Arterioscler Thromb Vasc Biol, 2009. **29**(7): p. 1074-9.
226. Hielscher, A., et al., *Fibronectin Deposition Participates in Extracellular Matrix Assembly and Vascular Morphogenesis*. PLoS One, 2016. **11**(1): p. e0147600.
227. Lou, X., et al., *SOX2 targets fibronectin 1 to promote cell migration and invasion in ovarian cancer: new molecular leads for therapeutic intervention*. Omics, 2013. **17**(10): p. 510-8.
228. Endoh, T. and T. Ohtsuki, *Cellular siRNA delivery using cell-penetrating peptides modified for endosomal escape*. Adv Drug Deliv Rev, 2009. **61**(9): p. 704-9.

229. Foerg, C., et al., *Differentiation restricted endocytosis of cell penetrating peptides in MDCK cells corresponds with activities of Rho-GTPases*. Pharm Res, 2007. **24**(4): p. 628-42.
230. Kumar, P., et al., *Transvascular delivery of small interfering RNA to the central nervous system*. Nature, 2007. **448**(7149): p. 39-43.
231. Lopez, M.V., et al., *A tumor-stroma targeted oncolytic adenovirus replicated in human ovary cancer samples and inhibited growth of disseminated solid tumors in mice*. Mol Ther, 2012. **20**(12): p. 2222-33.
232. Jefferson, A., V.E. Cadet, and A. Hielscher, *The mechanisms of genetically modified vaccinia viruses for the treatment of cancer*. Crit Rev Oncol Hematol, 2015. **95**(3): p. 407-16.
233. Thundimadathil, J., *Cancer treatment using peptides: current therapies and future prospects*. J Amino Acids, 2012. **2012**: p. 967347.
234. Ensenberger, M.G., et al., *Specific interactions between F1 adhesin of Streptococcus pyogenes and N-terminal modules of fibronectin*. J Biol Chem, 2001. **276**(38): p. 35606-13.
235. Garcia-Hernandez Mde, L., et al., *Adoptive transfer of tumor-specific Tc17 effector T cells controls the growth of B16 melanoma in mice*. J Immunol, 2010. **184**(8): p. 4215-27.
236. Wetterwald, A., et al., *Optical imaging of cancer metastasis to bone marrow: a mouse model of minimal residual disease*. Am J Pathol, 2002. **160**(3): p. 1143-53.
237. Wierzbicka-Patynowski, I., Y. Mao, and J.E. Schwarzbauer, *Analysis of fibronectin matrix assembly*. Curr Protoc Cell Biol, 2004. **Chapter 10**: p. Unit 10.12.
238. Towbin, H., T. Staehelin, and J. Gordon, *Electrophoretic transfer of proteins from polyacrylamide gels to nitrocellulose sheets: procedure and some applications*. 1979. Biotechnology, 1992. **24**: p. 145-9.
239. Hochuli, E., et al., *Genetic Approach to Facilitate Purification of Recombinant Proteins with a Novel Metal Chelate Adsorbent*. Bio/Technology, 1988. **6**(11): p. 1321-1325.
240. Sabrina, K., *Der Einfluss des Osteoblasten-und Tumorzellfibronectins auf die Immunzellen*, in *Institut für Immunologie und Serologie, Uniklinikum Heidelberg*. 2014, Universität Hohenheim: Hohenheim. p. 215.
241. Norman, J.H., *Die Rolle des Fibronektins bei der Entstehung und dem Wachstum von Tumoren*, in *Institut für Immunologie und Serologie, Uniklinikum Heidelberg*. 2010, Johannes Gutenberg-Universität in Mainz: Mainz. p. 184.
242. Altrock, E., et al., *Inhibition of fibronectin deposition improves experimental liver fibrosis*. J Hepatol, 2015. **62**(3): p. 625-33.
243. Beaumont, K.A., N. Mohana-Kumaran, and N.K. Haass, *Modeling Melanoma In Vitro and In Vivo*. Healthcare (Basel), 2013. **2**(1): p. 27-46.
244. Bingham, R.J., et al., *Crystal structures of fibronectin-binding sites from Staphylococcus aureus FnBPA in complex with fibronectin domains*. Proc Natl Acad Sci U S A, 2008. **105**(34): p. 12254-8.
245. Maurer, L.M., W. Ma, and D.F. Mosher, *Dynamic structure of plasma fibronectin*. Crit Rev Biochem Mol Biol, 2015. **51**(4): p. 213-27.
246. Maurer, L.M., et al., *Extended binding site on fibronectin for the functional upstream domain of protein F1 of Streptococcus pyogenes*. J Biol Chem, 2010. **285**(52): p. 41087-99.
247. Au, A.v., *Der Einfluss des extrazellulären Matrixproteins Fibronektin auf das Wachstum von Knochenmetastasen*, in *Institut für Immunologie und Serologie*,

- Uniklinikum Heidelberg*. 2012, Ruprecht-Karls-Universität Heidelberg: Heidelberg. p. 215.
248. Zhang, X., R. Goncalves, and D.M. Mosser, *The isolation and characterization of murine macrophages*. Curr Protoc Immunol, 2008. **Chapter 14**: p. Unit 14.1.
 249. Sabatier, L., et al., *Fibrillin assembly requires fibronectin*. Mol Biol Cell, 2009. **20**(3): p. 846-58.
 250. Zhou, X., et al., *Fibronectin fibrillogenesis regulates three-dimensional neovessel formation*. Genes Dev, 2008. **22**(9): p. 1231-43.
 251. Hanski, E. and M. Caparon, *Protein F, a fibronectin-binding protein, is an adhesin of the group A streptococcus Streptococcus pyogenes*. Proc Natl Acad Sci U S A, 1992. **89**(13): p. 6172-6.
 252. Ozeri, V., et al., *A two-domain mechanism for group A streptococcal adherence through protein F to the extracellular matrix*. Embo j, 1996. **15**(5): p. 989-98.
 253. Wennerberg, K., et al., *Beta 1 integrin-dependent and -independent polymerization of fibronectin*. J Cell Biol, 1996. **132**(1-2): p. 227-38.
 254. Sottile, J. and D.C. Hocking, *Fibronectin polymerization regulates the composition and stability of extracellular matrix fibrils and cell-matrix adhesions*. Mol Biol Cell, 2002. **13**(10): p. 3546-59.
 255. Grivennikov, S.I., F.R. Greten, and M. Karin, *Immunity, inflammation, and cancer*. Cell, 2010. **140**(6): p. 883-99.
 256. Lin, W.W. and M. Karin, *A cytokine-mediated link between innate immunity, inflammation, and cancer*. J Clin Invest, 2007. **117**(5): p. 1175-83.
 257. Sica, A., P. Allavena, and A. Mantovani, *Cancer related inflammation: the macrophage connection*. Cancer Lett, 2008. **267**(2): p. 204-15.
 258. Overwijk, W.W. and N.P. Restifo, *B16 as a mouse model for human melanoma*. Curr Protoc Immunol, 2001. **Chapter 20**: p. Unit 20.1.
 259. Watanabe, S., et al., *Tumor-induced CD11b+Gr-1+ myeloid cells suppress T cell sensitization in tumor-draining lymph nodes*. J Immunol, 2008. **181**(5): p. 3291-300.
 260. Porta, C., et al., *Macrophages in cancer and infectious diseases: the 'good' and the 'bad'*. Immunotherapy, 2011. **3**(10): p. 1185-202.
 261. Shi, F., et al., *Collagen I matrix turnover is regulated by fibronectin polymerization*. Am J Physiol Cell Physiol, 2010. **298**(5): p. C1265-75.
 262. Menzel, J. and W. Borth, *Influence of plasma fibronectin on collagen cleavage by collagenase*. Coll Relat Res, 1983. **3**(3): p. 217-30.
 263. Joh, D., et al., *Multiple specificities of the staphylococcal and streptococcal fibronectin-binding microbial surface components recognizing adhesive matrix molecules*. Eur J Biochem, 1998. **258**(2): p. 897-905.
 264. Zhang, Q. and D.F. Mosher, *Cross-linking of the NH₂-terminal region of fibronectin to molecules of large apparent molecular mass. Characterization of fibronectin assembly sites induced by the treatment of fibroblasts with lysophosphatidic acid*. J Biol Chem, 1996. **271**(52): p. 33284-92.
 265. Meenan, N.A., et al., *The tandem beta-zipper model defines high affinity fibronectin-binding repeats within Staphylococcus aureus FnBPA*. J Biol Chem, 2007. **282**(35): p. 25893-902.
 266. Atkin, K.E., et al., *The streptococcal binding site in the gelatin-binding domain of fibronectin is consistent with a non-linear arrangement of modules*. J Biol Chem, 2010. **285**(47): p. 36977-83.
 267. Zamarron, B.F. and W. Chen, *Dual roles of immune cells and their factors in cancer development and progression*. Int J Biol Sci, 2011. **7**(5): p. 651-8.

CIRRCULUM VITAE

268. Chang, C.I., J.C. Liao, and L. Kuo, *Macrophage arginase promotes tumor cell growth and suppresses nitric oxide-mediated tumor cytotoxicity*. *Cancer Res*, 2001. **61**(3): p. 1100-6.

7 CURRICULUM VITAE

Personal information

First name: Hiba
 Surname: Ghura
 Family status: Single
 Place & Date of birth: Syria- 09/11/1987
 Nationality: Syrian

Education:

1993-1999	Elementary school, Lattakia, Syria
1999-2005	Secondary school, Lattakia, Syria (Honor)
2005-2010	Education at Tishreen university, Lattakia, Syria, Faculty of pharmacy, Department of pharmacy and pharmaceutical sciences. Bachelor degree, average (80.32%- top 5 out of 200 students)
2011-2013	Research assistant at Tishreen university, Faculty of pharmacy Department of microbiology, hematology and immunology Master student, department of Biochemistry and Microbiology. Research project “ the diagnostic value of soluble transferrin receptor in differentiation of iron deficiency anemia and anemia of chronic disease ”.
2013- 2015	Research assistant at Damascus university, Faculty of pharmacy Department of pharmacology and medicinal chemistry
2015-2019	PhD student at institute of Immunology and Serology at the Medical Faculty of Heidelberg (Doctoral research grant from German Academic Exchange Service (DAAD))

Publications

1. A Subpopulation of Stromal Cells Controls Cancer Cell Homing to the Bone Marrow. Rosnagl S, **Ghura H**, Groth C, Altrock E, Jakob F, Schott S, Wimberger P, Link T, Kuhlmann JD, Stenzl A, Hennenlotter J, Todenhöfer T, Rojewski M, Bieback K, Nakchbandi IA. *Cancer Res.* 2018 Jan 1;78(1):129-142. doi: 10.1158/0008-5472.CAN-16-3507. Epub 2017 Oct 24.
2. Circulating fibronectin contributes to mesangial expansion in a murine model of type 1 diabetes. Klemis V, **Ghura H**, Federico G, Würfel C, Bentmann A, Gretz N, Miyazaki T, Gröne HJ, Nakchbandi IA. *Kidney Int.* 2017 Jun;91(6):1374-1385. doi: 10.1016/j.kint.2016.12.006. Epub 2017 Jan 31.

Poster presentations and attended events

Changing matrix composition suppresses cancer growth by modifying macrophage behavior. Hiba Ghura, Caren Zoeller, Inaam Nakchbandi. European Association for Cancer Research (EACR), "Defence is the best attack", Barcelona, Spain, 2019.

Pharmacologic inhibition of fibronectin accumulation suppresses bone metastasis growth. Hiba Ghura, Caren Zoeller, Inaam Nakchbandi. Deutsche Gesellschaft für Osteologie, Frankfurt, Germany, 2019. Speaker and Travel award

Characteristics of the stromal cells in the hematopoietic and premetastatic niches. Hiba Ghura, Stephanie Rosnagl, Inaam Nakchbandi. Cancer and Bone meeting, Oxford, UK, 2018.

Learning from osteoblasts how to fight cancer. Hiba Ghura, Carla Sens, Inaam Nakchbandi. Cancer and Bone meeting, Oxford, UK, 2018.

Honors and awards

Travel grant for attending and presenting my results under the title "pharmacologic inhibition of fibronectin accumulation suppresses bone metastasis growth" in "Osteologie Kongress, Frankfurt, Germany, 2019"

DAAD scholarship for PhD studies and research

Training exchange grant in Assiut, Egypt, 2009

Honor student third highest grade, faculty of Pharmacy, Tishreen University, Latakia, Syria, 2008

Course

- Application and assessment workshop which was organized by Heidelberg University and took place on 25th and 26th of April
- Application seminar "Expand your research with flow cytometry" in DKFZ which was organized by BD life science company
- Training course during a student exchange program with Egypt at faculty of pharmacy- Assiut University-Egypt, 2009
- Good manufacture practice course (GMP) at T3A pharmaceutical industries, Assiut, Egypt, 2009

8 ACKNOWLEDGEMENT

I would like to thank my project supervisor Prof. Dr. Inaam Nakchbandi for taking me as a PhD student and for the generous support and encouragement she offered during the years.

I would like to thank Prof. Dr.rer.nat. Peter Bugert and PD. Dr. Yu xi Feng for agreeing to be examiners.

I would like to express my thanks and appreciation to everybody who directly or indirectly contributed to this project. Thanks to the biochemical core facility of the Max Planck Institute in Martinsried for providing me with the biomass and raw peptides. Thanks to Jüri Habicht for his precious tips in performing my experiments. I would like to thank my colleagues in the lab, Franziska, Caren, Alexander, Stefan, Katrin and Carla for the wonderful atmosphere and for making me feel at home.

I am particularly grateful to DAAD (German Academic Exchange Service) for giving me the opportunity to work at the exciting scientific University with inspiring people.

A big thank to Aline Bendig for being such a nice person who always remembered me in Christmas and birthdays times with nice cards, making me feel loved in those nice days. Thanks for your precious friendship and for always reminding me that "alles wird gut". Rana, Nahed, Dima, Ahmad, Zaid and Ayham, thanks for your encouragement to always do better. Your love is deeply appreciated and will always be needed.

I am tremendously grateful to my family for supporting me: My father for his encouragement and putting the fundament of my scientific curiosity, my mother, who cared for and raised me with boundless love. This work should serve as a small token for your trust and continued belief in me.

Thanks to the inspirational person in my life since I was a child, my grandmother, I love you and I wish you were there now.....

Thanks to Syria which without I wouldn't have been in this place.